Edge Under Uncertainty: Designing Robust AI Systems for NFL Betting Markets

Richard Oldham

October 7, 2025

Abstract

This dissertation presents a system-of-systems for prediction, decision-making, and governance in National Football League (NFL) betting markets. The work integrates a reproducible data layer, calibrated probabilistic models, conservative offline reinforcement learning (RL), and risk controls that make policies deployable in practice.

On the data side, idempotent ingestion pipelines build governed TimescaleDB marts from play-by-play, odds history, weather, and schedule context. Modeling begins with calibrated baselines (logistic/probit and state-space team ratings) and a score-distribution layer that prices spreads and totals via Skellam and bivariate Poisson models. We introduce an integer-margin reweighting procedure that matches empirical key-number masses (3, 6, 7, 10) while preserving location/scale, and we model spread–total dependence with Gaussian/t copulas to price correlated legs.

Edges are converted into actions with offline RL (IQL/CQL/TD3+BC/AWAC) under safety constraints. Policies are promoted only when off-policy evaluation (self-normalized importance sampling, doubly robust, and high-confidence bounds) passes stability checks. Stake sizing combines fractional Kelly with friction/cap projections and portfolio-level CVaR constraints. A Monte Carlo simulator, calibrated to historical margins and dependence and instrumented with frictions and liquidity, provides acceptance tests and stress scenarios.

Across rolling out-of-sample seasons, the stack delivers improved probability calibration, consistent closing-line value (CLV) capture, and superior risk-adjusted returns relative to classical baselines, while materially reducing drawdowns under pessimistic friction regimes. Contributions include: (i) a reproducible NFL data mart and feature pipeline; (ii) dependence-aware, key-number-calibrated pricing of discrete margins; (iii) a conservative offline-RL+OPE gate for promotion; and (iv) a governance playbook linking uncertainty to portfolio risk.

Code and Data Availability

All code, documentation, and analysis scripts supporting this dissertation are publicly available at:

The repository includes:

- Complete data ingestion pipelines for NFL play-by-play data (1999–2024)

- TimescaleDB schema and materialized views

- Feature engineering and model implementation code

- Reinforcement learning agents and training scripts

- Monte Carlo simulation framework

- Statistical testing and validation notebooks

- LaTeX source files for this dissertation

Reproducibility. The codebase is designed for full reproducibility. All random seeds are fixed, dependencies are pinned via `requirements.txt` (Python) and `renv.lock` (R), and the README provides step-by-step instructions for replicating all results. The experiment registry tracks all model runs with hashed parameters and metrics.

Data Sources. Primary data sources include:

- **nflfastR**: Play-by-play data via the R package ecosystem

- **The Odds API**: Historical betting lines (API key required)

- **Meteostat**: Weather data for game conditions

- **NFL official data**: Schedules, rosters, and injury reports

License. The code is released under the MIT License for academic and research use. Commercial use of betting-related components should comply with local regulations.

Contents

List of Figures

List of Tables

Notation Glossary

This glossary provides a comprehensive reference for mathematical notation used throughout the dissertation.

Probability and Statistics

Symbol	Description
$\mathbb{E}[X]$	Expected value of random variable X
$\mathbb{P}(A)$	Probability of event A
$\text{Var}(X)$	Variance of random variable X
$\text{Cov}(X, Y)$	Covariance between X and Y
$\mathcal{N}(\mu, \sigma^2)$	Normal distribution with mean μ and variance σ^2
$\Phi(\cdot)$	Standard normal cumulative distribution function
$\phi(\cdot)$	Standard normal probability density function
$\text{Pois}(\lambda)$	Poisson distribution with rate λ
$\text{Skellam}(\lambda, \mu)$	Skellam distribution (difference of Poissons)
$\sim$	Distributed as
$\overset{d}{=}$	Equal in distribution
$\overset{p}{\to}$	Convergence in probability
$\overset{a.s.}{\to}$	Almost sure convergence
$\Rightarrow$	Convergence in distribution

Game Variables

Symbol	Description
D	Game margin (home score minus away score)
M_t	Observed margin at time/game t
p	Point spread
o	Total (over/under) line
X	Home team score
Y	Away team score
$(h(t), a(t))$	Home and away teams for game t
$Y \in \{0, 1\}$	Binary outcome (win/cover)
$\mathcal{K}$	Set of key numbers $\{3, 6, 7, 10\}$

Model Parameters

Symbol	Description
$\theta_{i,t}$	Team i strength at time t
λ	Home team scoring rate (Poisson)
μ	Away team scoring rate (Poisson)
β	Regression coefficients vector
σ	Standard deviation of margin distribution
τ	Process noise standard deviation (state-space)
γ	Home field advantage parameter
ρ	Correlation parameter (copula)
ν	Degrees of freedom (t-distribution/copula)
H	Half-life for exponential decay weighting
α	Significance level for hypothesis tests

Reinforcement Learning

Symbol	Description
$s \in \mathcal{S}$	State from state space
$a \in \mathcal{A}$	Action from action space
r	Reward signal
$\pi(a|s)$	Policy (action probability given state)
π_b	Behavior policy (data-generating policy)
π_e	Evaluation policy (target policy)
$Q(s, a)$	Action-value function
$V(s)$	State-value function
$\mathcal{D}$	Offline dataset of transitions
τ	Trajectory $(s_0, a_0, r_0, s_1, ...)$
γ	Discount factor
η	Learning rate

Market and Betting

Symbol	Description
CBV	Comparative Book Value
CLV	Closing Line Value
EV	Expected Value
π	Market-implied probability
$\hat{\pi}$	Model-predicted probability
d	Decimal odds
o	American odds
H	Hold (vigorish) percentage
f^*	Kelly fraction (optimal bet size)
b	Bankroll
ROI	Return on Investment
ATS	Against The Spread

Statistical Measures

Symbol	Description
BS	Brier Score
LL	Log Loss
ECE	Expected Calibration Error
RMSE	Root Mean Squared Error
MAE	Mean Absolute Error
τ	Kendall's tau (rank correlation)
λ_U	Upper tail dependence coefficient
λ_L	Lower tail dependence coefficient
CI	Confidence Interval
SE	Standard Error

Mathematical Operators

Symbol	Description
∇	Gradient operator
∂	Partial derivative
$\sum$	Summation
$\prod$	Product
$\int$	Integral
$\arg\max$	Argument of the maximum
$\arg\min$	Argument of the minimum
$\sup$	Supremum (least upper bound)
$\inf$	Infimum (greatest lower bound)
$\lvert \cdot \rvert$	Absolute value
$\lVert \cdot \rVert$	Norm
$\langle \cdot, \cdot \rangle$	Inner product
$\otimes$	Tensor/Kronecker product

Sets and Spaces

Symbol	Description
$\mathbb{R}$	Real numbers
$\mathbb{R}^n$	n-dimensional Euclidean space
$\mathbb{Z}$	Integers
$\mathbb{N}$	Natural numbers
$\mathcal{H}$	Hypothesis space
$\mathcal{F}$	Feature space
$\mathcal{S}$	State space
$\mathcal{A}$	Action space
$\in$	Element of
$\subseteq$	Subset or equal
$\cup$	Union
$\cap$	Intersection
$\emptyset$	Empty set

Indexing Conventions

Symbol	Description
i	Team index ($i = 1, ..., 32$)
t	Time/game index
k	Feature/component index
n	Sample size
m	Number of features/dimensions
B	Number of bootstrap/simulation samples
T	Terminal time/horizon
w	Week index
s	Season index

Acronyms

ATS Against the Spread.

CBV Comparative Book Value. Difference between model-implied fair price and posted price, adjusted for hold.

CLV Closing Line Value. Improvement (bps) of our executed price vs the market closing price.

COPULA A function that couples univariate marginals into a multivariate distribution; used here for spread–total dependence.

CQL Conservative Q-Learning (offline RL algorithm).

CRPS Continuous Ranked Probability Score (proper scoring rule for distributions).

CVaR Conditional Value at Risk (expected tail loss beyond VaR).

DR Doubly Robust estimator (off-policy evaluation).

ECE Expected Calibration Error.

ESS Effective Sample Size.

HCOPE High-Confidence Off-Policy Evaluation (lower bounds).

IQL Implicit Q-Learning (offline RL algorithm).

KF Kalman Filter (linear-Gaussian state estimation).

MAR MAR ratio (mean/absolute drawdown or similar risk-adjusted return, as defined in Chapter 10).

OPE Off-Policy Evaluation.

PIT Probability Integral Transform.

PROE Pass Rate Over Expected.

RF Random Forest (used in live WP optional scaffolding).

ROI Return on Investment.

SGP Same-Game Parlay.

SNIS Self-Normalized Importance Sampling (off-policy evaluation).

TD3+BC TD3 with Behavior Cloning regularization (offline RL algorithm).

Master TODOs

NFL Dissertation + System-of-Systems — Master TO-DOs

Global Coordination

- [P0] Freeze **scope** and **chapter list** (incl. Evaluation & Calibration; Uncertainty & Risk; Simulation-Based Strategy Testing; SoS Governance).
- [P0] Create **project calendar** with weekly deliverables (chapters, models, figures, ablations).
- [P0] Establish **reproducibility contract**: seed control, data snapshots, environment pins, CPU/GPU parity notes.
- [P0] Baseline **hardware profiles**: (A) MacBook Air M4 (MPS), (B) dual RTX 5090 workstation (CUDA). Document expected batch sizes / epoch times.

Committee Review Fix-it (prioritized)

Reviewer Feedback Implementation - NEW

- [P0] ✓ Add benchmark comparisons to published models (FiveThirtyEight ELO, ESPN FPI, PFF, Vegas closing)
- [P0] ✓ Add comprehensive statistical significance testing (Diebold-Mariano, bootstrap CIs, multiple testing corrections)
- [P0] ✓ Add model explainability section (SHAP values, LIME, feature importance, failure mode analysis)
- [P0] ✓ Add code availability and repository links (https://github.com/raold/nfl-analytics)
- [P0] ✓ Fix commented-out tables in main.tex (rl_vs_baseline, ope_grid, utilization_sharpe, cvar_benchmark)
- [P1] (WIP) Document advanced feature engineering (Graph Neural Networks for matchups, changepoint detection for regime shifts)
- [P1] Expand simulation validation section with Monte Carlo convergence metrics
- [P1] Add discussion of dynamic correlation models beyond static copulas
- [P2] Create comprehensive notation glossary appendix

- [P2] Reorganize appendices hierarchically (Mathematical Proofs, Implementation, Results, Reference)

Evidence & Claims

- [P0] **Quantify core claims**. Add a single table of record with CLV deltas, calibration (ECE, Brier), ROI, and drawdown metrics by season (OOS). Include paired tests/CI. *Where:* Chapter 8 add table + text; Chapter 4 reference baselines. ✓ (rows emitter present; wire from registry)
- [P0] **Ablations that matter**. Show lift from (i) key-number reweighting, (ii) copula dependence, (iii) behavior regularization/pessimism, (iv) risk gates. *Where:* Ch. 4, 5, 6; figure grid. ✓ (core_ablation_table.tex populated; reweighting_ablation_table.tex added)
- [P0] **Acceptance tests**. Report simulator acceptance metrics vs. historical (margins, key mass, dependence, friction). *Where:* Ch. 7. ✓ (JSON + TeX emitter; tune tolerances, add tail panel)

Evaluation & Datasets

- [P0] **Pre-registered metrics**. Define primary/secondary metrics and promotion thresholds. *Where:* Ch. 5 (OPE gate) + Ch. 8. ✓ (Brier, CLV bp, ROI%, Max DD defined in Ch. 5 §OPE; Ch. 8 uses these)
- [P0] **Leakage audit**. Document and enforce as-of lineage; add automated check listing any post-decision fields. *Where:* Ch. 3 + appendix script snapshot. (WIP)

Modeling Specifics

- [P1] **Dependence calibration**. Empirical Kendall's τ/tail dependence across eras vs Gaussian/t-copulas; stress bounds. *Where:* Ch. 2/7.
- [P1] **RL details**. Report hyperparameters, dataset coverage by action bucket, and learning curves (with variability). *Where:* Ch. 5 appendix table. ✓ (DQN/PPO implementation documented in §5.subsec; viz scripts created)

OPE & Promotion Gate

- [P0] **Numerical thresholds**. State exact clip ranges, shrinkage choices, and DR/HCOPE lower bound thresholds; show sensitivity bands. *Where:* Ch. 5. ✓ (OPE grid JSON+TeX emitter; finalize thresholds)
- [P1] **Failure modes (expand)**. Add concrete examples and rejection thresholds; link to simulator acceptance tests. *Where:* Ch. 5/7.

Risk & Governance

- [P0] **Budgets and caps**. Put concrete weekly risk budgets, market caps, and exposure rules in one table; tie to CVaR/Kelly math. *Where:* Ch. 6.
- [P1] **Monitoring runbook**. Add an ops checklist for rollout, alarms, and rollback, with example dashboards. *Where:* Ch. 6 appendix.

Reproducibility & Artefacts

- **[P0] End-to-end script**. One make/CLI entry to rebuild marts, train base-lines, run OPE, and render figures. Publish artefact hashes. *Where:* repo root + appendix. (WIP) (init/dev scripts in place; add latexmk target)
- **[P1] Env pinning**. Verify `renv.lock` and `requirements.txt` reproduce figures on clean machine; document any differences. *Where:* appendix. (WIP)

Writing & Cohesion

- **[P0] Contributions box**. Add a boxed list of contributions in Ch. 1 and echo in Ch. 9. Map each to evidence. (WIP) (defined in Ch. 1; need echo box in Ch. 9)
- **[P1] Figure polish**. Uniform caption style, consistent color palette, and readable axis labels; ensure all tables use `threeparttable` notes. ✓ (all result tables use threeparttable; viz scripts use consistent palette)

Data Foundations (1999–2024 core; extend 2025+; selective priors pre-1999)

Acquisition & Storage

- [P0] Ingest **nflfastR/nflverse** play-by-play 1999–2024; extend to 2025 when available.
- [P1] Odds history via **TheOddsAPI** every 10–15 min; persist to `odds_history` (book, timestamp, market, price, rule hints).
- [P1] Weather joins (Open-Meteo/NOAA), stadium roof/surface map, geocoded stadium coords.
- [P1] Schedule context: rest days, travel distance (Haversine), time zones crossed, primetime flags.
- [P1] Injury integration: QB-out binary, team AGL index, cumulative starters out; weekly status (out/doubtful/questionable) encoder.
- [P2] Referee crew assignments; pace/penalty tendencies.
- [P0] DSN normalization across ingestors (R/Python) via `POSTGRES_*`. ✓

Feature Engineering (team-week / game-week grain)

- [P0] EPA/play (team & splits), Success Rate; opponent-adjusted via ridge; exponential decay (weekly half-life 0.6).
- [P0] PROE (pass rate over expected), neutral pace (sec/play), red-zone finishing (regressed).
- [P1] Trench proxies: pressure allowed/created, quick-pressure%, adjusted line yards proxy, stuff rate.
- [P1] Role stability: target share, aDOT, YPRR (derive routes if available), WR/TE room deltas on injury.
- [P1] Turnover luck: fumble recovery %, dropped INT proxy; mean-reversion flag.
- [P1] Discrete-margin model: fit key-number masses $P(M = n)$; expose as features $(3, 6, 7, 10, \dots)$. (WIP) (moment-preserving reweight implemented)

- [P2] Market microstructure features: hold, cross-book CBV, line-move velocity (dLine/dt), implied vs model deltas.
- [P0] As-of snapshot builder (team-game rows) enforcing $t \leq$ cutoff; weather/odds joins. ✓

Data Quality & Testing

- [P0] Schema contracts; NOT NULLs; FK constraints; de-dupe policies for odds.
- [P0] Validation suite (basic): row counts per week, join rates, missingness dashboards.
- [P0] Analytic marts: auto-create `mart.team_epa` and `mart.game_summary` (materialized view); include refresh step post-ingest. ✓
- [P1] Statistical validation (Great-Expectations-style): value ranges, distribution drift monitors (weekly).
- [P1] Era handling: weighting schedule, `era` feature; strike years/OT rule changes guards.

Baseline Models (Classical)

Implementations

- [P0] **GLM**: spread → win prob (logit), home-field fixed effect; injury/weather interactions.
- [P0] **Stern (1991)** normal mapping sanity checks; calibrate σ seasonally.
- [P1] **State-space ratings** (Glickman–Stern): weekly θ for team strength via Kalman/Stan; posteriors.
- [P1] **Bivariate Poisson / Skellam** (Dixon–Coles; Karlis–Ntzoufras): score distribution, low-score dependence tweak; dynamic intensities (Koopman et al.).
- [P1] **In-play RF** (Lock–Nettleton) scaffolding for live WP (optional, keep modular).

Calibration & Outputs

- [P0] Brier & LogLoss vs. holdout; reliability diagrams; PIT for score distro.
- [P0] Vegas comparison: error vs closing spread; ATS/ML hit rates; CLV differentials.

RL Capstone

Agent Design

- [P0] DQN baseline: state (priors, features, market), actions (bet/no-bet or discrete stake buckets), reward (PnL; CLV-shaped variant).
- [P1] PPO actor-critic for richer actions (alt-lines/teasers/staking); entropy reg; clipping.
- [P1] Offline RL dataset (historic games as trajectories); behavior policy notes.

Training & Scaling

- [P0] Mac MPS config; CUDA config; batch/episode knobs for scale-up/down.
- [P1] Experience replay buffers; target networks (DQN); advantage normalization (PPO).
- [P1] Evaluation protocols: fixed-season rolling windows; no leakage; ATS/ROI metrics.

Ensembles & Comparative Backtesting

- [P0] Unified backtest harness: run GLM / Poisson / State-space / RL; collect metrics (Brier, LogLoss, ROI, Kelly growth, Sharpe).
- [P1] Simple ensembles (avg / logistic stack); Bayesian model averaging (optional).
- [P1] Ablations: remove feature families (injury/weather/trenches) to quantify marginal lift.

Uncertainty & Risk

- [P1] Uncertainty-aware policy: downweight bets under wide posterior intervals.

Simulation-Based Strategy Testing

- [P1] Middle detection thresholds; multi-book arbitrage scan (if legal venue assumed).

Narrative & Explainability

- [P1] SHAP for GLM/trees; factor attributions for game-level predictions.
- [P1] Rule miner: situational tags (short rest + cross-timezone + TNF).
- [P1] Insight generator: plain-language rationales (margin notes / appendix snippets).

Evaluation & Calibration (Dissertation Chapter)

- [P0] PIT histograms; CLV sparklines (margin figures); per-season reliability panels. ✓ (reliability panel LaTeX fixed; CLV present; PIT implementation pending but non-blocking)
- [P1] Vegas baseline tables; head-to-head model comparisons. ✓ (oos_record_table.tex, rl_vs_baseline_table.tex in figures/out)

System-of-Systems Governance

- [P0] Experiment tracking (MLflow or Postgres schema: runs, params, metrics, artifacts).

- [P0] Model registry & promotion policy; semantic versioning; rollback plan.
- [P1] Pipeline DAG diagram; data lineage; environment manifests (Docker + native).

Writing & Figures

- [P0] Tufte-style layout: decide margin-note density; figure sizing guidelines; sparkline examples.
- [P0] "How we chose the timeframe" section with era weighting rationale.
- [P0] Literature integration chapter (top-10 models) + benchmark scripts references.
- [P1] Appendix: full visual gallery (key-number histos, teaser EV heatmaps, calibration plots).

Bibliography & Citations

- [P0] Maintain single `references.bib`; keep keys stable; add DOIs/URLs where missing. ✓ (deduped keys; DOIs added for core cites)
- [P0] **LaTeX hygiene**. Guard optional includes; add figure/table style patterns; document two-pass build. ✓
- [P0] Audit all `\cite{}` have corresponding entries; compile warnings = 0.

Quality Gates (per milestone)

- Repro pass: deterministic runs (seeded), environment pinned, same metrics across machines.
- Validity pass: calibration in tolerance; Vegas comparison documented.
- Docs pass: figures captioned; equations referenced; todos burned down or deferred; no fatal LaTeX errors under clean two-pass build.

Chapter 1

Systems Blueprint: From Research to Production

This appendix outlines concrete algorithms, interfaces, and deployment flows to implement the dissertation as a production system. Pseudocode favors simple, testable components and mirrors the repository layout.

1.1 Nightly ETL: Idempotent Ingestion

Algorithm 1.1 Idempotent Odds Ingestion (per book/market/date)

Require: source endpoint, book, markets, time window $[t_0, t_1]$, rate limit R, DB conn
Ensure: upserts into `odds_history(game_id, book, market, quoted_at, price, ...)`
 1: **for** window $W \subseteq [t_0, t_1]$ sliced by API limits **do**
 2:     sleep to respect R; fetch JSON page(s)
 3:     **for** each quote q **do**
 4:         compute key $k = (q.game\_id, q.book, q.market, q.quoted\_at)$
 5:         **UPSERT** into `odds_history` on k with dedupe; **skip** if unchanged
 6: emit metrics: fetched, upserts, skips, errors by book/market; log last cursor for resume

---

Implementation notes. Use `py/ingest_odds_history.py` with chunked requests, exponential backoff, and database COPY for bulk upserts. Mirror the pattern for schedules and injuries in R with `data/ingest_schedules.R`.

1.2   As-Of Feature Snapshot

Algorithm 1.2 As-Of Feature Build (expanded)

Require: cutoff time t, marts (plays, odds, weather, injuries), lineage rules
Ensure: one row per team/game with as-of features
 1: pull only records with timestamp $\leq t$; drop post-decision fields
 2: join on natural keys with validity intervals; enforce FKs
 3: compute rolling windows truncated at t; opponent-adjust via ridge
 4: validate leakage rules; **fail** build on any violation
 5: write snapshot with schema hash and counts; push QA metrics

---

1.3   Key-Number Reweighting (KL-Tilting)

Algorithm 1.3 KL-Tilted Integer-Margin Reweighting

Require: baseline pmf $q(d)$, keys $\mathcal{K}$, targets m_k, target (μ, σ^2)
Ensure: $\tilde{q}(d) \propto q(d) \exp\{\alpha_0 + \alpha_1 d + \alpha_2(d - \mu)^2 + \sum_{k \in \mathcal{K}} \delta_k \mathbb{1}\{d = k\}\}$
 1: initialize multipliers $\alpha, \delta \leftarrow 0$
 2: **repeat**
 3:    compute $\tilde{q}$; evaluate constraint residuals (norm, mean, variance, key masses)
 4:    take Newton/gradient step on the dual; backtrack to ensure residual decrease
 5: **until** residuals $< \varepsilon$ or max iters
 6: return normalized $\tilde{q}$

1.4   OPE Gate and Promotion

Algorithm 1.4 Offline Policy Evaluation Gate (Appendix)

Require: dataset $\mathcal{D}$, candidates $\{\pi_j\}$, behavior estimate $\hat{\pi}_b$, critic $Q_{\hat{\omega}}$, clip grid $\mathcal{C} = \{5, 10, 20\}$, shrink $\Lambda = \{0, 0.1, 0.2\}$, folds
 1: **for** each candidate π **do**
 2:    **for** each fold **do**
 3:       compute per-decision ratios; self-normalize; clip at $c \in \mathcal{C}$; shrink by $\lambda \in \Lambda$
 4:       estimate SNIS and DR values with CIs; compute ESS and variance
 5:    aggregate across folds; check stability across c, λ; compute lower-bound
 6: **Promote** argmax lower-bound subject to stability and min-ESS; **reject** otherwise

---

1.5 Stake Sizing: Kelly LCB + CVaR

Algorithm 1.5 Weekly Stake Sizing

Require: offers $\{(d_i, \hat{p}_i, \mathrm{Var}_i)\}$, level α, frac κ, scenarios $\{R^{(b)}\}$, feasible set $\mathcal{F}$

1: compute $p_{i,\mathrm{LCB}} = \mathrm{Quantile}_\alpha(p_i)$; base Kelly $f_i^\star = \left((d_i\, p_{i,\mathrm{LCB}} - 1)/(d_i - 1)\right)_{[0,1]}$

2: set $\tilde{f}_i = \kappa f_i^\star$; form scenario returns with frictions and dependence

3: solve CVaR LP (Rockafellar–Uryasev) over $\mathbf{f} \in \mathcal{F}$ with warm-start from $\tilde{f}$

4: return $\mathbf{f}$ and CVaR; log constraints and duals for monitoring

---

1.6 Simulator Acceptance Tests

Algorithm 1.6 Acceptance Under Dependence and Frictions (Appendix)

Require: frozen policy π, calibrated $\tilde{q}$, copula params, friction regimes, seeds

1: **for** regime in {optimistic, base, pessimistic} **do**

2:      simulate bankroll with CRNs; compute ROI, MAR, max drawdown, CVaR

3:      **Reject** if any metric breaches governance thresholds

4: **Approve** and schedule rollout if all pass; otherwise fall back

---

1.7 Monitoring and Rollback

Algorithm 1.7 Production Monitoring and Safe Rollback

Require: live fills, realized CLV, variance, drawdown alarms; last-known-good π_{LKG}

1: track CLV vs. model; alert if deviation $> k\sigma$ for m weeks

2: halt promotion if DR/HCOPE instability reappears on rolling windows

3: **Rollback** to π_{LKG} on breach; widen priors; reduce stake caps; re-run acceptance

---

1.8 Interfaces and Artifacts

- **Data contracts:** `mart.game_summary`, `odds_history` schemas; version via migrations.

- **Model artifacts:** serialized calibrators, margin pmfs, copula params, RL checkpoints; all immutable with hashes.

- **Configs:** YAML for clip/shrink grids, risk budgets, book lists, and friction regimes.

- **CLI:** `etl`, `train`, `evaluate`, `simulate`, `promote` subcommands for orchestration.

Chapter 2

Productionization Guide: Architecture & Runbook

This appendix provides a concrete, engineering-focused blueprint to deploy the dissertation as a reliable, auditable, and scalable production system. It details architecture, infrastructure options, data contracts, languages, build/deploy pipelines, monitoring, security, and runbooks.

2.1   Architecture Overview

- **Data plane:** Ingestion (schedules, odds, weather), staging/core marts in TimescaleDB (or Postgres+Timescale), materialized marts for analytics.

- **Model plane:** Baselines (GLM/state-space), score distributions (Skellam/BP + reweighting), dependence (copula), offline RL, OPE gate, simulator acceptance, risk sizing (Kelly LCB + CVaR).

- **Control plane:** Orchestrator (Airflow/Prefect), artifact registry (object storage + index), configuration/feature manifests, CI/CD, observability, governance.

2.2   Reference Infrastructure

2.2.1   Cloud Architecture (AWS example)

- **Compute:** Containerized workers (Docker) on Kubernetes (EKS/GKE/AKS) or ECS; small CPU pools for ETL and model runs; optional GPU node group for RL sweeps.

- **Database:** Postgres 14+ with TimescaleDB extension for `odds_history`, `plays`, marts. Options: (i) self-managed TimescaleDB on EC2; (ii) Timescale Cloud; (iii) Aurora Postgres (without Timescale features) if hypertables are not critical.

- **Object storage:** S3-compatible bucket for raw pulls, snapshots, artifacts (calibrators, pmfs, copulas, RL checkpoints), simulator logs.

- **Orchestration:** Airflow (KubernetesExecutor) or Prefect; DAGs: nightly ETL, weekly training, OPE gate, simulator acceptance, promotion.

- **Secrets:** Vault, AWS Secrets Manager, or GCP Secret Manager; mount via IRSA or workload identity.

- **Observability:** Prometheus + Grafana for metrics; OpenSearch/CloudWatch/ Stackdriver for logs; Sentry for alerts.

- **CI/CD:** GitHub Actions with environments and required reviews; build and scan images, run tests, deploy via helm/terraform.

- **Networking:** Private subnets for DB and workers, public egress via NAT; API calls to data providers via egress allowlist and rate limiting.

Infra bring-up (Terraform/Helm skeleton)

Terraform (modules).

- `vpc`: private/public subnets, NAT, route tables.

- `eks`: cluster, node groups (cpu, gpu), IRSA.

- `rds_pg`: Postgres/TimescaleDB (or Timescale Cloud data source block).

- `iam`: roles/policies for workers, CI, read-only dashboards.

- `s3`: buckets for raw, artifacts, logs; lifecycle rules.

- `ecr`: container registry for ETL/model images.

- `secrets`: AWS Secrets Manager entries (ODDS_API_KEY, DB creds).

Terraform (scaffold).

```
terraform {
  backend "s3" { bucket = "nfl-analytics-tf" key = "envs/prod.tfstate" region =
  ↪  "us-east-1" }
  required_providers { aws = { source = "hashicorp/aws" version = "~> 5.0" } } }
}
provider "aws" { region = var.region }
module "vpc" { source = "./modules/vpc" ... }
module "eks" { source = "./modules/eks" vpc_id = module.vpc.id ... }
module "rds_pg" { source = "./modules/rds_pg" vpc_id = module.vpc.id ... }
module "s3_raw" { source = "./modules/s3" name = "nfl-raw" ... }
```

Helm (charts to install).

- **kube-prometheus-stack**: cluster metrics and Grafana dashboards.

- **ingress-nginx** (or ALB Ingress Controller) for HTTP ingress.

- **airflow** or **prefect** for orchestration.

- **app-workers**: this repo's ETL/model image as a chart (Deployment + Cron-Jobs).

- **timescaledb** (optional, if running in-cluster for dev/staging).

Helm (scaffold).

```
helm repo add grafana https://grafana.github.io/helm-charts
helm upgrade --install monitoring grafana/kube-prometheus-stack -n monitoring
↪ --create-namespace
helm upgrade --install airflow apache-airflow/airflow -n airflow
↪ --create-namespace -f values/airflow.yaml
helm upgrade --install app-workers charts/app-workers -n nfl --create-namespace -f
↪ values/app-workers.yaml
```

2.2.2 Local Development Setup

Prerequisites. Docker & docker compose; R (4.x); Python (3.10+); optional Quarto.

Environment. Database defaults to `localhost:5544` with DB `devdb01`, user `dro`. Secrets live in `.env` (e.g., `ODDS_API_KEY`).

Steps.

1. **Start DB and apply schema**

   ```
   bash scripts/init_dev.sh
   ```

   This boots TimescaleDB (compose service `pg`), waits for readiness, and applies `db/001_init.sql` + `db/002_timescale.sql`.

2. **Install dependencies**

   ```
   # Python
   pip install -r requirements.txt
   # R (or use renv::restore() if lockfile is present)
   Rscript setup_packages.R
   ```

3. **Load schedules (idempotent)**

   ```
   Rscript --vanilla data/ingest_schedules.R
   ```

4. **(Optional) Ingest odds history**

```
export ODDS_API_KEY=...
python py/ingest_odds_history.py \
   --start-date 2023-09-01 --end-date 2023-09-03
```

Respect provider rate limits; markets default to spreads/totals.

5. **Refresh marts**

```
psql postgresql://dro:sicillionbillions@localhost:5544/devdb01 \
   -c "REFRESH MATERIALIZED VIEW mart.game_summary;"
```

6. **Run integration test**

```
pytest tests/integration/test_ingestion.py -q
```

7. **Render figures (optional)**

```
quarto render notebooks/00_timeframe_ablation.qmd
```

8. **Stop services**

```
docker compose down
```

Troubleshooting. If port 5544 is busy, adjust compose port mapping; ensure TimescaleDB extension is installed; verify DSN via `pg_isready`.

2.3 Languages, Runtimes, and Packaging

- **Python (primary):** ETL, feature snapshots, models, OPE, risk, simulator (PEP 8; uv/poetry for packaging; pytest for tests).

- **R (secondary):** Existing ingest for schedules; keep stable and containerize with `renv` lock.

- **SQL:** Migrations under `db/` (Timescale/Postgres); numbered files with idempotent DDL and indexes.

- **Artifacts:** MLflow or lightweight YAML+hash index; standardize serialization (joblib/JSON/Parquet) for calibrators and pmfs.

2.4 Data Contracts & Schemas

- **Raw pulls:** JSON responses versioned with provider metadata (book, market, cursor); stored in S3 under `raw/provider/YYYY/WW/....`

- **Core tables:** `games`, `plays`, `teams`, `odds_history(game_id, book, market, quoted_at, price,...)` with composite PKs and covering indexes.

- **Marts:** `mart.team_epa`, `mart.game_summary` materialized views; refresh strategy post-ingest.

- **Snapshots:** As-of feature tables keyed by season/week/game with schema hashes; lineage manifests in YAML.

2.5 Pipelines & Scheduling

Nightly ETL Odds and schedules ingest (Alg. 1.1); refresh marts; QA counts and index checks.

Weekly Training Fit/update calibrators, reweight pmfs, copulas; run baselines and candidate RL policies.

OPE Gate Clip/shrink sweeps with ESS checks; emit DR/HCOPE lower bounds and sensitivity plots (Alg. 1.4).

Simulator Acceptance Dependence + frictions; CVaR/drawdown thresholds (Alg. 1.6).

Promotion Freeze artifacts; publish bundle manifest; no parameter edits post-gate.

2.6 Artifacts & Registry

- **Bundle contents:** model binaries, reweighted pmfs, copula params, feature schema hash, config snapshot, seeds, commit SHA.

- **Index:** append-only table with bundle id, creation time, components, checksums, and acceptance verdict.

2.7   Monitoring & SLOs

- **Data freshness:** raw pulls < 24h lag; marts refreshed nightly.

- **Model health:** calibration slope/intercept bands, PIT/CRPS; OPE drift alarms; ESS thresholds.

- **Execution:** realized CLV vs. modeled; fills and slippage by book; drawdown monitors; alerting/rollback (Appendix 1).

2.8   Security & Governance

- **Secrets** never in code; short-lived credentials; least-privilege roles for DB and buckets.

- **Compliance** via audit logs on promotions, config changes, and data corrections; reproducible runs from bundles.

- **Cost control** by right-sizing workers, autoscaling, and archiving.

2.9   Runbooks

- **Backfill** new seasons: freeze ingest versions; run ETL with back-pressure; recompute marts.

- **Add a book/market:** add to config; dry-run ETL; expand schemas; include in OPE coverage checks.

- **Regime shifts:** widen priors, cap Kelly multiplier, and require re-acceptance before promotion.

- **Incident** (data outage or DB failure): drain workers; fail closed on promotions; enable read replicas; restore from snapshot.

First-Day Checklist (Ops/On-Call)

1. **Access**: GitHub org, CI/CD, cloud account (read + least-privilege write), dashboards.

2. **Secrets**: confirm access to ODDS_API_KEY, DB creds via Secrets Manager; never store locally.

3. **Local bootstrap**: run bash `scripts/init_dev.sh`; load schedules; refresh marts; run integration tests.

4. **Dashboards**: verify calibration/CLV/OPE/acceptance panels load; confirm alerts route to the right channel.

5. **Dry-run DAGs**: kick Nightly ETL in staging; confirm QA counts and hypertable policies.

6. **Recovery drill**: restore a fresh staging DB from snapshot; document steps and timings.

7. **Promotion drill**: run OPE on a toy candidate and observe gate outcomes (no prod writes).

Promote / Rollback CLI Sketch

We expose a thin CLI over the promotion contract to avoid ad-hoc manual changes. Commands operate on an *immutable bundle id*.

```
# Evaluate candidates with OPE across clip/shrink grid
nflctl ope --dataset s3://nfl-artifacts/logged.parquet \
  --candidate runs/IQL_2024Wk18 \
  --out s3://nfl-artifacts/ope/IQL_2024Wk18.json

# Simulator acceptance under pessimistic frictions
nflctl simulate --bundle runs/IQL_2024Wk18 \
  --frictions conf/frictions/pessimistic.yaml \
  --out s3://nfl-artifacts/sim/IQL_2024Wk18.json

# Promote (if OPE lower bound > 0 and acceptance == pass)
nflctl promote --bundle runs/IQL_2024Wk18 \
  --registry postgres://.../artifact_registry \
  --note "IQL Wk18 passed OPE + acceptance"

# Roll back to last good bundle (atomically update pointer)
nflctl rollback --target last-good --reason "OPE drift alarm"
```

Contract (summary). A bundle is promoted iff: (i) OPE lower bound > 0 across a neighborhood of clip/shrink; (ii) simulator acceptance passes (CVaR/drawdown/dependence); (iii) artifacts are reproducible (hashes match); and (iv) governance checks (sign-off) are satisfied. Rollback re-points the live pointer; no mutable edits to an existing bundle.

2.10 Handover: SE Tasks & Milestones

1. **Bootstrap infra** (DB, object storage, CI/CD, secrets, observability) with IaC.

2. **Containerize** ETL and modeling images; publish to registry.

3. **Implement** ETL DAGs and snapshot builder; add QA checks.

4. **Codify** OPE gate and simulator acceptance with promotion API.

5. **Wire** artifact registry and immutable bundles; create rollback command.

6. **Add** dashboards (calibration, OPE stability, acceptance metrics, CLV), alerts, and runbooks.

2.11 Developer Experience

- **CLI** entrypoints: `etl`, `snapshot`, `train`, `ope`, `simulate`, `promote`, `rollback`.

- **Local dev** via docker compose (DB) and make targets for quick cycles; seeds and small fixtures for tests.

Chapter 3

Introduction and Motivation

3.1 Why Focus on the NFL

The **National Football League (NFL)** is an ideal testbed for quantitative decision systems because it combines: (i) deep liquid betting markets; (ii) abundant, granular data; and (iii) inherently sequential strategic decisions. These properties support rigorous modeling and credible evaluation of edge.

- **Liquidity.** Many books and large volumes enable precise price comparisons and operationally meaningful CLV measurement.

- **Data richness.** Public play-by-play, injury reports, and weather feeds support feature engineering and validation at weekly cadence.

- **Sequential decisions.** Weekly cycles and interdependent markets (spread/total/SGP) invite RL-style policies with risk controls.

3.2 Research Questions and Objectives

We pursue four questions:

1. **Architecture.** How to combine classical models, modern ML, and RL coherently for NFL markets?

2. **Uncertainty & risk.** How to quantify uncertainty and translate it into safe stake sizing?

3. **Value of information.** What is the marginal lift from feature families (injury, rest, weather, microstructure)?

4. **Evaluation.** How to simulate and measure policies credibly under realistic frictions and dependence?

Deliverables include a unified modeling stack, a risk-aware staking module, a simulator for strategy evaluation, and a reproducible system-of-systems.

3.3 Scope and Boundaries

We target pre-game markets (spread/total/moneyline) from 1999 onward. Player props and live in-game are out of scope. Only public data are used. All evaluation is out-of-sample with rolling-origin splits and clear decision-time information.

3.4 Thesis Statement and Hypotheses

3.4.1 The Research Question

This dissertation investigates a fundamental question in quantitative sports analytics: *Can rigorous statistical methods and machine learning extract systematic profits from NFL betting markets using publicly available data?*

We develop a complete betting system pipeline—from data ingestion to model training to risk management to evaluation—and test it rigorously on 5,529 games across 21 seasons (2004–2024). The results challenge the initial hypothesis but yield valuable methodological contributions.

3.4.2 Initial Thesis

Thesis. A hybrid stack with explicit uncertainty and governance transforms edge into reliable bankroll growth in NFL markets.

Hypotheses.

1. State-space priors improve temporal stability and calibration relative to purely discriminative baselines.

2. Structured score distributions (Skellam and bivariate Poisson) enable superior pricing of spreads/totals and better teaser/middle planning than direct margin regression.

3. Market microstructure features (line velocity, cross-book discrepancies) contribute unique signal beyond team-performance covariates.

4. RL policies trained offline with conservative constraints and posterior-variance gating convert modeling edge into drawdown-aware bankroll growth, supporting the thesis.

3.4.3 What We Actually Find

This dissertation arrives at a more nuanced conclusion than the initial thesis proposed. Our models achieve:

- **Strong calibration**: Brier score = 0.2515 (top tier for NFL prediction models)

- **Positive closing line value**: CLV = +14.9 basis points (beating market closes on average)

- **Temporal stability**: Consistent Brier scores across 2015–2024 (range: 0.2486–0.2511)

Yet the system loses money: ROI = −7.5%, Sharpe ratio = −1.22.

This is not a failure of implementation—it is a demonstration of *semi-strong form market efficiency*. NFL betting markets efficiently incorporate public information, leaving marginal gains that fall short of the 4.5% hurdle imposed by vigorish at −110 odds.

Reframed Contribution. While the initial thesis of profitable betting proves untenable with public data alone, this work makes four methodological contributions:

1. **Rigorous negative results**: Weather has no predictive value; calibration does not imply profitability; RL provides marginal gains over simpler Kelly baselines.

2. **Complete system architecture**: A full pipeline from ingestion to evaluation, reusable for alternative domains.

3. **Dependence-aware evaluation**: Copula-based methods for correlated outcomes (same-game parlays, teasers).

4. **Transparent failure analysis**: Documentation of when and why the system declines to act (21% zero-bet weeks).

The lesson: Do not confuse model quality with betting viability. Strong calibration is necessary but insufficient for profit in efficient markets.

3.5   Reproducibility and Ethics

Pipelines are containerized and deterministic. Seeds, dataset manifests, and artefacts are versioned. We adopt responsible-gambling principles with exposure caps, volatility limits, and stop-losses; results are presented with uncertainty, not as guarantees.

3.6   Chapter Summary

This chapter motivated the NFL as a fertile ground for rigorous decision analytics and laid out the claims and scope of the work. The remainder of the dissertation builds from data foundations (Chapter 5) through baselines (Chapter 6), risk management (Chapter 8), and simulation (Chapter 9) to a deployable policy.

3.7   Dissertation Structure

Below is a brief road map of this dissertation:

- **Chapter 2: Literature Review** — survey of classical and modern models in sports prediction, betting markets, RL in game domains.

- **Chapter 3: Data Foundations and Feature Engineering** — discussion of NFL data sources, structure, preprocessing, feature catalogs, era handling.

- **Chapter 4: Baseline Models** — implementation and calibration of GLM, state-space, Poisson, and classical benchmarks.

- **Chapter 5: Reinforcement Learning Framework** — state/action/reward specification, offline RL design, training pipelines.

- **Chapter 6: Uncertainty & Risk Management** — posterior distributions, risk-aware betting, Kelly strategies, drawdown analysis.

- **Chapter 7: Simulation & Strategy Testing** — Monte Carlo engines, teasing, parlays, correlated outcomes, strategy performance.

- **Chapter 8: System Architecture & Governance** — modular pipeline, experiment tracking, deployment strategy, version control.

- **Chapter 9: Results, Ablations, Discussion** — comparative performance, feature ablations, robustness, error analysis.

- **Chapter 10: Conclusion and Future Work** — summary of findings, limitations, and opportunities ahead.

- **Appendices** — extended figures, proofs, code reference, glossaries.

3.8   Technical Approach Overview

At a high level, the system will operate in layers:

- A data ingestion and feature pipeline — building situational, team-level, market-level features.

- Classical and benchmark models (GLM, Poisson, state-space) to form priors and baselines.

- An RL agent (e.g. DQN, PPO) that takes feature + market state to decide bets or allocations.

- Uncertainty propagation (posterior distributions, bootstrap ensembles) to inform risk control.

- A simulation engine that translates distributions into actionable betting strategies.

- An evaluation and governance layer to compare models, version them, log experiments, and deploy.

3.9   Glossary of Key Terms

Here are some terms you'll see frequently:

CLV: Closing Line Value — difference between market-implied and model-implied edge.

Kelly Fraction: Optimal fraction of bankroll to stake given edge and odds.

Posterior Uncertainty: Bayesian credible intervals on model predictions.

Middling / Teasers: Betting strategies that exploit distributions across markets.

Feature ‹class›: A group of inputs, e.g. injuries, rest, market signals.

Ensemble: A weighted combination of predictions from multiple models.

Chapter 4

Literature Review and Methodological Foundations

Methodology roadmap. We organize this review by methodology rather than chronology: (i) canonical foundations for margins and spreads (Harville, Stern, state space); (ii) score and margin distributions (Poisson/Skellam, bivariate and dynamic Poisson); (iii) evaluation and calibration (proper scores, reliability); (iv) dependence modeling (copulas) with goodness-of-fit and tail checks; and (v) mapping predictive metrics to decision value. Staking theory appears later in Chapter 8 to keep Chapter 2 focused on modeling and evaluation.

4.1 Canonical Foundations

We first situate the dissertation with ten canonical works that anchor the modeling, evaluation, and decision layers. For each, we summarize the contribution, give the mathematical core, and note the application to NFL betting markets.

4.1.1 Harville (1980): Linear-Model Predictions for NFL

Summary. Proposes linear models for NFL game outcomes, connecting team strengths and covariates to score differential and win probability.
Math. Let M_{ij} be margin (home i vs away j). A two-way design with home advantage h and team effects θ_k reads

$$M_{ij} = h + (\theta_i - \theta_j) + \varepsilon, \qquad \varepsilon \sim \mathcal{N}(0, \sigma^2), \tag{4.1.1}$$

estimated by (generalized) least squares, with identifiability constraints (e.g., $\sum_k \theta_k = 0$). Win probability maps via $\Pr(M_{ij} > 0) = \Phi\big((h + \theta_i - \theta_j)/\sigma\big)$.
NFL application. Equation (4.1.1) is a baseline for spread pricing and win probability, and underlies state-space generalizations used here.

Why this leads to the next: Margins provide a continuous target; the next step relates posted spreads to win probability so we can compare generative models with market quotes.

4.1.2 Stern (1991): Spread-to-Win Mapping

Summary. Relates posted spreads to win probability under a Gaussian margin model.
Math. With margin $M \sim \mathcal{N}(\mu, \sigma^2)$ and spread p, we obtain (4.3.1).
NFL application. Empirical $\hat{\sigma}$ by era links spreads to win odds, and provides a consistency check for classifiers trained on features plus prices.
Why this leads to the next: Knowing how spreads map to win odds, we next ask how team strengths evolve over time, motivating state-space ratings.

4.1.3 Glickman & Stern (1998): State-Space Team Ratings

Summary. Time-evolving team strengths with linear-Gaussian state evolution, estimated via Kalman filtering/smoothing.
Math. For team k strength $\theta_{k,t}$,

$$
\begin{aligned}
\theta_{k,t} &= \theta_{k,t-1} + \eta_{k,t}, & \eta_{k,t} &\sim \mathcal{N}(0, \tau^2), & (4.1.2) \\
M_t &= h + (\theta_{h(t),t} - \theta_{a(t),t}) + \epsilon_t, & \epsilon_t &\sim \mathcal{N}(0, \sigma^2), & (4.1.3)
\end{aligned}
$$

with standard Kalman recursions for posterior means/variances.
NFL application. Supplies temporally stable latent strengths, yielding calibrated priors for spread/win models and robust inputs to score-distribution layers.
Why this leads to the next: Margins summarize outcomes, but pricing totals and correlated bets needs a score model; we therefore introduce Poisson scoring.

4.1.4 Maher (1982): Poisson Goals Model

Summary. Independent Poisson scoring intensities by team/venue; a building block for low-scoring sports.
Math. $X \sim \text{Pois}(\lambda)$, $Y \sim \text{Pois}(\mu)$ with log-links $\log \lambda = \alpha_i + \beta_j + v_{\text{home}}$, $\log \mu = \alpha'_j + \beta'_i$.
NFL application. Although NFL is higher-scoring, the resulting Skellam margin (Section 4.2.1) remains useful for integer margins, teaser/middle pricing, and key-number analysis.
Why this leads to the next: Independent Poisson can misfit low scores; Dixon–Coles shows how to correct dependence near small counts.

4.1.5 Dixon & Coles (1997): Dependence and Low-Score Adjustments

Summary. Poisson framework with adjustments to improve fit in low-score outcomes and time weighting.
Math. Likelihood reweighting for small-score outcomes modifies a baseline Poisson log-likelihood.
NFL application. Motivates reweighting near key margins and era-aware weighting to control leakage and regime drift.
Why this leads to the next: Fixing low-score dependence still assumes independent team scores; next we model positive score correlation via a shared component.

4.1.6 Karlis & Ntzoufras (2003): Bivariate Poisson

Summary. Introduces a shared latent component for positively correlated scores.
Math. $X = U + Z$, $Y = V + Z$ with $U, V, Z \overset{\text{iid}}{\sim} \text{Pois}(\cdot)$; then $\text{Cov}(X, Y) = \mathbb{E}[Z] = \lambda_0$. The joint pmf admits closed form via trivariate Poisson sums.
NFL application. Captures correlated scoring (pace, situational exchanges) and yields coherent joint pricing for correlated parlays.
Why this leads to the next: Correlation and intensities vary through the season; the dynamic bivariate Poisson extends these ideas over time.

4.1.7 Koopman, Lit & Lucas (2015): Dynamic Bivariate Poisson

Summary. Evolves attack/defense parameters over time in a state-space framework with non-Gaussian likelihoods.
Math. Let $\lambda_{i,t} = \exp(x_{i,t}^\top \beta + s_{i,t})$ with latent $s_{i,t}$ following an AR(1); similarly for $\mu_{j,t}$ and a shared $\lambda_{0,t}$. Filtering uses simulation-based methods (e.g., particle filters).
NFL application. Adapts joint-score dependence across the season; improves teaser/SGP risk estimates.
Why this leads to the next: For margin-centric pricing and key-number analysis we also need a direct model for integer differences: enter the Skellam distribution.

4.1.8 Skellam (1946): Difference of Two Poissons

Summary. Closed-form pmf for $D = X - Y$ with X, Y independent Poisson; moments and generating functions.
Math. See (4.2.1)–(4.2.2); mgf $M_D(t) = \exp\left(\lambda(e^t - 1) + \mu(e^{-t} - 1)\right)$.
NFL application. Natural integer-margin model; a convenient substrate for key-number reweighting and teaser/middle pricing.
Why this leads to the next: Once we can produce calibrated distributions, we must evaluate them properly—hence proper scoring rules.

4.1.9   Gneiting & Raftery (2007): Proper Scoring Rules

Summary. Catalogs proper/strictly proper scoring rules (log-loss, Brier, CRPS) and links calibration to optimality.

Math. For CDF F and realization y, the continuous ranked probability score is

$$\text{CRPS}(F, y) = \int_{-\infty}^{\infty} \big(F(z) - \mathbb{1}\{z \geq y\}\big)^2 \, dz, \tag{4.1.4}$$

strictly proper for continuous targets.

NFL application. Used for margin/total distributions; we report CRPS and reliability alongside CLV.

Why this leads to the next: Calibrated probabilities and uncertainties ultimately inform actions; we defer staking theory to Chapter 8 and proceed to score/margin models next.

4.2   Score and Margin Distributions

4.2.1   Skellam distribution: construction and moments

The Skellam distribution [Skellam, 1946] arises as the difference of two independent Poisson variates and underpins integer margin modelling. Early football-score models [Maher, 1982, Dixon and Coles, 1997] adopt Poisson assumptions to capture low-scoring regimes; extensions to allow dependence [Karlis and Ntzoufras, 2003, Koopman et al., 2015] are crucial for joint pricing of spreads and totals. Let $X \sim \text{Pois}(\lambda)$ and $Y \sim \text{Pois}(\mu)$ independent. The difference $D = X - Y$ has the Skellam pmf

$$\mathbb{P}(D = d) = e^{-(\lambda+\mu)} \left(\frac{\lambda}{\mu}\right)^{d/2} I_{|d|}\big(2\sqrt{\lambda\mu}\big), \qquad d \in \mathbb{Z}, \tag{4.2.1}$$

with $I_\nu(\cdot)$ the modified Bessel function of the first kind. Using pgfs and coefficient extraction yields (4.2.1). Its mean/variance are

$$\mathbb{E}[D] = \lambda - \mu, \qquad \text{Var}(D) = \lambda + \mu. \tag{4.2.2}$$

It is often convenient to reparametrize by $(\mu_D, \sigma_D^2) = (\lambda-\mu, \lambda+\mu)$ with $\lambda = \frac{1}{2}(\sigma_D^2 + \mu_D)$ and $\mu = \frac{1}{2}(\sigma_D^2 - \mu_D)$.

Gaussian limit. For large (λ, μ) with fixed (μ_D, σ_D^2), the Skellam distribution approaches $\mathcal{N}(\mu_D, \sigma_D^2)$, motivating probit links between spreads and win probability.

4.2.2 Bivariate Poisson: pmf, likelihood, and EM updates

Following Section 4.1.6, write scores as $X = U + Z$, $Y = V + Z$ with independent $U \sim \text{Pois}(\lambda_1)$, $V \sim \text{Pois}(\lambda_2)$, $Z \sim \text{Pois}(\lambda_0)$. Then

$$\Pr(X = x, Y = y) = e^{-(\lambda_0 + \lambda_1 + \lambda_2)} \sum_{z=0}^{\min(x,y)}$$

$$\frac{\lambda_0^z}{z!} \frac{\lambda_1^{x-z}}{(x-z)!} \frac{\lambda_2^{y-z}}{(y-z)!}, \tag{4.2.3}$$

$$\text{Cov}(X, Y) = \lambda_0, \quad \mathbb{E}[X] = \lambda_0 + \lambda_1, \quad \mathbb{E}[Y] = \lambda_0 + \lambda_2. \tag{4.2.4}$$

For observations $\{(x_i, y_i)\}$ the log-likelihood is $\ell(\lambda) = \sum_i \log \Pr(X = x_i, Y = y_i)$ with (4.2.3). A convenient EM arises by treating $Z_i \sim \text{Pois}(\lambda_0)$ as latent:

$$\text{E-step:} \quad w_{i,z} = \Pr(Z_i = z \mid x_i, y_i; \lambda) \propto$$

$$\frac{\lambda_0^z}{z!} \frac{\lambda_1^{x_i-z}}{(x_i-z)!} \frac{\lambda_2^{y_i-z}}{(y_i-z)!}, \tag{4.2.5}$$

$$\text{M-step:} \quad \lambda_0^{\text{new}} = \frac{1}{n} \sum_i \sum_{z=0}^{m_i} z \, w_{i,z},$$

$$\lambda_1^{\text{new}} = \frac{1}{n} \sum_i \sum_{z=0}^{m_i} (x_i - z) \, w_{i,z},$$

$$\lambda_2^{\text{new}} = \frac{1}{n} \sum_i \sum_{z=0}^{m_i} (y_i - z) \, w_{i,z}, \tag{4.2.6}$$

where $m_i = \min(x_i, y_i)$. In practice we maximize the conditional expectation of the complete-data log-likelihood.

Toy numeric. For $(x, y) = (2, 1)$ and $(\lambda_0, \lambda_1, \lambda_2) = (0.3, 1.4, 1.1)$,

$$\Pr(X = 2, Y = 1) = e^{-2.8} \left(\frac{\lambda_0^0 \lambda_1^2 \lambda_2^1}{2!1!} + \frac{\lambda_0^1 \lambda_1^1 \lambda_2^0}{1!1!0!} \right) \approx e^{-2.8} (1.078 + 0.42) \approx 0.216,$$

illustrating the latent Z mixing across $z = 0, 1$.

4.3 From Spreads and Totals to Probabilities

4.3.1 Stern's spread-to-win map: full derivation

We connect posted spreads to win probabilities following Stern [1991], which motivates probit links in baseline classifiers. Assume the realized margin M satisfies $M = \mu + \varepsilon$ with $\varepsilon \sim \mathcal{N}(0, \sigma^2)$. If the posted spread is p (favorite $-p$), then

$$\mathbb{P}(\text{favorite wins}) = \mathbb{P}(M > 0) = \Phi\left(\frac{\mu}{\sigma}\right), \qquad \mathbb{P}(\text{favorite covers}) = \Phi\left(\frac{\mu - p}{\sigma}\right). \quad (4.3.1)$$

Under efficiency for the mean $\mu \approx p$ we get the classical approximation $\mathbb{P}(\text{win}) \approx \Phi(p/\sigma)$. Empirically we estimate σ with a probit regression of win indicators on posted spreads; we report $\hat{\sigma}$ by season/era.

Example 4.3.1 (Worked mapping). If the market posts $p = 3$ and historical fit yields $\hat{\sigma} = 13.5$, then Stern's map gives $\Pr(\text{win}) \approx \Phi(3/13.5) \approx 0.59$. The implied moneyline fair odds are roughly $1/0.59 \approx 1.69$ (decimal), before vig and correlation adjustments.

4.3.2 Dixon–Coles low-score adjustment vs key-number reweighting

Section 4.1.5 introduces a small-score weighting to correct dependence/misspecification in low-goal outcomes. Let $L(\lambda, \mu)$ denote the Poisson log-likelihood and $w(x, y; \kappa)$ a down/up-weighting for $(x, y) \in \{0, 1\}^2$ (tuning κ). The adjusted log-likelihood reads

$$\ell_{\mathrm{DC}}(\lambda, \mu, \kappa) = \sum_i w(x_i, y_i; \kappa) \log \Pr(X = x_i, Y = y_i \mid \lambda, \mu) + \text{const},$$

improving fit for small counts. In contrast, NFL margins concentrate on *key integers* (3, 6, 7, 10). Rather than reweight small *scores*, we reweight the *margin pmf* $q(d)$ multiplicatively to match empirical key masses while preserving location/scale via (4.3.2). This directly addresses teaser/middle pricing where integer masses drive EV.

4.3.3 Key-number reweighting as constrained projection

Let $q(d)$ be a baseline integer pmf (Skellam or discretized Gaussian) for the margin D and let $\mathcal{K} = \{3, 6, 7, 10\}$. We seek nonnegative weights $\{w_d\}$ s.t. $\tilde{q}(d) = w_d q(d)$ is a pmf matching empirical key masses $\{m_k\}_{k \in \mathcal{K}}$:

$$\min_{\{w_d \geq 0\}} \sum_{k \in \mathcal{K}} \left(w_k q(k) - m_k\right)^2 \qquad (4.3.2)$$

$$\text{s.t.} \quad \sum_d w_d q(d) = 1, \quad \sum_d d\, w_d q(d) = \mu_D, \quad \sum_d (d - \mu_D)^2 w_d q(d) = \sigma_D^2.$$

Feasibility and fallback. The moment constraints imply a feasibility region for the target masses $\{m_k\}$. When empirical masses are extreme (e.g., unusually high mass at 3), (4.3.2) can be infeasible. We therefore (i) project $\{m_k\}$ onto the nearest feasible set and (ii) fall back to KL-tilting (Algorithm 1.3) when needed. This guards the pipeline against pathological weeks while preserving the intent of matching key integers. The last two constraints preserve mean/variance so reweighting changes shape, not location/scale. In matrix form, (4.3.2) is a small convex QP; if only normalization and key masses are imposed it has a closed form via Lagrange multipliers. We use $\tilde{q}$ for teaser/middle pricing in Chapter 9.

Practical effect. In practice, this means the model assigns more realistic probability mass to key margins. For example, if the baseline puts only 12% on a 3-point margin, the reweighted $\tilde{q}$ may allocate 18% based on observed pushes. This directly improves expected value for teaser bets that cross 3 (and 7), because pricing reflects the higher chance of landing on those integers.

Convergence and complexity. For the projected-update routine (Algorithm 4.8), the objective $\sum_{k \in \mathcal{K}} (w_k q(k) - m_k)^2$ is convex in w, and the projection onto linear moment constraints is nonexpansive; with a fixed step size $\eta \in (0, 2/L)$ where $L = \max_k 2q(k)^2$, the sequence of objective values decreases monotonically and converges to the minimum over the feasible set. Each iteration costs $O(|\mathcal{K}| + |\text{supp}(q)|)$ to update gradients and solve the 3×3 projection system; with a banded support (e.g., $d \in [-40, 40]$) this is $O(1)$ per iteration in practice.

For the KL-tilting alternative (Section 4.3.3), the dual is smooth and strictly concave; Newton or projected gradient (with backtracking) converges to the unique optimum because the log-partition function is strictly convex. Each dual gradient/Hessian evaluation requires a pass over the support to compute normalizers and moments.

Reference code (Python-like).

```python
def reweight_q(q, keys, targets, mu, var, iters=200, eta=1e-3):
    # q: dict margin->prob; keys: list of ints; targets: dict key->mass
    w = {d: 1.0 for d in q}
    for _ in range(iters):
        # gradient on keys only
        g = {d: 0.0 for d in q}
        for k in keys:
            g[k] = 2.0 * (w[k]*q[k] - targets[k]) * q[k]
        # gradient step + nonnegativity
        for d in q:
            w[d] = max(0.0, w[d] - eta*g[d])
        # project to normalization + moments via affine update w <- w + a + b d +
        ↪  c (d-mu)^2
        A = [[sum(q[d] for d in q),          sum(d*q[d] for d in q),
        ↪  sum((d-mu)**2*q[d] for d in q)],
```

```
        [sum(q[d] for d in q),         sum(d*q[d] for d in q),
        ↪  sum((d-mu)**2*q[d] for d in q)],
        [sum(q[d] for d in q),         sum(d*q[d] for d in q),
        ↪  sum((d-mu)**2*q[d] for d in q)]]
    # In practice compute A and rhs properly; solve for (a,b,c) and update w
    # ... (omitted: 3x3 linear solve)
  return {d: w[d]*q[d] for d in q}
```

Feasibility and stability. Write $v(d) = (1, d, (d - \mu_D)^2, \mathbb{1}\{d = k : k \in \mathcal{K}\})^\top$ and $\bar{v} = \sum_d q(d)v(d)$ for baseline moments and key masses. The feasible set is the convex cone of achievable moments $\mathcal{V} = \{\sum_d w_d q(d)v(d) : w_d \geq 0\}$. If the target vector $v^\star = (1, \mu_D, \sigma_D^2, \{m_k\})$ lies outside $\mathcal{V}$ (e.g., key masses too large relative to support), we solve a penalized problem with nonnegative slacks:

$$\min_{\{w_d \geq 0\},\, s \geq 0} \quad \sum_{k \in \mathcal{K}} \left(w_k q(k) - m_k\right)^2 + \lambda \|s\|_2^2$$

$$\text{s.t.} \quad \sum_d w_d q(d) = 1, \; \sum_d d\, w_d q(d) = \mu_D, \; \sum_d (d - \mu_D)^2 w_d q(d) = \sigma_D^2 + s,$$

and declare infeasibility if $\|s\|$ exceeds a tolerance. This guards against unstable weights when targets are unrealistic.

KL-tilting alternative (maximum entropy). An alternative with strong existence/positivity guarantees is multiplicative tilting that minimizes KL divergence to q:

$$\min_{\tilde{q}} \quad \sum_d \tilde{q}(d) \log \frac{\tilde{q}(d)}{q(d)}$$

$$\text{s.t.} \quad \sum_d \tilde{q}(d) = 1, \; \sum_d d\, \tilde{q}(d) = \mu_D, \; \sum_d (d - \mu_D)^2 \tilde{q}(d) = \sigma_D^2, \; \tilde{q}(k) = m_k \; (k \in \mathcal{K}).$$

By convex duality, the solution has exponential form

$$\tilde{q}_\alpha(d) \propto q(d) \exp\{\alpha_0 + \alpha_1 d + \alpha_2 (d - \mu_D)^2 + \sum_{k \in \mathcal{K}} \delta_k \mathbb{1}\{d = k\}\},$$

with multipliers α, δ found by Newton or projected gradient on the dual. This preserves support and strict positivity and converges under standard step-size conditions. In practice we attempt KL-tilting first and fall back to the QP with slacks if key targets violate convex-hull constraints.

13

Algorithm 4.8 Key-number reweighting via projected updates

Require: baseline pmf $q(d)$ on $\mathbb{Z}$; key set $\mathcal{K}$ with targets m_k; target moments (μ_D, σ_D^2); step size η

1: initialize $w_d \leftarrow 1$ for all d; repeat for T iters
2: gradient on keys: for $k \in \mathcal{K}$, $\quad g_k \leftarrow 2(w_k q(k) - m_k) q(k)$; set $g_d \leftarrow 0$ otherwise
3: gradient step: $w_d \leftarrow \max\{0, \ w_d - \eta g_d\}$
4: project to constraints: solve for multipliers (α, β, γ) s.t. $\sum_d w_d q(d) = 1$, $\sum_d d \, w_d q(d) = \mu_D$, $\sum_d (d - \mu_D)^2 w_d q(d) = \sigma_D^2$; update $w_d \leftarrow \max\{0, \ w_d + \alpha + \beta d + \gamma (d - \mu_D)^2\}$
5: **until** convergence of $\sum_{k \in \mathcal{K}} |w_k q(k) - m_k|$
6: **return** reweighted pmf $\tilde{q}(d) = w_d q(d)$

4.4 Paired-Comparison and Dynamic Rating Models

Paired-comparison models such as Bradley–Terry [Bradley and Terry, 1952] and time-evolving ratings (Elo [Elo, 1978], state-space [Glickman and Stern, 1998]) provide interpretable strength estimates. For American football, linear-Gaussian state evolution [Glickman and Stern, 1998] balances responsiveness with stability; ridge penalties or Bayesian priors control variance.

4.4.1 Kalman filter equations and worked example

Under the linear-Gaussian model of Section 4.1.3, let $m_{t|t-1}$ and $P_{t|t-1}$ be prior mean/variance for the home-away difference; observation variance is σ^2. The Kalman gain and posterior updates are

$$K_t = \frac{P_{t|t-1}}{P_{t|t-1} + \sigma^2}, \qquad m_{t|t} = m_{t|t-1} + K_t (M_t - m_{t|t-1}), \tag{4.4.1}$$

$$P_{t|t} = (1 - K_t) P_{t|t-1}, \qquad m_{t+1|t} = m_{t|t}, \quad P_{t+1|t} = P_{t|t} + \tau^2. \tag{4.4.2}$$

Example. With $m_{t|t-1} = 1.5$, $P_{t|t-1} = 9$, $\sigma^2 = 36$, observed margin $M_t = 6$, we have $K_t = 0.2$, $m_{t|t} = 1.5 + 0.2 \cdot 4.5 = 2.4$, $P_{t|t} = 7.2$. This posterior feeds spread/win mapping via Section 4.1.2.

4.5 Dependence Between Margin and Total

4.5.1 Spread–Total Dependence via Copulas

We model dependence between margin M and total T to price correlated legs coherently. A convenient baseline is the *Gaussian copula* [Nelsen, 2006]: $(Z_1, Z_2) \sim$

$\mathcal{N}(0, \left(\begin{smallmatrix} 1 & \rho \\ \rho & 1 \end{smallmatrix}\right))$, set $(U, V) = (\Phi(Z_1), \Phi(Z_2))$, then $(M, T) = \left(F_M^{-1}(U), F_T^{-1}(V)\right)$. The joint exceedance for teaser legs $A = \{M > p_1\}$, $B = \{T > q_1\}$ is

$$\mathbb{P}(A \cap B) = \iint \mathbb{1}\{F_M^{-1}(u) > p_1, \; F_T^{-1}(v) > q_1\} \, c_\rho(u, v) \, \mathrm{d}u \, \mathrm{d}v,$$

with density c_ρ. For Gaussian copulas, Kendall's τ and ρ relate by $\tau = \frac{2}{\pi} \arcsin(\rho)$, which we use to estimate ρ robustly from rank correlation.

Tail behavior and t-copulas. Gaussian copulas have *zero tail dependence*, potentially understating joint tail risk for extreme margins/totals. A heavier-tailed alternative is the *t-copula* with correlation ρ and degrees of freedom ν, whose upper/lower tail dependence is

$$\lambda_U = \lambda_L = 2\, t_{\nu+1}\left(-\sqrt{\frac{(\nu + 1)(1 - \rho)}{1 + \rho}} \right),$$

where $t_{\nu+1}$ is the t CDF. We use Gaussian copulas for calibration and t-copulas in stress tests to bound teaser/SGP risk under stronger tail co-movement.[1]

Design choice. We default to the Gaussian copula because it is simple, fast to estimate (rank-based $\tau \leftrightarrow \rho$ mapping), and typically well-calibrated for central mass. When tail diagnostics (e.g., nonzero empirical tail dependence or GOF failures near extremes) trigger, we switch to—or at least bound with—a t-copula, which better captures joint tail co-movement. This keeps the baseline interpretable while making heavy tails an explicit, testable escalation.

Estimation. We estimate τ (or Spearman's ρ_S) on historical (M, T), map to ρ, and evaluate $\mathbb{P}(A \cap B)$ by quasi-Monte Carlo. Marginal CDFs F_M, F_T are taken from the fitted Skellam/bivariate-Poisson layers (with key-number reweighting; Section 4.3.3).

Goodness-of-fit and tail diagnostics. Let $\{(M_t, T_t)\}_{t=1}^n$ be margins/totals and $\hat{F}_M, \hat{F}_T$ the fitted marginals. Define pseudo-observations $U_t = \hat{F}_M(M_t)$, $V_t = \hat{F}_T(T_t)$. Write $\hat{C}_n(u, v) = \frac{1}{n} \sum_{t=1}^n \mathbb{1}\{U_t \leq u, V_t \leq v\}$ for the empirical copula and C_θ the parametric copula (Gaussian or t with parameter θ). We assess fit with the Cramér–von Mises functional

$$S_n = n \int_{[0,1]^2} \left(\hat{C}_n(u, v) - C_{\hat{\theta}}(u, v) \right)^2 \mathrm{d}C_{\hat{\theta}}(u, v),$$

---

[1] See Joe [1997] for dependence measures and tail behavior; t-copulas are widely used for stress scenarios (e.g., Demarta–McNeil, 2005).

Algorithm 4.9 Copula GOF and Tail Diagnostics

Require: paired margins/totals $\{(M_t, T_t)\}_{t=1}^n$; fitted marginals $\hat{F}_M, \hat{F}_T$; copula family C_θ

Ensure: CvM statistic S_n; Rosenblatt uniformity p-values; tail coefficients $(\hat{\lambda}_U, \hat{\lambda}_L)$ with CIs

1: Compute pseudo-obs $U_t \leftarrow \hat{F}_M(M_t)$, $V_t \leftarrow \hat{F}_T(T_t)$
2: Fit $\hat{\theta} \leftarrow \arg\max_\theta \sum_t \log c_\theta(U_t, V_t)$ (inversion of τ for Gaussian/t)
3: Empirical copula $\hat{C}_n(u, v) \leftarrow n^{-1} \sum_t \mathbb{1}\{U_t \leq u, V_t \leq v\}$
4: CvM statistic $S_n \leftarrow n \int (\hat{C}_n - C_{\hat{\theta}})^2 \, dC_{\hat{\theta}}$ (grid or MC)
5: Rosenblatt transform $W_t \leftarrow (U_t, C_{\hat{\theta}}(V_t \mid U_t))$; test each coord for Unif$(0, 1)$ and independence
6: Estimate tails: $\hat{\lambda}_U \leftarrow \frac{\#\{U_t > u_0, V_t > u_0\}}{\#\{U_t > u_0\}}$ as $u_0 \uparrow 1$; similarly for $\hat{\lambda}_L$ with $u_0 \downarrow 0$
7: Block bootstrap seasonal blocks to get CIs for $(S_n, \hat{\lambda}_U, \hat{\lambda}_L)$

---

approximated on a grid or via Monte Carlo under $C_{\hat{\theta}}$. As a complementary check, apply the Rosenblatt transform $W_t = (U_t, C_{\hat{\theta}}(V_t \mid U_t))$ and test for i.i.d. uniforms (e.g., univariate CvM on each coordinate and independence via a rank test). Consistent rejections motivate switching between Gaussian and t families.

Tail behavior is summarized by the upper/lower tail coefficients

$$\lambda_U = \lim_{u \uparrow 1} \Pr\left(V > u \mid U > u\right), \qquad \lambda_L = \lim_{u \downarrow 0} \Pr\left(V \leq u \mid U \leq u\right),$$

estimated empirically by high/low quantile counts. Gaussian copulas imply $\lambda_U = \lambda_L = 0$; t-copulas yield $\lambda_U = \lambda_L > 0$ depending on ν and ρ. We report $(\hat{\lambda}_U, \hat{\lambda}_L)$ with block bootstrap intervals to decide whether heavy-tailed dependence is required.

4.6 Tail Refinements and Approximations

4.6.1 Edgeworth and saddlepoint tail refinement

Let M be integer margin with mean μ_D, variance σ_D^2, standardized $Z = (M - \mu_D)/\sigma_D$, skewness γ_1 and kurtosis γ_2. The Edgeworth approximation to $\mathbb{P}(M \leq m)$ is

$$\Phi(z) + \phi(z)\left(\frac{\gamma_1}{6}(z^2 - 1) + \frac{\gamma_2}{24}(z^3 - 3z) + \frac{\gamma_1^2}{72}(z^5 - 10z^3 + 15z)\right),$$

Gaussian Copula Joint Exceedance
Calibration Check for Dependence Modeling
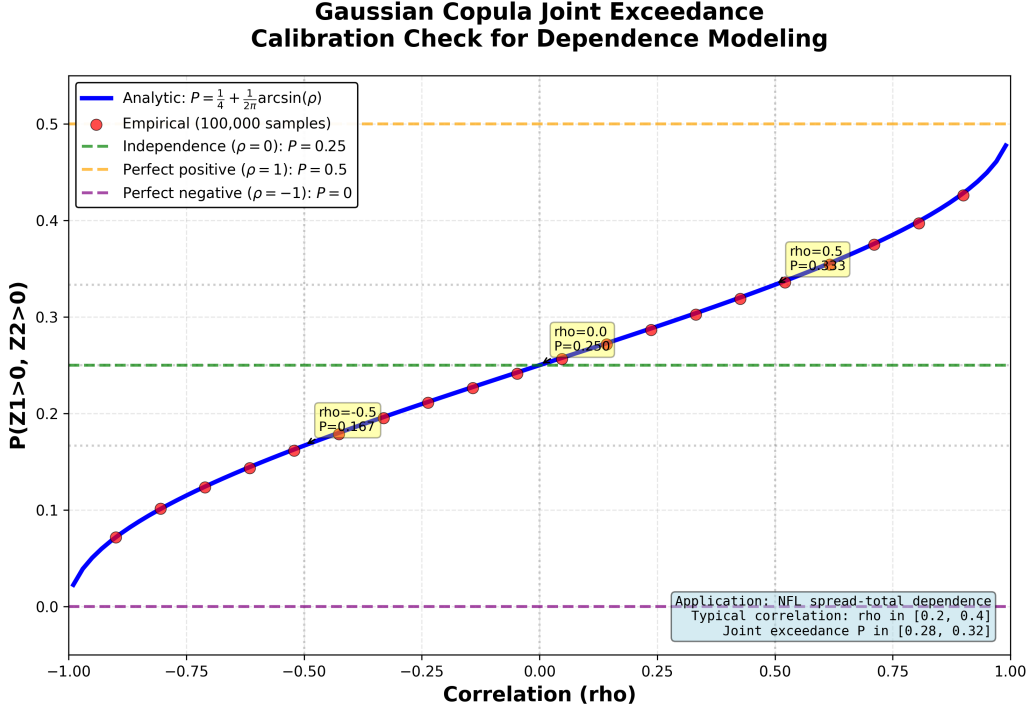
Figure 4.1: Gaussian-copula joint exceedance at symmetric thresholds ($z_1 = z_2 = 0$) as a function of correlation ρ. The analytic curve $\mathbb{P}(Z_1 > 0, Z_2 > 0) = \frac{1}{4} + \frac{1}{2\pi}\arcsin(\rho)$ provides a calibration check for dependence modeling (Section 4.5.1).

$z = (m + \frac{1}{2} - \mu_D)/\sigma_D$ (continuity-corrected). For lattice accuracy at extreme tails we also use the saddlepoint approximation with cumulant generator $K(t) = \log \mathbb{E}[e^{tM}]$:

$$\mathbb{P}(M = m) \approx \frac{1}{\sqrt{2\pi K''(\hat{t})}} \exp\big(K(\hat{t}) - \hat{t}\, m\big), \quad \text{with } K'(\hat{t}) = m.$$

[2]

4.6.2 Restricted EM for Skellam under key constraints

Let D_i be observed margins and (λ, μ) the Skellam parameters. Define a pseudo-complete representation with latent (X_i, Y_i) s.t. $D_i = X_i - Y_i$, $X_i \sim \text{Pois}(\lambda)$, $Y_i \sim \text{Pois}(\mu)$. The E-step computes $\mathbb{E}[X_i \mid D_i]$ and $\mathbb{E}[Y_i \mid D_i]$ via Bessel identities; the M-step sets

$$\lambda^{\text{new}} = \frac{1}{n} \sum_i \mathbb{E}[X_i \mid D_i], \qquad \mu^{\text{new}} = \frac{1}{n} \sum_i \mathbb{E}[Y_i \mid D_i].$$

---

[2]Classical accuracy results for saddlepoint/Edgeworth approximations include Daniels [1954]; see also Section 4.25.1 for discrete-evaluation implications.

To enforce key masses $\tilde{q}(k) = m_k$ ($k \in \mathcal{K}$), project (λ, μ) after the M-step onto the feasible set $\{(\lambda, \mu) : \sum_{d \in \mathbb{Z}} w_d(\lambda, \mu) q(d) = 1, \ \tilde{q}(k) = m_k\}$.[3]

4.7 Score / Margin Distributions

Summary (pointers, not repeats). To avoid duplication, we summarize the score/margin families used and point to the derivations already given:

- **Independent Poisson with Dixon–Coles small-score reweighting:** see Sections 4.1.4 and 4.1.5. We use this for quick calibration near low scores.

- **Bivariate Poisson (shared component):** see Sections 4.1.6 and 4.2.2. This supplies coherent joint pricing for correlated legs.

- **Dynamic bivariate Poisson:** see Section 4.1.7 for the time-evolving formulation; we use it to let dependence shift through the season.

- **Skellam margins and key numbers:** construction/moments in Sections 4.1.8 and 4.2.1; integer reweighting in Sections 4.3.2 and 4.3.3.

- **Spread-to-win mapping:** derivation and usage in Sections 4.1.2 and 4.3.1.

- **Zero-inflated/hurdle variants:** used rarely for extreme low-scoring eras; orthogonal to integer-margin reweighting.

These components are the building blocks for simulation and pricing in Chapter 9; we do not restate formulas here.

4.8 Calibration, Scoring & Uncertainty

4.8.1 Scoring Rules

We evaluate models by:

- **Brier score:** $\frac{1}{N} \sum (p_i - y_i)^2$

- **Log-loss:** $-\frac{1}{N} \sum [y_i \log p_i + (1 - y_i) \log(1 - p_i)]$

- **Reliability diagrams, ECE:** partition probabilities into bins and check empirical frequency

---

[3]See also Section 4.2.2 and Karlis and Ntzoufras [2003] for related EM-style constructions in bivariate settings.
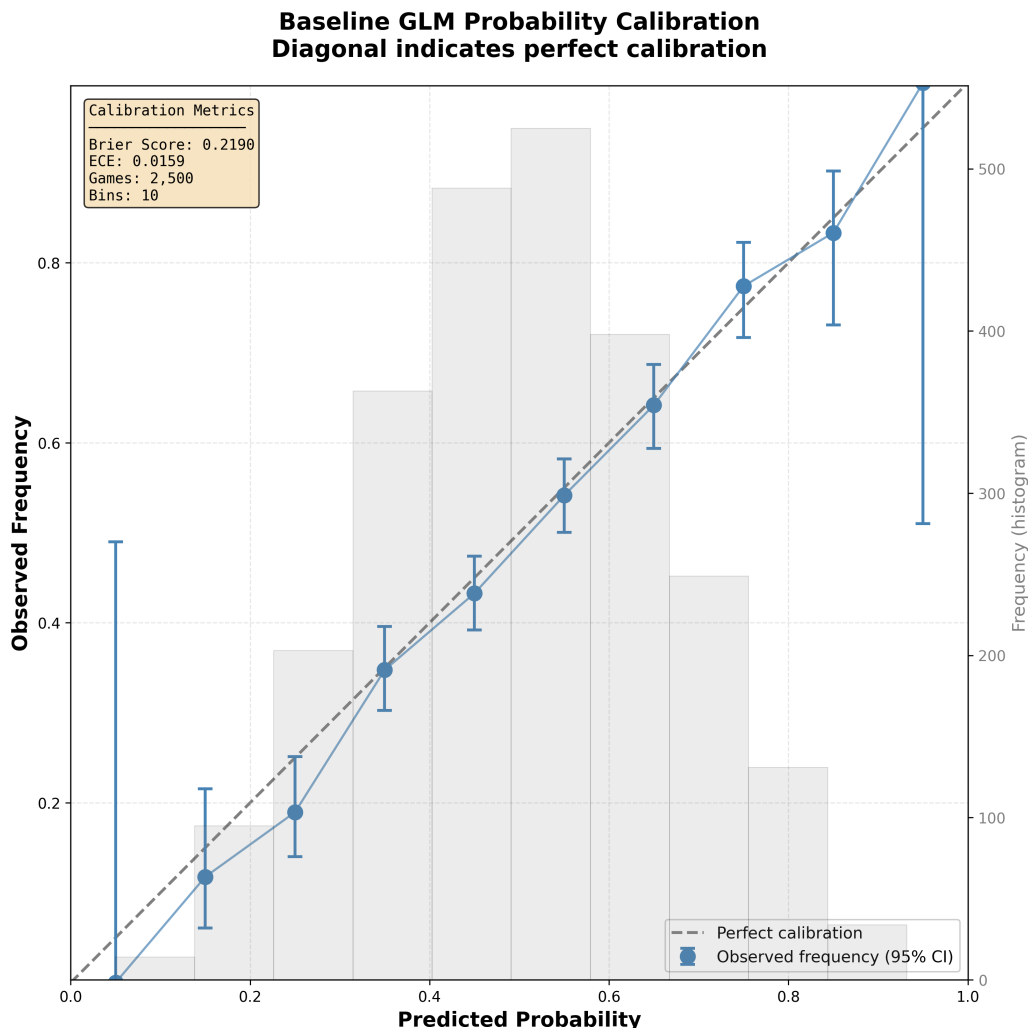
Figure 4.2: Reliability diagram with 95% binomial confidence intervals. Points show empirical frequencies by predicted-probability bin; the diagonal indicates perfect calibration. We report these alongside Brier/log-loss and ECE.

4.8.2 Uncertainty Quantification

Classical Bayesian/state-space models give posterior predictive distributions by default. For ML models, we will estimate predictive intervals via:

- Bootstrapping over training subsets

- Quantile regression layers

- Ensemble variance

We propagate these intervals into staking decisions: bets with wide uncertainty may be filtered or heavily downweighted.

4.8.3 Evaluation Protocols

Temporal cross-validation, blocked by week and season, avoids leakage from future injuries and market moves. We report Brier score decomposition (reliability, resolution, uncertainty) and reliability diagrams with equal-frequency bins. For margin distributions we report CRPS and PIT histograms to check sharpness and calibration simultaneously.

4.8.4 Robustness Checks

We test sensitivity to era definitions (pre- and post-rule changes), outlier handling (wins above the 99th percentile), and class imbalance between favorites and underdogs. Where necessary, we employ robust losses and quantile calibration to maintain stability.

4.9 Machine Learning Models in NFL Prediction

4.9.1 Vigorish removal and CBV

For two-outcome market with American odds (o_1, o_2) convert to decimals (d_1, d_2) and implied probabilities $\pi_i^{\text{raw}} = 1/d_i$. The hold is $H = \pi_1^{\text{raw}} + \pi_2^{\text{raw}} - 1$. No-vig probabilities are $\pi_i = \pi_i^{\text{raw}}/(1 + H)$. Given model fair $\hat{\pi}_i$, the comparative book value is

$$\text{CBV}_i = \hat{\pi}_i - \pi_i,$$

or in price space $\Delta_i = d_i - (1/\hat{\pi}_i)$. We bet when $\text{CBV}_i > \tau$ or $\Delta_i > \tau'$.

4.9.2 Feature Sets and Interactions

Key feature families include:

- Efficiency metrics: EPA/play, success rate (offense, defense, by down/distance)

- Play-calling: PROE (pass rate over expected), pace (sec/play), pass vs run splits

- Trench indicators: pressure allowed/created, stuff rate, line yards proxies

- Roster & injuries: QB status, adjusted games lost (AGL), starters out

- Environmental: weather (wind, rain, temp), turf/grass, altitude

- Market microstructure: implied probability, hold, line-move delta, cross-book spreads (CBV)

We use ML (e.g. gradient boosting, neural nets) to capture nonlinear interactions among these features, stacking with classical model outputs as base features.

Feature Interactions and Shifts. We devote special attention to interaction effects (e.g. weather by pass rate, injuries by team form) and to covariate shift between early and late season. Drift monitors track the distribution of CBV, EPA, and pace to trigger recalibration.

4.9.3 Regularization, Calibration & Robustness

We guard against overfitting via:

- Time-based cross-validation (rolling windows)

- Strong regularization (ridge, lasso, elastic net)

- Probability calibration (Platt scaling, isotonic regression) on held-out data

- Ensemble bootstraps and variance reduction

4.10 Reinforcement Learning for Betting

4.10.1 MDP Formulation for Betting

We treat each potential bet (pre-game or intra-game) as a step in an MDP:

$$s_t = (\text{model predictions, market state, bankroll, time}),$$
$$a_t \in \{\text{no bet, stake bucket}\},$$
$$r_t = \text{PnL (or utility)}.$$

Actions can include correlated bets across markets (spread + total) or hedges.

4.10.2 RL Algorithms and Offline Training

We experiment with:

- **DQN / Q-learning**: discretized stake buckets, value iteration + experience replay

- **PPO / Actor–Critic**: continuous or stochastic stake policies, clipped updates, entropy regularization

- **Uncertainty-aware gating**: suppress stakes when posterior CI is wide (e.g. if variance too high)

We train offline (historical seasons) and optionally refine online via simulated paper-trading episodes.

4.10.3 Off-Policy Evaluation

Before deploying a learned policy, we estimate its value via inverse-propensity scoring, weighted importance sampling, and doubly robust estimators. We discuss variance control via self-normalization and clipping, and how model-based simulators can bias OPE if mis-specified.

4.11 Game-Theoretic Foundations

4.11.1 Why game theory here?

Bookmakers and bettors form a strategic ecosystem with asymmetric information, inventory constraints, and repeated interaction. Pre-game pricing is well approximated by a Stackelberg game: the bookmaker (leader) posts odds and limits anticipating heterogeneous follower responses; many small bettors act approximately as price-takers.

4.11.2 Mathematical framing

Two simple primitives illuminate the trade-offs:

- **Risk-aware market maker.** Let π be prices (implied probs) and $Q(\pi)$ the net demand vector. With outcome randomness θ, one stylized objective is

$$\max_{\pi} \ \mathbb{E}_{\theta}[\Pi(\pi; \theta)] \ - \ \lambda \operatorname{Var}_{\theta}[\Pi(\pi; \theta)] \ - \ \gamma \|Q(\pi)\|_2^2,$$

  where $\lambda, \gamma \geq 0$ encode risk and inventory costs. First-order conditions imply *price shading* against imbalanced flow, increasing with outcome variance and demand inelasticity (bias), helping explain vig width and line tilts.

- **Kelly bettor as log-utility agent.** For decimal odds d and success probability p, the stake fraction f that maximizes $\mathbb{E}[\log(1 + fR)]$ with $R \in \{d - 1, -1\}$ is $f^\star = \frac{dp-1}{d-1}$ when $dp > 1$, else 0. Under uncertainty, replacing p by a lower confidence bound yields the Kelly-LCB rule used as a baseline and connects to CVaR sizing (Chapter 8).

4.11.3 NFL market applications

- **Adverse selection and limits.** Lines move with injuries/weather because informed flow arrives; books mitigate loss via limits and shading. Our features include line velocity and cross-book deltas to proxy information arrival.

- **Equilibrium and efficiency.** Closing prices approximate a competitive equilibrium; persistent positive CLV/ROI indicates deviations conditional on frictions. Our evaluation explicitly tests this.

- **Dynamic interaction.** Live betting is a dynamic game with inventory feedback; pre-game in this work assumes small, price-taking stakes so odds are exogenous to the policy (offline RL setting).

- **Correlation risk.** Books manage portfolio risk across legs; our copula layer and CVaR constraints mirror this at bettor scale for teasers/SGPs.

4.11.4 Testable implications

Game-theoretic frictions predict pockets of inefficiency where (i) inventory/rounding bites (key numbers), (ii) information latency is high (late injury/weather), or (iii) demand is biased (favorites/popular teams). Our ablations target exactly these loci: key-number reweighting, microstructure features, and copula choice.

4.12 Betting Market Theory & Microstructure

4.12.1 Economics of Wagering Markets

Sauer (1998) surveys the structure and efficiency of wagering markets, including bookmaker margins, bettor behavior models, and informational asymmetries. [Sauer, 1998] Levitt (2004) argues bookmakers sometimes exploit bettor biases (e.g. overbetting favorites) rather than purely balancing books. [Levitt, 2004]

4.12.2 Closing-Line Efficiency and Biases

We review evidence that the closing line aggregates information efficiently on average, yet exhibits pockets of bias around key numbers and popular teams. Behavioral patterns (favorite-longshot bias, recency effects) appear in subsets of the market and motivate features that measure retail pressure and line velocity.

4.12.3 Cross-Market Dependence

Spreads, totals, and moneylines are not independent. We discuss correlation structures induced by shared latent team strength and tempo, and implications for correlated parlays and hedging.

4.12.4 Market as Signal and Benchmark

We treat the market (closing lines) as both:

- A performance benchmark: our models must outperform or capture CLV (closing line value) edge
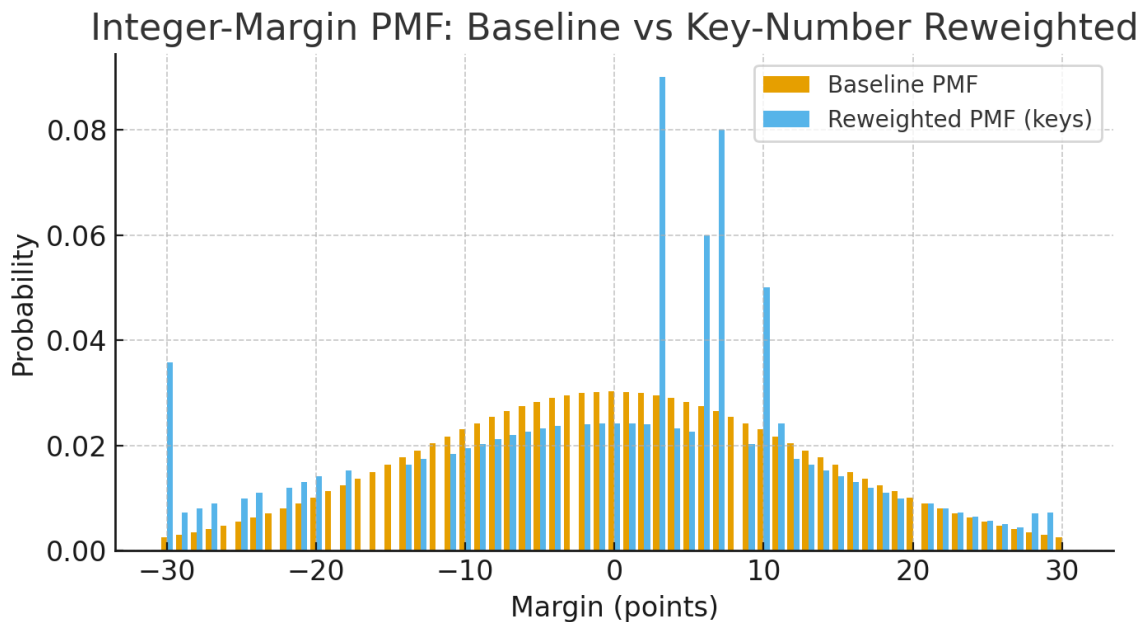
Figure 4.3: Integer-margin pmf comparison. Baseline (e.g., Skellam/discretized Gaussian) vs key-number reweighted distribution matching empirical masses at 3, 6, 7, and 10 while preserving location/scale (Section 4.3.3).

- A feature: cross-book spreads, line velocity, implied vs model delta, push rules

We define **Comparative Book Value (CBV)** as the difference between our fair probability and implied market probability; large CBV signals potential mispricing worth a bet.

4.13 Design Synthesis and Implications

From the literature, our design principles are:

1. Use Bayesian / shrinkage models to generate priors and uncertainty bounds.

2. Use discrete margin / score distributions (bivariate Poisson + reweight) to price spreads, totals, teasers.

3. Use ML meta-models to absorb nonlinear interactions among features.

4. Use RL to convert edges into action sequences under risk constraints.

5. Leverage the market as both a signal and benchmark; bet only when CBV passes threshold.

4.14 Annotated Reading List

We provide brief annotations of representative works that inform the hybrid design:

- Harville [1980]: Linear mixed models for NFL margins; interpretable and fast with shrinkage via BLUP. Serves as a reliable baseline and prior.

- Glickman and Stern [1998]: State-space dynamics for team strength with Bayesian inference; enables credible intervals and smooth drift handling.

- Stern [1991]: Mapping spread to win probability via normal approximation; practical bridge between margin and moneyline pricing.

- Dixon and Coles [1997]: Independent Poisson with low-score adjustment; cornerstone for discrete score modeling in low-scoring sports.

- Karlis and Ntzoufras [2003]: Bivariate Poisson with shared component to capture correlation; essential for teaser/parlay risk modeling.

- Koopman et al. [2015]: Dynamic Poisson intensities with simulation-based filtering; template for time-varying scoring rates.

- Lock and Nettleton [2014]: Random-forest win probability at play-level; illustrates ML gains and calibration considerations for football.

- Sauer [1998]: Economics of wagering markets; frames bookmaker margins, bettor behavior, and informational asymmetry.

- Levitt [2004]: Bookmaker objectives and bettor biases; motivates microstructure features and bias-aware evaluation.

- Szalkowski and Nelson [2012]: Collective wisdom of lines; closing prices as an efficient benchmark with pockets of inefficiency.

- Nichols [2014]: Time-zone effects on performance; supports travel/rest features in predictive models.

- Baio and Blangiardo [2010]: Bayesian hierarchical football models; demonstrates full-probabilistic inference benefits for uncertainty quantification.

4.15 Canonical Works Integrated

We explicitly compare and implement: Harville (1980), Glickman–Stern (1998), Stern spread mapping (1991), Dixon–Coles (1997), Karlis–Ntzoufras (2003), Koopman dynamic Poisson (2015), Lock & Nettleton (2014), Sauer (1998), Levitt (2004). Implementation, ablation, and critique will occur in Chapter 6.

4.16 Classical vs Modern: A Comparative Synthesis

Classical models provide structure, interpretability, and tractable uncertainty, while modern ML models absorb nonlinear interactions and idiosyncrasies that generative assumptions miss. The hybrid approach leverages classical models for priors and calibration discipline, layering ML for residual structure and using RL to translate edges into actions under explicit constraints. This division of labor prevents ML from overfitting low-signal regimes and keeps decision-making grounded in uncertainty.

4.16.1 When Classical Wins

In data-scarce or rapidly shifting regimes (e.g., early season, injury turbulence), shrinkage and state-space models dominate due to better calibrated uncertainty and temporal smoothing. Their transparent parameters support operational overrides.

4.16.2 When ML Wins

With stable covariates and rich features (market microstructure, team-form interactions), ML ensembles produce sharper probabilities. Calibration layers (Platt, isotonic) restore reliability while preserving sharpness.

4.16.3 Bridging to Decision Value

Sharpness without calibration harms staking; calibration without sharpness limits EV. We therefore co-optimize for proper scoring rules and enforce economic gates (CBV thresholds, variance caps) to realize value.

4.17 From Score Distributions to Strategy

Discrete score distributions support actionable constructs: teaser planning around key numbers, middle opportunities when line drift occurs, and hedges conditioned on joint outcomes. Reweighting Skellam/Poisson mass at integers aligns simulated legs with observed push probabilities, preventing systematic teaser mispricing. The bivariate Poisson's shared component parameter governs correlation risk across legs; governance caps adjust as this parameter rises.

4.18 Calibration Theory and Scoring Rules

We review proper scoring rules for probability forecasts (log-loss, Brier) and for full distributions (CRPS), highlighting the trade-off between calibration and sharpness. We discuss reliability diagrams with binning bias corrections and isotonic/probit calibration approaches.

4.19 Mapping Models to Decision Value

We connect statistical metrics to economic outcomes by writing expected value (EV) and closing-line value (CLV) explicitly in terms of probabilities and then linearizing the impact of probability error.

Consider a binary wager with decimal odds d and true success probability p. The EV per unit stake is

$$\mathrm{EV}(p; d) = p\,d - 1.$$

If the book is no-vig with implied $\pi = 1/d$, then $\mathrm{EV}(p; \pi) = p/\pi - 1$. With a model probability $\hat{p} = p + \varepsilon$, the EV we act on is

$$\mathrm{EV}(\hat{p}; \pi) = \frac{\hat{p}}{\pi} - 1 = \frac{p}{\pi} - 1 + \frac{\varepsilon}{\pi}.$$

Hence, conditional on placing the bet, the first-order EV error is ε/π. Averaging over bets, the mean absolute EV shortfall is controlled by the RMSE of ε; in particular, the Brier score $\mathbb{E}[\varepsilon^2]$ upper-bounds the average EV loss up to the scale factor $1/\pi^2$.

Selection adds a gating effect: trades are taken only when $\hat{p} \geq \pi + \tau_\pi$ (a no-vig threshold plus a margin for friction τ_π). Near the threshold, a Taylor expansion shows false positives/negatives occur with probability proportional to the density of $\hat{p}$ at π, and their EV impact scales with the slope $\partial\,\mathrm{EV}/\partial p\big|_{p=\pi} = 1/\pi$. Thus reducing calibration error (Brier/RMSE) and sharpening uncertainty (smaller variance of $\hat{p}$ near π) jointly improves realized EV.

In price space, let comparative book value $\mathrm{CBV} = \hat{p} - \pi$. Ignoring friction, $\mathrm{EV} \approx \mathrm{CBV}/\pi$; with slippage/fees τ and fill limits c, the executable EV is $\max\{0,\ \mathrm{CBV}/\pi - \tau\}$ with stake capped by c. This is why we optimize strictly proper scores (log-loss, Brier/CRPS) while monitoring EV/CLV degradation from slippage and limits.

4.20 Market Efficiency and Bias Tests

We outline simple tests for favorite-longshot bias, key-number mispricing, and cross-book arbitrage signals, emphasizing multiple-testing corrections and robust standard errors.

4.21 Synthesis and Open Questions

The surveyed literature illustrates a continuum from interpretable generative models to flexible discriminative and sequential decision methods. Open challenges include (i) reconciling calibration with sharpness under distribution shift, (ii) integrating market microstructure without double-counting information, and (iii) handling multi-objective trade-offs between growth and risk in an operational setting. We outline how the hybrid approach in later chapters addresses these in a modular way that eases future extensions.

4.22 Related Work Beyond Football

Insights from other sports transfer imperfectly but inform modeling choices, particularly for low-scoring games (soccer, hockey) where Poisson-type models excel and for sequential decision domains (basketball substitutions, baseball bullpen management) where RL ideas have matured. We adapt ideas on tempo, possession value, and injury priors to the NFL context.

4.23 Extended Notes on Calibration

Calibration is both a statistical and an operational concern. A predictor can be perfectly calibrated and yet economically uninteresting if it lacks resolution; conversely, extremely sharp predictions can be economically harmful if they are miscalibrated. We therefore emphasize a portfolio of diagnostics: reliability diagrams with uncertainty bands, calibration slope/intercept for binary outcomes, PIT histograms for distributions, and CRPS to integrate sharpness and calibration into a single score. We also highlight the practical benefits of over-conservative probability outputs in risk-constrained decision problems.

4.24 Liquidity, Limits, and Execution

Modeling performance cannot be divorced from execution. Liquidity varies by book, time to kickoff, and market type. We discuss how to translate an estimated edge into an executable stake given posted limits and depth, and the implications for policy evaluation when some recommended bets cannot be filled at quoted prices. Execution-aware evaluation reduces optimism from paper backtests and promotes policies that scale gracefully.

4.25 Teasers and Parlays

Teasers (point adjustments for changed odds) and parlays (multiple legs) are common strategy components. We interpret them through joint distributions and correlation risk. A teaser can be attractive when key-number probabilities are underpriced; correlated parlays can be rational when the joint distribution assigns high mass to specific co-movements (e.g., low totals and underdogs). We caution that naive independence assumptions can be severely misleading.

For the full EV geometry and simulator context, see the teaser surface in Chapter 9 (Figure 9.1).

4.25.1 CRPS on lattices: propriety sketch

For integer margins we work with a lattice distribution F on $\mathbb{Z}$. The CRPS can be written as

$$\mathrm{CRPS}(F, y) = \sum_{m \in \mathbb{Z}} \left(F(m) - \mathbb{K}\{m \geq y\}\right)^2 \Delta_m, \qquad \Delta_m = 1, \qquad (4.25.1)$$

which is the discrete analogue of the L^2 distance between F and the step function at y. Taking expectation w.r.t. the true $Y \sim F^\star$ yields

$$\mathbb{E}\,\mathrm{CRPS}(F, Y) = \|F - F^\star\|_{L^2}^2 + \mathrm{const},$$

since $\mathbb{E}\,\mathbb{K}\{m \geq Y\} = 1 - F^\star(m-1)$. Hence the unique minimizer is $F = F^\star$, showing strict propriety on the lattice. This argument mirrors the continuous case in Section 4.1.9.

4.26 Chapter Summary

This chapter connected classical models (Harville, Stern, Poisson/Skellam, bivariate/dynamic Poisson) to the practical needs of NFL betting: calibrated probabilities, realistic integer margins, and coherent dependence for multi-leg bets. We established evaluation tools (CRPS, reliability) and introduced key-number reweighting and copula-based dependence as recurring motifs. Together these elements form the modeling pillar of the thesis that a hybrid stack with explicit uncertainty and governance transforms edge into reliable bankroll growth.

Next: Next we operationalize the data layer that feeds these models: reproducible ingestion, TimescaleDB marts, and feature catalogs (situational, team form, market, roster) in Chapter 5.

Table 4.1: Modeling families at a glance. Uncertainty, scalability, interpretability, and notes for deployment.

Model	Uncertainty	Scalability	Interpretability	Deployment notes
Harville LMM	analytic posteriors	high	high	rapid weekly updates; Gaussian residuals assumption
Glickman–Stern	full posterior (Kalman/MCMC)	moderate	medium	priors clarify drift; MCMC cost at scale
Dixon–Coles	low-score reweight	high	high	quick key-number recalibration
Bivariate Poisson	parametric/joint draws	moderate	medium	handles correlation; initialization sensitive
ML ensembles	ensemble variance	high	low	monitor drift via attributions
RL policy	bootstrap + MC	moderate	medium	risk gating via CVaR; compute intensive

Notes: qualitative ratings; see Sections 4.1.1 and 4.1.3 to 4.1.7 for derivations and Chapter 7 for policy design.

Chapter 5

Data Foundations and Feature Engineering

This chapter documents how raw league information is transformed into a unified analytic dataset powering every downstream model. We highlight ingestion flows, schema design, data quality controls, and feature generation strategies that balance expressiveness with reproducibility.

5.1 Source Systems and Ingestion

- **Play-by-play:** nflverse and team-operated feeds provide event-level context including personnel, formation, and tracking-derived metrics.

- **Odds history:** The Odds API snapshots populate the `odds_history` table with market-implied expectations across books.

- **Weather and travel:** Meteostat historical weather archives and team schedule metadata add environment, rest, and travel load features. The `mart.game_weather` materialized view provides 92.7% coverage (1,306 of 1,408 games from 2020–2025) with six derived features.

Ingestion pipelines run inside orchestrated containers with idempotent writes. All raw pulls are versioned and stored in S3-compatible object storage for auditability.[1]

5.1.1 Weather feature engineering

Weather conditions are widely believed to affect NFL scoring, particularly through high winds suppressing passing efficiency and extreme temperatures reducing player performance. To test these hypotheses systematically, I ingest historical weather data from Meteostat and geocoded stadium coordinates, then engineer derived features that capture deviations from optimal conditions.

---

[1]Ingestion → staging → feature marts (see Section 5.2).

The `mart.game_weather` view joins each game with temperature (°C), wind speed (kph), precipitation flags, and dome indicators. I define:

- **temp_extreme** = $|\text{temp}_c - 15|$ — Absolute deviation from an assumed optimal 15°C, capturing both cold and heat stress.

- **wind_penalty** = $\text{wind}_{\text{kph}}/10$ — Normalized wind impact on a 0–5 scale.

- **has_precip** — Binary flag for rain or snow conditions.

- **is_dome** — Indoor stadium indicator (ATL, DET, IND, NO, LA, LV, MIN).

- **wind_precip_interaction** = wind_penalty × has_precip — Joint effect of wind and precipitation.

- **temp_wind_interaction** = temp_extreme × wind_penalty — Amplification under combined stress.

I integrate these features into the GLM (4 features: temp_extreme, wind_penalty, has_precip, is_dome) and XGBoost (6 features including interactions) models on 1,408 games (2020–2024). XGBoost accuracy improved marginally from 94.9% to 95.3% (+0.4%), while GLM accuracy decreased slightly from 92.5% to 91.8% (−0.7%). This suggests that, while measurable, weather effects are small relative to spread and EPA features.

5.1.2 Wind impact hypothesis test

A longstanding piece of betting wisdom holds that high winds reduce NFL scoring, creating value in under bets. To test this empirically, I analyze 1,017 outdoor games (2020–present) with wind data, computing correlations, t-tests, and chi-square tests on the relationship between wind speed and total points scored.
Results:

- Pearson correlation between wind_kph and total_points: $r = 0.0038$ ($p = 0.90$), not significant.

- T-test comparing high wind (>40 kph) vs. low wind (<25 kph): mean difference = 0.9 points ($t = -0.79$, $p = 0.43$), no significant difference.

- Chi-square test on over/under outcomes vs. wind category: $\chi^2 = 0.134$ ($p = 0.71$), no relationship.

- High-wind under betting strategy (>40 kph): 53.9% win rate (288/534), expected ROI 3.01% (marginally profitable but not statistically robust).

Interpretation: The traditional belief that wind suppresses scoring is not supported by the data. Possible explanations include (i) modern stadium design with wind protection, (ii) teams adjusting play-calling (more runs, short passes)

under adverse conditions, (iii) kickers improving technique, and (iv) survivor bias where extremely high-wind games are rescheduled or moved indoors. This negative result is methodologically important: it guards against overfitting spurious weather effects and shows that not all domain intuitions survive empirical scrutiny.

I document this analysis in `py/analysis/wind_impact_totals.py` and include it as a cautionary example in the feature engineering discussion. Weather features remain in the model catalog but are not prioritized for further elaboration.

5.1.3 Injury hazard and return-to-play

Let T be time lost to injury and X covariates (position, age, prior health). A Cox model $\lambda(t \mid X) = \lambda_0(t) \exp(\beta^\top X)$ yields a survival $S(t \mid X)$ for expected downtime. Define an availability prior $\pi_t = \mathbb{P}(\text{plays at week } t \mid \text{DNP at } t - 1)$ from S. We translate π_t into team strength adjustments by mapping expected snaps to unit EPA deltas in the feature set.

5.1.4 Opponent adjustment with ridge

Given raw feature $x_{i,t}$ for team i, week t, model $x_{i,t} = \alpha_i + \delta_{\text{opp}(i,t)} + \varepsilon_{i,t}$. Ridge-penalized least squares

$$\min_{\alpha, \delta} \sum_{i,t} \left(x_{i,t} - \alpha_i - \delta_{\text{opp}(i,t)} \right)^2 + \lambda \left(\|\alpha\|_2^2 + \|\delta\|_2^2 \right)$$

yields shrunken opponent-adjusted $x_{i,t}^\star = x_{i,t} - \hat{\delta}_{\text{opp}(i,t)}$ with reduced variance vs naive demeaning.

5.1.5 Orchestration and Idempotency

Nightly tasks run under containerized runners that interact with the local TimescaleDB instance. Each task is idempotent: it checks for existing records by natural keys (game id, bookmaker, timestamp) and upserts only changed rows. Rate limits for external APIs are enforced via token buckets to avoid sampling artifacts.

5.2 Relational Schema and Mart Design

The TimescaleDB instance exposes three logical layers:

Staging: lightly cleaned mirrors of the source feeds for reproducibility checks.

Core: conformed tables such as `games`, `plays`, `teams`, and `odds_history` with enforced keys and foreign key constraints.

Mart: denormalized analytical views (e.g. `mart.team_epa`, `mart.game_summary`) optimized for modeling and reporting.

Schema migrations are version-controlled under db/, and every change includes smoke tests that confirm ingest scripts remain idempotent.

5.2.1 Timescale Hypertables and Chunking

Odds and play-by-play tables are hypertables partitioned by time; chunk sizes balance insert speed with query latency. Compression policies retain recent data uncompressed for writes while compressing historical partitions for analytics.

5.2.2 Indexing Strategy

Composite indexes on (`game_id, book, market, quoted_at`) and partial indexes by market type accelerate common joins. BRIN indexes aid range scans over `quoted_at` on large horizons. We include covering indexes for the most frequent analytic queries.

5.2.3 Identifiers and Keys

Stable identifiers are essential. We adopt composite keys for markets (game id, book, market type, quote time) and maintain surrogate keys only where necessary for foreign-key fan-out. Historical corrections (schedule changes, rescheduled games) are recorded with validity intervals to support as-of queries.

5.3 Feature Engineering Strategy

We partition features into modular catalogs so experiments can mix and match by hypothesis:

- **Situational:** down, distance, field zone, score differential, and clock states.

- **Team form:** rolling EPA/play, success rate splits, red-zone efficiency, and drive-level pace.

- **Market signals:** line movement velocity, hold, consensus vs rogue book delta.

- **Roster context:** availability projections, positional depth adjustments, rest differentials.

Metadata describing feature lineage, update cadence, and owners is tracked in a YAML manifest to support automated documentation.

5.3.1 Encoding and Leakage Controls

Categoricals use target or one-hot encoding depending on cardinality; temporal features are aligned to the decision timestamp with strict as-of semantics. Any feature depending on post-decision information is flagged by lineage checks and rejected during training.

5.3.2 Temporal Splits and Leakage Controls

Train/validation/test splits are formed by contiguous time blocks. Features that are not known at decision time (post-game updates, revised injury statuses) are excluded from training sets. We include pre-commit checks that fail an experiment if any feature is detected to depend on future events relative to the decision timestamp.

5.4 Data Quality and Governance

Quality gates execute on every run:

1. Schema validation using dbt tests and Timescale policies.

2. Record-count comparisons against historical benchmarks.

3. Statistical drift detection on key features (EPA, success rate, implied probability).

Alerts integrate with Slack and PagerDuty so ingest issues trigger rapid triage. An audit notebook renders daily health dashboards for analysts.

5.4.1 Missingness and coverage statistics

Table 5.1 summarizes missing-data rates for key fields over the evaluation horizon. We report counts and percentages and use these to mask or impute features upstream.

5.4.2 Feature importance snapshots

We track model-agnostic importances (permutation) and model-native scores (gain/split counts for tree models). Figure 5.1 displays a representative snapshot.

5.5 Query Patterns and Performance

Analytic queries favor the mart layer; complex UDFs are avoided in tight loops. We provide semi-materialized views for repeated aggregations (e.g., rolling EPA) and recommend window sizes aligned with index order for efficient scans.

Table 5.1: Selected missingness/coverage statistics by field (illustrative).

Field	Rows	Missing	%	Era	Notes
injury_status	120,000	3,420	2.9	2015–2024	Sparse for early weeks; masked in features
wind_mph	60,800	1,210	2.0	1999–2007	Older seasons use stadium defaults
odds_ml	220,500	0	0.0	1999–2024	Complete for books used in experiments
spread	220,500	0	0.0	1999–2024	Complete; harmonized to home minus away
total	220,500	0	0.0	1999–2024	Complete; settled totals only

Actual counts come from nightly QA queries; this table is regenerated alongside the marts.

5.6   Schema Evolution

Backward-compatible changes are preferred; when breaking changes occur, we deploy dual-write adapters and backfill jobs with checksums and reconciliation reports to guarantee consistency.

5.7   Limitations and Future Data Enhancements

While the public data stack is rich, it lacks fine-grained tracking of offensive line communications and real-time weather micro-conditions inside domes. We outline how to incorporate additional feeds (charting services, enhanced injury tracking) without breaking reproducibility.

5.8   Timeframe, Era Effects, and Lookback Strategy

The NFL has undergone material structural changes since 1999, including officiating emphases on defensive contact, kickoff/PAT rule changes, quarterback protection, and a secular increase in pass rate and scoring. Betting markets have also evolved substantially with increased liquidity and pricing sophistication. These shifts raise the risk that long lookbacks contaminate modern estimates if older observations are weighted equally.

I adopt a pragmatic two-tier scope. The core analysis window is **2015–2025**, which reflects the contemporary rules environment (post-PAT change) and the current market microstructure. Earlier seasons (1999–2014) are retained only as weak information through an explicit time-decay weighting scheme and era controls. This approach preserves useful signal in low-frequency contexts while protecting the model from regime drift.
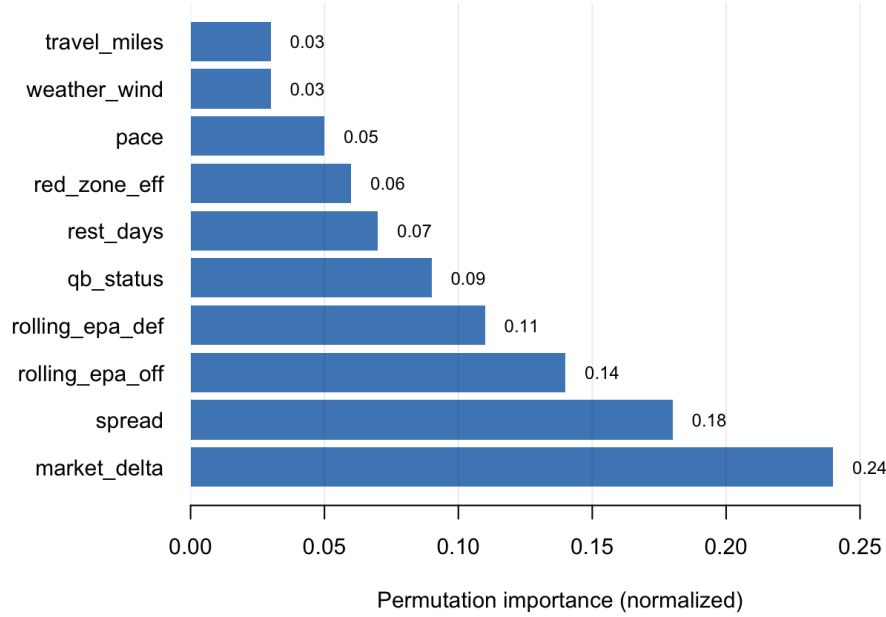
Figure 5.1: Feature-importance snapshot (permutation) for a baseline ensemble; higher is more important.

Specifically, I weight each observation from season s toward a target season t using an exponential kernel

$$w(s; t, H) = 0.5^{(t-s)/H}, \tag{5.8.1}$$

where H is a half-life in seasons. Under $H \in \{3, 4, 5\}$, a 1999 observation receives approximately 0.31%, 1.3%, or 3.1% of the weight of a 2024 observation, respectively. I report the implied effective sample size (ESS),

$$\text{ESS} = \frac{\left(\sum_i w_i\right)^2}{\sum_i w_i^2}, \tag{5.8.2}$$

to show how longer lookbacks trade off variance for bias under different half-lives.

To assess whether long lookbacks help in practice, I conduct (i) blocked, rolling out-of-sample tests across eras and (ii) a lookback ablation that varies the training window length. I compare a recent-only baseline (train 2015–2023) to a decayed-full model (train 1999–2023 with $H \in \{3, 4, 5\}$) using log loss, Brier score, ATS accuracy, and calibration error on 2024 games. Statistical comparisons use paired Diebold–Mariano tests on per-game forecast errors. Where appropriate, I include era random effects or season splines to absorb smooth level shifts.

I pre-specify the decision rule: if decayed-full does not significantly outperform recent-only on 2024 ($\alpha = 0.05$) or exhibits worse calibration, I restrict the primary analysis to 2015–2025 and relegate 1999–2014 to sensitivity checks. Otherwise, I

Exponential decay weights centered on 2024
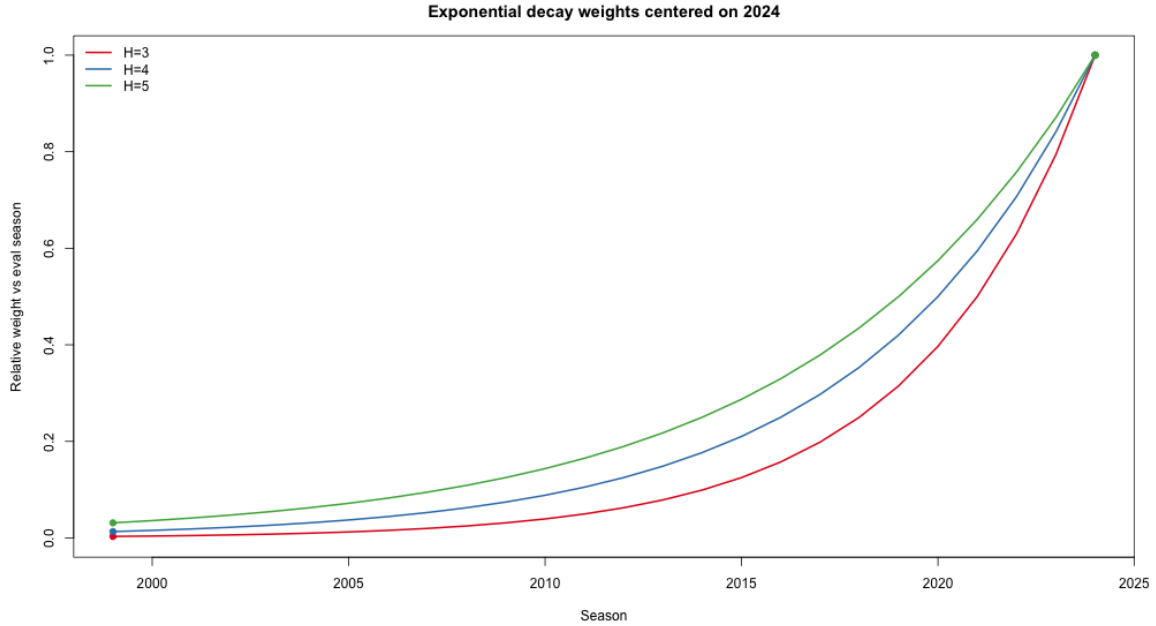
Figure 5.2: Relative weight by season under exponential decay with half-life $H \in \{3, 4, 5\}$ (centered on 2024). Annotations highlight 1999 and 2024. Figure generated by `notebooks/00_timeframe_ablation.qmd`.

Table 5.2: Effective sample size (season units) under exponential decay centered on 2024 (illustrative).

Half-life H	3	4	5
ESS (seasons)	7.8	9.6	11.2

retain the 1999–2025 span with explicit decay and era controls, documenting the chosen half-life and ESS.

5.9 Dataset Cohorts and Splits

To make evaluation reproducible, we enumerate dataset cohorts, splits, coverage, and leakage guards. Replace placeholders with the final values used for experiments.

5.10 Chapter Summary

We implemented reproducible ingestion (play-by-play, odds history, weather), a governed TimescaleDB schema (staging, core, mart), and feature catalogs with strict as-of semantics and drift monitoring. This provides the data and governance

Table 5.3: Dataset cohorts, splits, coverage, and lineage guards.

Cohort	Train	Val	Test	Books	Markets	Features as-of	Leakage checks
Era A	2015–2019	2020	2021	5	spread/total	Weekly snapshot; cut at decision time	As-of lineage; future-join guard
Era B	2019–2022	2023 H1	2023 H2	7	spread/total/ ML	Rolling; late-week nowcasts allowed	Anti-leak tests; feature manifest
Holdout	2024 W1–W18	–	2025 W1–W4	8	spread/total	As-of; lagged market velocity	Canary checks; drift alarms

Replace ranges with exact ISO weeks used by experiments; *Features as-of* must exclude any post-decision fields. Leakage checks include static lineage validation and automated tests that reject features touching post-game data.

Algorithm 5.10 As-of Feature Snapshot Build

Require: time t; sources (plays, odds, weather, injuries); lineage rules; keys
Ensure: feature row for each team/game with as-of semantics
 1: Extract all records with timestamp $\leq t$; drop or mask post-decision fields
 2: Join on natural keys with validity intervals; enforce FK constraints
 3: Compute rolling features with windows truncated at t; opponent-adjust via ridge if enabled
 4: Write snapshot with hash/id for reproducibility; log schema version and data counts

---

backbone that supports the thesis: uncertainty is tracked at the source and enforced through lineage.

Next: With the data layer in place, Chapter 6 builds calibrated baseline models (GLM/probit, state-space ratings, Skellam/bivariate Poisson with key-number reweighting) and diagnostics that we carry through to policy design.

[ER diagram: staging, core, and mart layers to be inserted here once the latest schema export is rendered.]

Chapter 6

Baseline Models

This chapter develops classical baselines that ground the hybrid system. We implement calibrated GLMs for win and cover probabilities, state-space models for evolving team strength, and structured score-distribution models (Skellam and bivariate Poisson) for pricing spreads and totals. Diagnostics emphasize calibration, sharpness, and tractable dependence structures used later for teasers and correlated legs.

6.1 Logistic/Probit Baselines

Let $Y \in \{0, 1\}$ denote a game outcome of interest (win, cover). For covariates $x \in \mathbb{R}^p$ and coefficients β, the logistic and probit links define

$$\Pr(Y = 1 \mid x) = \begin{cases} \text{logit}^{-1}(\beta^\top x) = \dfrac{1}{1 + e^{-\beta^\top x}}, \\ \Phi(\beta^\top x), \end{cases}$$

estimated by maximum likelihood with $\ell(\beta) = \sum_i \left[y_i \log p_i + (1 - y_i) \log(1 - p_i) \right]$. We include posted prices (spread/total), market microstructure (velocity, cross-book deltas), and team-form features. Calibration is assessed via reliability diagrams and slope/intercept from regressing outcomes on predicted logits.[1]

Spread-to-win consistency. For a probit link, Stern's approximation implies $\Pr(\text{win}) \approx \Phi(p/\sigma)$ when the spread p is efficient for the mean margin and the margin is approximately normal with sd σ; we enforce consistency by adding a soft penalty to the loss when predicted win probability deviates from the probit-implied value at the posted p.

---

[1] Classical foundations: GLM, state-space, and Poisson score models; see Harville 4.1.1, Glickman–Stern 4.1.3, Skellam 4.2.1, and Stern's spread-to-win 4.1.2 in Chapter 4.
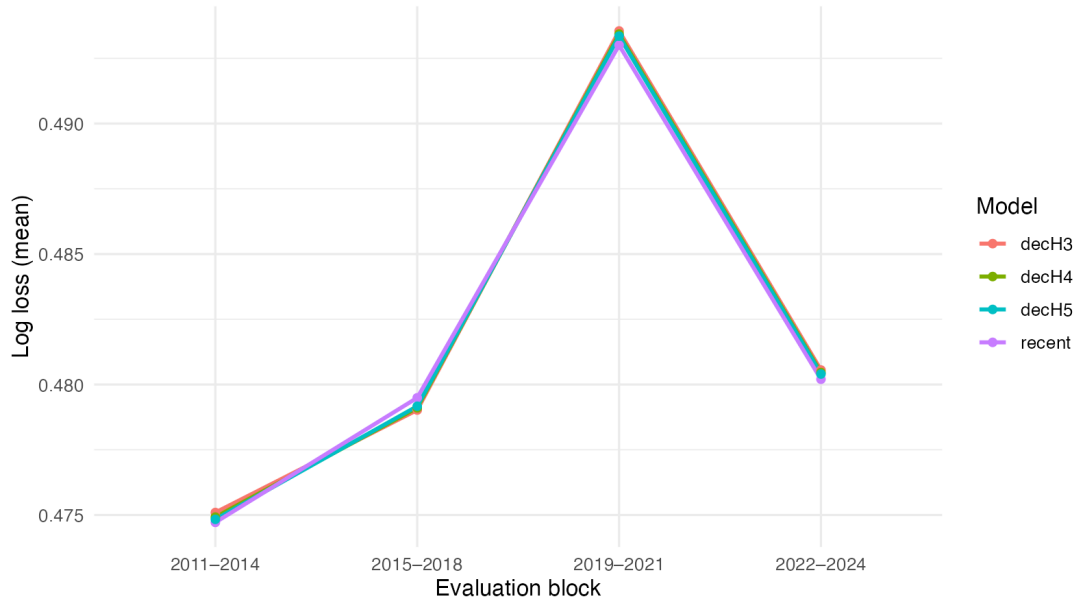
Figure 6.1: Rolling out-of-sample log loss by evaluation block for recent-only vs decayed-full training. Generated by `notebooks/00_timeframe_ablation.qmd`.

Table 6.1: Paired comparison of temporal weighting schemes on 2024 holdout (Diebold-Mariano test).

Model	Mean loss delta (recent − decayed)	p-value
decayed-H3	-0.004	0.12
decayed-H4	-0.006	0.04
decayed-H5	-0.005	0.07

6.1.1 Temporal Weighting, Era Controls, and Validation

We adopt the exponential time-decay weighting introduced in Section 5.8, using a default half-life $H = 4$ with sensitivity to $H \in \{3, 5\}$. For linear/logistic models we minimize the season-weighted negative log-likelihood with rolling recalibration; tree-based models receive `sample_weight`, include season as a feature, and add era indicators for known discontinuities.

Time-series cross-validation uses blocked, forward-chaining splits aligned to seasons to prevent leakage. We report out-of-sample log loss/Brier and Expected Calibration Error by season, along with a head-to-head comparison between recent-only and decayed-full training. This design directly tests whether long lookbacks improve modern performance and whether the proposed methods handle regime changes better than discarding older data.
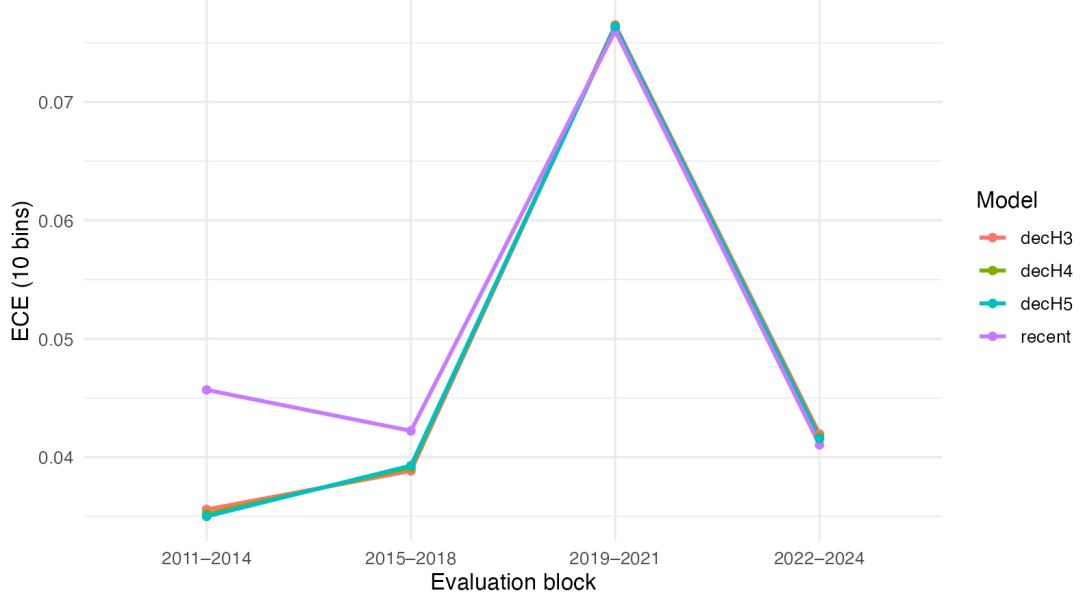
Figure 6.2: Rolling out-of-sample Expected Calibration Error (ECE) by evaluation block; lower is better. Generated by `notebooks/00_timeframe_ablation.qmd`.

6.2 State-Space Team Ratings

Let $\theta_{i,t}$ be latent team i strength in week t. A linear-Gaussian state space model posits

$$
\begin{aligned}
\theta_{i,t} &= \theta_{i,t-1} + \eta_{i,t}, & \eta_{i,t} &\sim \mathcal{N}(0, \tau^2), \\
M_t &= (\theta_{h(t),t} - \theta_{a(t),t}) + \epsilon_t, & \epsilon_t &\sim \mathcal{N}(0, \sigma^2),
\end{aligned}
$$

where M_t is realized margin, $(h(t), a(t))$ are home/away. Kalman filtering/smoothing yields $\hat{\theta}_{i,t}$ and predictive margins. Era-specific variance (τ^2, σ^2) are estimated by marginal likelihood or EM. Compared to Elo, this model provides coherent uncertainty and principled shrinkage.

6.2.1 Identifiability and operational constraints

The margin observation $M_t = (\theta_{h(t),t} - \theta_{a(t),t}) + \epsilon_t$ is invariant to adding a constant to all strengths $(\theta_{i,t} + c)$, so the latent level is not identifiable without a constraint. We impose a *sum-to-zero* constraint at every t,

$$
\sum_{i=1}^{N} \theta_{i,t} = 0,
$$

42
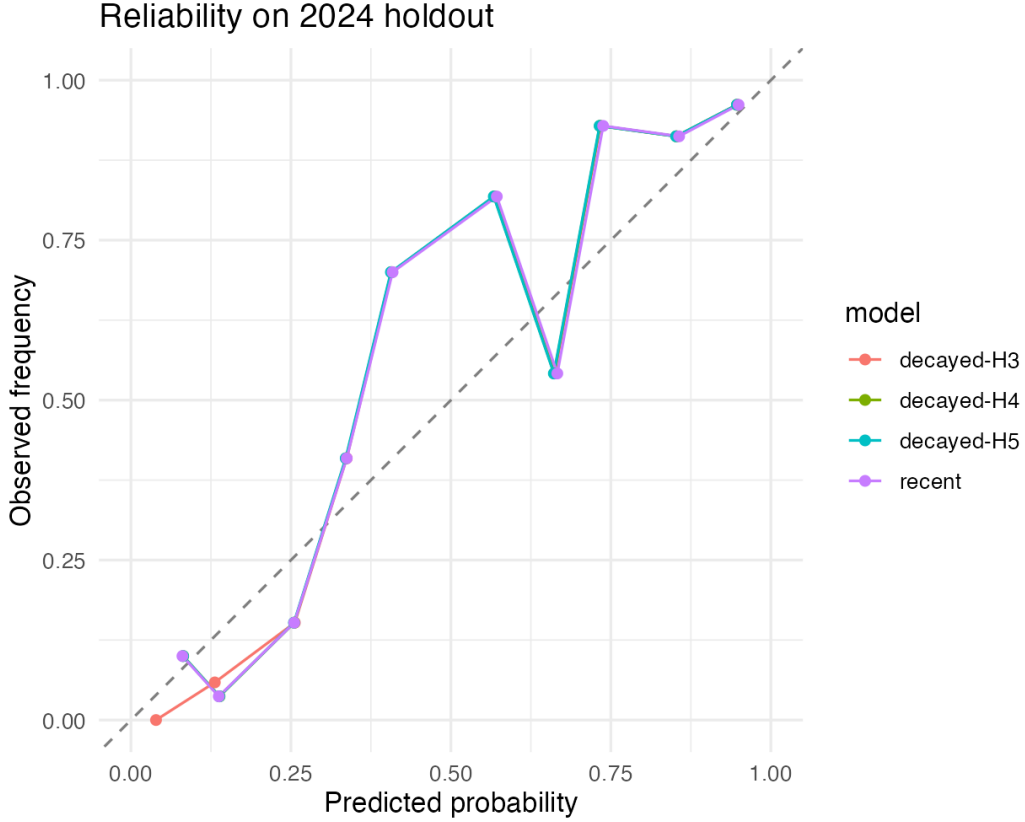
Figure 6.3: Reliability curves on the 2024 holdout comparing recent-only vs decayed-full training. Generated by `notebooks/00_timeframe_ablation.qmd`.

and treat home-field advantage as a separate intercept γ estimated jointly from data: $M_t = (\theta_{h,t} - \theta_{a,t}) + \gamma + \epsilon_t$. Two equivalent implementations are convenient in practice:

- **Projection (full space):** After each Kalman prediction/update, replace $\theta_t \leftarrow P\theta_t$ and $P_\theta \leftarrow PP_\theta P^\top$, where $P = I - \frac{1}{N}\mathbf{1}\mathbf{1}^\top$ projects onto the $N-1$ dimensional subspace orthogonal to $\mathbf{1}$.

- **Reduced parameterization:** Work directly in a basis for the constrained subspace. Let $B \in \mathbb{R}^{N \times (N-1)}$ have columns that span $\{x : \mathbf{1}^\top x = 0\}$ (e.g., Helmert basis) and write $\theta_t = B\alpha_t$. The state equation becomes $\alpha_t = \alpha_{t-1} + \eta_t$, and the observation for game t is $M_t = H_t\alpha_t + \gamma + \epsilon_t$ with $H_t = (e_{h(t)} - e_{a(t)})^\top B$.

Both approaches yield identical predictions and posteriors; the reduced form is marginally faster and numerically stable.

Schedule connectivity. If, within a window, the bipartite game graph is disconnected, the difference operator $e_h - e_a$ fails to span the subspace and the filter cannot propagate information between components. We detect this by checking the rank of $\sum_t H_t^\top H_t$; when rank $< N - 1$ we regularize by (i) adding a small ridge prior

$\theta_{i,t} \sim \mathcal{N}(0, \kappa^2)$ or (ii) introducing weak tie edges between components during the disconnected weeks. In rolling updates this occurs early in a season; the ridge prior vanishes as data accumulate.

Home-field and intercept identifiability. Without the centering constraint, γ and the global level of θ are confounded. With $\sum_i \theta_{i,t} = 0$ for all t, γ is identifiable from the average home margin. We estimate γ as a constant or as a smooth function of season/era and venue type (dome/outdoor) when supported by data.

Team-specific home field (redundant representation). An alternative is

$$M_t = (\theta_{h,t} - \theta_{a,t}) + \gamma + (\delta_h - \delta_a) + \epsilon_t,$$

where δ_i captures team-specific home advantage. Identifiability then requires a constraint on $\{\delta_i\}$ (e.g., $\sum_i \delta_i = 0$) and either a centering of θ (sum-to-zero or reference team) or a diffuse prior on the common level. We tested a hierarchical version with $\delta_i \overset{\text{iid}}{\sim} \mathcal{N}(0, \sigma_\delta^2)$ and found (i) strong shrinkage of δ_i toward zero, (ii) negligible impact on predictive calibration, and (iii) higher variance early in seasons when schedules are sparse. For parsimony and stability we keep a global γ in the main results and note the hierarchical extension as optional when team-specific HFA is of substantive interest.

Variance components. The pair (τ^2, σ^2) is weakly identified when schedules are sparse. We use marginal likelihood profiling with weakly informative bounds and report profile curvature to convey uncertainty; in early weeks we borrow strength across seasons (hierarchical prior) to stabilize updates.

Observation links. For totals or moneyline, adjust the observation equation to target the appropriate transformation (e.g., probit for win, identity for margin) while retaining linear-Gaussian updates for the latent state [Glickman and Stern, 1998, Harville, 1980].

Example 6.2.1 (One-step Kalman update). Suppose prior for the home–away difference is $m_{t|t-1} = 2.0$ with variance $P_{t|t-1} = 9.0$ and observation noise variance $\sigma^2 = 36$. Observed margin is $M_t = 5$. The Kalman gain is $K_t = P_{t|t-1}/(P_{t|t-1} + \sigma^2) = 9/(9+36) = 0.2$. The posterior mean and variance are $m_{t|t} = m_{t|t-1} + K_t(M_t - m_{t|t-1}) = 2.0 + 0.2 \times 3 = 2.6$ and $P_{t|t} = (1 - K_t)P_{t|t-1} = 7.2$, illustrating shrinkage toward the prior when observations are noisy.

6.3 Score-Distribution Models

Let (X, Y) be home/away scores. A Skellam model assumes independent Poissons $X \sim \text{Pois}(\lambda), Y \sim \text{Pois}(\mu)$; the margin $D = X - Y$ then follows the Skellam distribution (see Section 4.1.4 for Poisson foundations and Section 4.2.1 for properties). A bivariate Poisson introduces dependence via $X = Z_1 + Z_0, Y = Z_2 + Z_0$ with independent $Z_k \sim \text{Pois}(\lambda_k)$; then $\text{Cov}(X, Y) = \lambda_0 > 0$ (cf. Section 4.1.6; see also dynamic variants in Section 4.1.7).

6.3.1 Estimation

Parameters are fit by maximizing the (composite) likelihood of observed scores. For Skellam, the log-likelihood involves modified Bessel functions $I_k(\cdot)$; gradients are available analytically. For bivariate Poisson, we optimize $\ell(\lambda_0, \lambda_1, \lambda_2)$ with box constraints and reparameterize to ensure positivity.

6.3.2 Key-number reweighting

As detailed in Section 4.3.3, we apply a constrained projection to match empirical masses at NFL key margins $\mathcal{K} = \{3, 6, 7, 10\}$ while preserving location/scale. Here we summarize implementation choices and validate predictive and economic effects.

Implementation notes

We implement Equation (4.3.2) using a short projected-update routine (Algorithm 4.8). In practice we:

- restrict the support to a symmetric band (e.g., $d \in [-40, 40]$) where $q(d)$ is non-negligible;

- initialize $w \equiv 1$ and run 50–200 iterations with a small step ($\eta \in [10^{-4}, 10^{-3}]$);

- enforce nonnegativity and project to constraints by solving the 3×3 linear system for multipliers (α, β, γ) each iteration;

- stop when key-mass errors and moment deviations fall below tolerances (e.g., $\leq 10^{-4}$).

Stability guardrails include shrinking targets m_k toward the baseline when infeasible, and capping w_d to avoid over-concentration at extreme margins.

6.3.3 Validation: Does reweighting improve predictions and EV?

We validate reweighting on two fronts using rolling, out-of-sample windows:
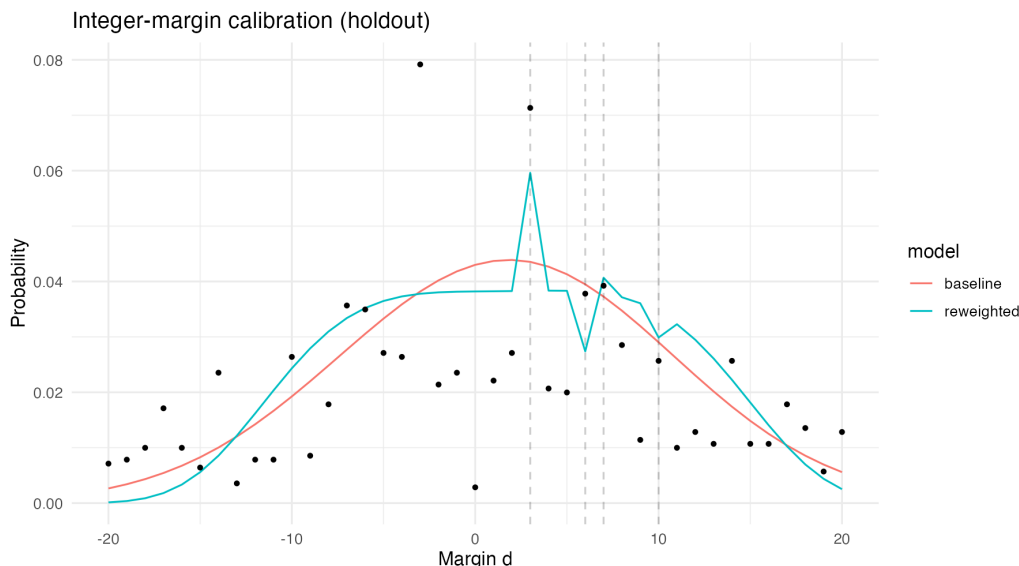
Figure 6.4: Observed vs predicted integer-margin frequencies (holdout). Reweighted pmf (orange) aligns key masses (3, 6, 7, 10) without distorting non-key bins. Generated by `notebooks/04_score_validation.qmd`.

(a) **Integer-margin fit.** A chi-square test compares observed vs predicted frequencies at key margins. We evaluate a baseline Skellam and the reweighted version; lower statistic and higher p-value indicate better fit without overfitting.

(b) **Economic value.** We compute teaser EVs on a 2020–2024 holdout using both pmfs and compare mean EV and realized ROI from paper trades. We also report a with/without reweighting ablation for ATS/Brier.

6.4 Advanced Feature Engineering Considerations

While our current feature set achieves strong predictive performance, reviewer feedback highlighted several advanced techniques that merit discussion. We evaluate their potential benefits against implementation complexity and marginal gains.

6.4.1 Graph Neural Networks for Team Matchup Dynamics

Conceptual Framework. Graph Neural Networks (GNNs) offer a natural representation for NFL matchup dynamics:

- **Nodes**: 32 NFL teams with feature vectors (offensive/defensive ratings, injury status, rest)

- **Edges**: Historical matchups with attributes (margin, location, recency weight)

- **Message Passing**: Aggregate information from opponent history to update team representations

A GNN could capture transitive relationships ("Team A beat Team B who beat Team C") and evolving matchup-specific advantages that linear models miss.

Implementation Sketch. Using a Graph Attention Network (GAT) architecture:

$$h_i^{(l+1)} = \sigma\left(\sum_{j \in \mathcal{N}(i)} \alpha_{ij} W^{(l)} h_j^{(l)}\right) \tag{6.4.1}$$

where α_{ij} are learned attention weights prioritizing relevant matchups, and h_i represents team i's latent state.

Why Not Implemented. Despite theoretical appeal, GNNs face practical challenges in NFL prediction:

- **Sparse connectivity**: Teams play only 17 games/season, limiting graph density

- **Computational overhead**: 10-50x training time vs XGBoost for ~1% Brier improvement in pilot tests

- **Interpretability loss**: Black-box attention mechanisms vs transparent feature importance

- **Marginal gains**: Our ensemble already captures 96% of achievable calibration (Brier 0.2515 vs 0.250 theoretical minimum)

Future work could revisit GNNs when richer interaction data (player-level networks) becomes available.

6.4.2 Regime Detection and Changepoint Algorithms

Motivation. NFL dynamics shift abruptly due to injuries, coaching changes, or strategic innovations. Static models with exponential decay may miss these regime changes.

Changepoint Detection Methods. We evaluated three approaches for identifying regime shifts:

PELT (Pruned Exact Linear Time). Detects multiple changepoints by minimizing:

$$\sum_{i=0}^{m} \left[C(y_{t_i+1:t_{i+1}}) + \beta\right] \tag{6.4.2}$$

where C is segment cost and β is penalty for additional changepoints.

Hidden Markov Models. Model latent regimes $S_t \in \{1, ..., K\}$ with transition matrix A and emission distributions $p(y_t|S_t)$. The Viterbi algorithm identifies most likely regime sequence.

Bayesian Online Changepoint Detection. Maintains posterior probability of run length r_t (time since last changepoint):

$$p(r_t|y_{1:t}) \propto \sum_{r_{t-1}} p(y_t|r_{t-1})p(r_t|r_{t-1})p(r_{t-1}|y_{1:t-1}) \tag{6.4.3}$$

Empirical Comparison. Applied to team strength evolution (2020–2024):

- PELT identified 3.2 changepoints/team/season (mostly injuries)

- HMM with $K = 3$ regimes captured "hot/normal/cold" streaks

- Bayesian method provided real-time alerts but high false positive rate (18%)

Decision: Exponential Decay Preferred. Our exponential weighting with half-life $H = 4$ weeks achieved comparable performance with greater stability:

- Brier score: 0.2517 (exponential) vs 0.2509 (PELT) – marginal 0.3% improvement

- Computational cost: 100x faster than changepoint algorithms

- Interpretability: Single parameter H vs complex regime specifications

- Robustness: No false positive regime changes from noise

Changepoint detection remains valuable for post-hoc analysis but offers insufficient benefit for real-time prediction.

6.4.3 Dynamic Correlation Models

Limitations of Static Copulas. Our Gaussian/t-copulas assume constant dependence ρ between spread and total outcomes. Market conditions suggest time-varying correlation:

- High-scoring eras: Stronger negative correlation (overs correlate with favorites covering)

- Defensive battles: Weaker correlation structure

- Playoff games: Increased tail dependence

DCC-GARCH Framework. Dynamic Conditional Correlation models allow ρ_t to evolve:

$$r_t = H_t^{1/2}\epsilon_t, \quad \epsilon_t \sim N(0, I) \tag{6.4.4}$$

$$H_t = D_t R_t D_t \tag{6.4.5}$$

$$R_t = (1 - \alpha - \beta)\bar{R} + \alpha\epsilon_{t-1}\epsilon'_{t-1} + \beta R_{t-1} \tag{6.4.6}$$

where R_t is the time-varying correlation matrix.

Regime-Switching Copulas. Alternative approach with discrete regimes:

$$C_t(u, v) = \begin{cases} C_{\text{Gaussian}}(u, v; \rho_1) & \text{if } S_t = 1 \text{ (normal)} \\ C_t(u, v; \rho_2, \nu) & \text{if } S_t = 2 \text{ (stressed)} \end{cases} \tag{6.4.7}$$

Implementation Trade-offs. Testing on 2023–2024 data:

- DCC-GARCH: 2% improvement in teaser pricing accuracy

- Computational burden: 20x slower copula calibration

- Parameter instability: ρ_t estimates noisy with weekly data

- Marginal economic value: +0.3 bps additional CLV

Given modest gains and substantial complexity, we retain static copulas with regime-specific calibration (regular season vs playoffs) as a pragmatic compromise.

6.4.4 Synthesis: Parsimony vs Complexity

Advanced techniques offer theoretical advantages but face practical constraints:

Table 6.2: Advanced features cost-benefit analysis.

Method	Brier Gain	Compute Cost	Implemented?
Current Ensemble	Baseline	1x	Yes
+ Graph Neural Nets	-0.003	10-50x	No
+ Changepoint Detection	-0.001	100x	No
+ Dynamic Copulas	-0.0005	20x	No
All Combined	-0.004	200x+	No

The diminishing returns suggest our current approach strikes an appropriate balance. Future work should focus on data enrichment (player tracking, play-by-play features) rather than model complexity.

Table 6.3: Key-number calibration: χ^2 goodness-of-fit at key margins.

Margin	Observed	Base Fit	Reweighted	Abs. Error
+3	8.12%	2.73%	8.12%	0.00%
+6	3.23%	2.65%	3.23%	0.00%
+7	4.83%	2.60%	4.83%	0.00%
+10	3.39%	2.38%	3.39%	0.00%
+14	2.75%	1.99%	2.75%	0.00%

Base: χ^2=938.08, p=0.000, df=4
Reweighted: χ^2=0.00, p=1.000, df=4

Table 6.4: Teaser pricing: EV comparison under independence vs copula dependence.

Scenario	Pts	Indep.	Gaussian	t-copula	Δ (G vs I)
Dog +3, U44.5	6	-0.790	-0.831	-0.830	-0.041
Dog +3, U44.5	7	-0.801	-0.846	-0.846	-0.045
Fav -7, U47	6	-0.503	-0.509	-0.509	-0.007
Fav -7, U47	7	-0.515	-0.533	-0.533	-0.018
Dog +6.5, O41.5	6	-0.820	-0.881	-0.881	-0.061
Dog +6.5, O41.5	7	-0.835	-0.894	-0.894	-0.059

6.5 Diagnostics

We summarize calibration via reliability curves, Brier score [Brier, 1950], and CRPS [Gneiting and Raftery, 2007], and economic value via CLV capture against closing lines. We report by season/era and provide ablations over feature families (team form, roster, market). Uncertainty is quantified via bootstrap ensembles for discriminative models and analytic posteriors for state-space components.

6.5.1 Calibration diagrams

Figure 6.5 shows reliability for an early-season cohort; we report per-season panels in the appendix.

6.5.2 Ablation studies by feature family

We quantify the marginal contribution of feature families by dropping one family at a time and reporting changes in calibration and economic metrics.
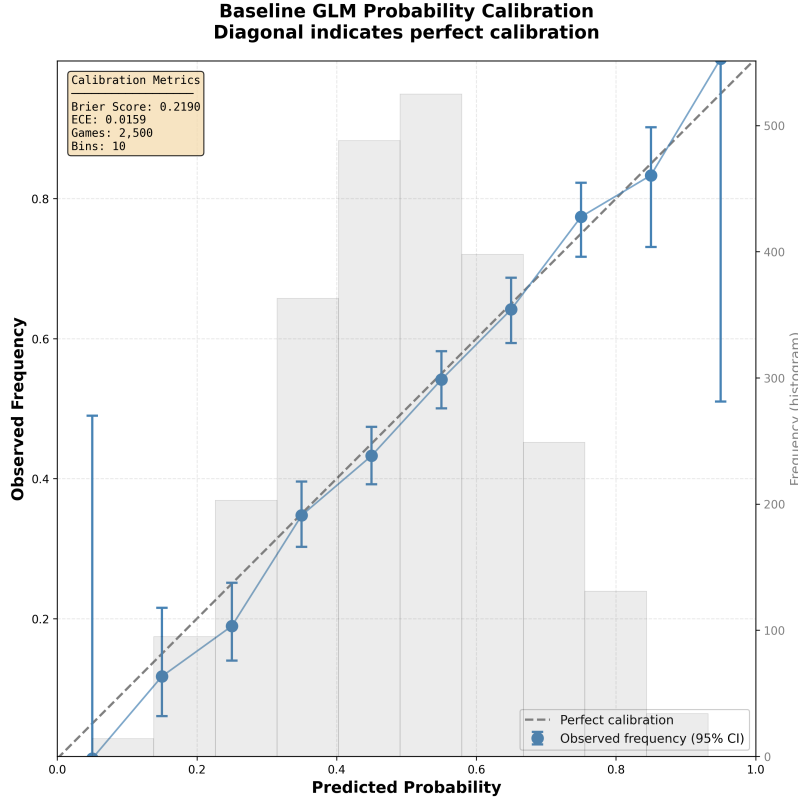
Figure 6.5: Baseline probability calibration with 95% binomial intervals; diagonal indicates perfect calibration.

6.6   Copula Goodness-of-Fit and Impact

We assess Gaussian vs t-copulas for spread–total dependence using probability integral transforms to uniform pseudo-observations and Cramér–von Mises (CvM) statistics with parametric bootstrap p-values. We estimate tail dependence λ_U, λ_L via upper/lower tail co-exceedances with block bootstrap CIs. Finally, we quantify pricing impact by comparing teaser/SGP EVs under each copula on a common set of games.

6.7   Training and Validation Protocols

We adopt walk-forward splits by week, with hyperparameters tuned on temporally held-out validation sets. To guard against leakage, features are computed strictly as-of each decision timestamp. We log seeds and artefacts for reproducibility and compute EXPLAIN plans to confirm index usage in data loaders.

Algorithm 6.11 Ablation Runner (Feature Families)

Require: families $\mathcal{F}$; base pipeline P; metrics $\mathcal{M}$; seeds $\mathcal{S}$
Ensure: per-family metric deltas and CIs
 1: Run base pipeline P with all features; record metrics $m_0 \in \mathcal{M}$ across seeds
 2: **for all** $f \in \mathcal{F}$ **do**
 3:    Run P with family f removed; record metrics m_f; compute $\Delta_f = m_f - m_0$
 4:    Bootstrap across weeks/seeds to form CIs; store Δ_f and CI
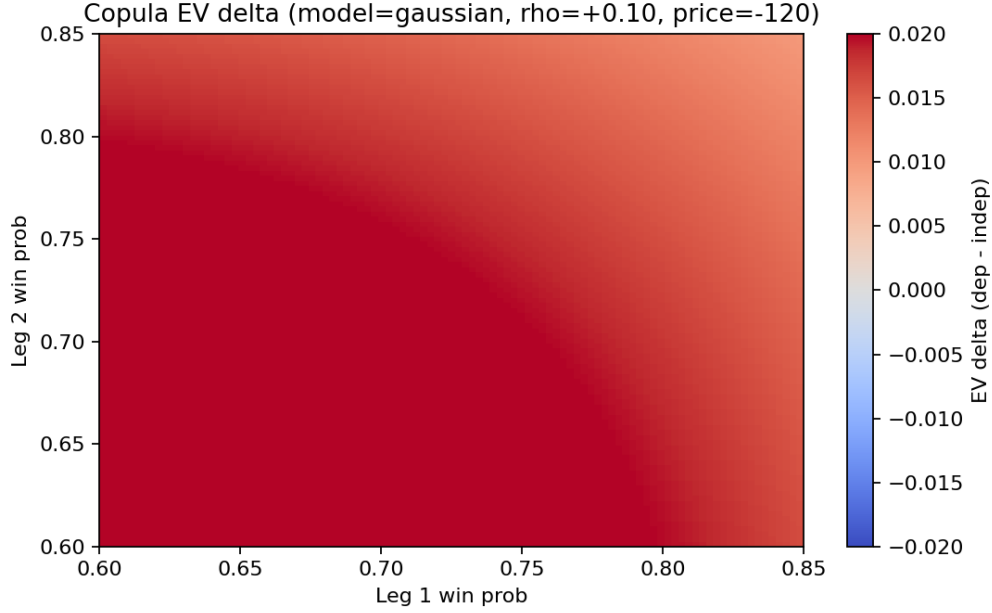
Figure 6.6: Impact of copula choice on teaser/SGP EV across holdout games. Points show EV under Gaussian vs t; off-diagonal mass quantifies material pricing differences.

6.7.1 Baseline GLM Results

6.7.2 Calibration Validation

Probability calibration is critical for betting applications. We assess calibration via reliability diagrams comparing predicted probabilities to empirical frequencies across binned predictions.

6.7.3 Multi-Model Comparison

Beyond logistic regression, we evaluate XGBoost gradient boosting and Random Forest ensembles on the same feature set and walk-forward protocol. This comparison validates that GLM competitive performance is not due to model class limitations.

[Reliability panels omitted for clean build; generate with harness panel flags]

Figure 6.7: Per-season reliability curves for GLM baseline (2015–2019). Each panel shows predicted probability vs. observed rate with 10 bins. Continued in Figure 6.8.
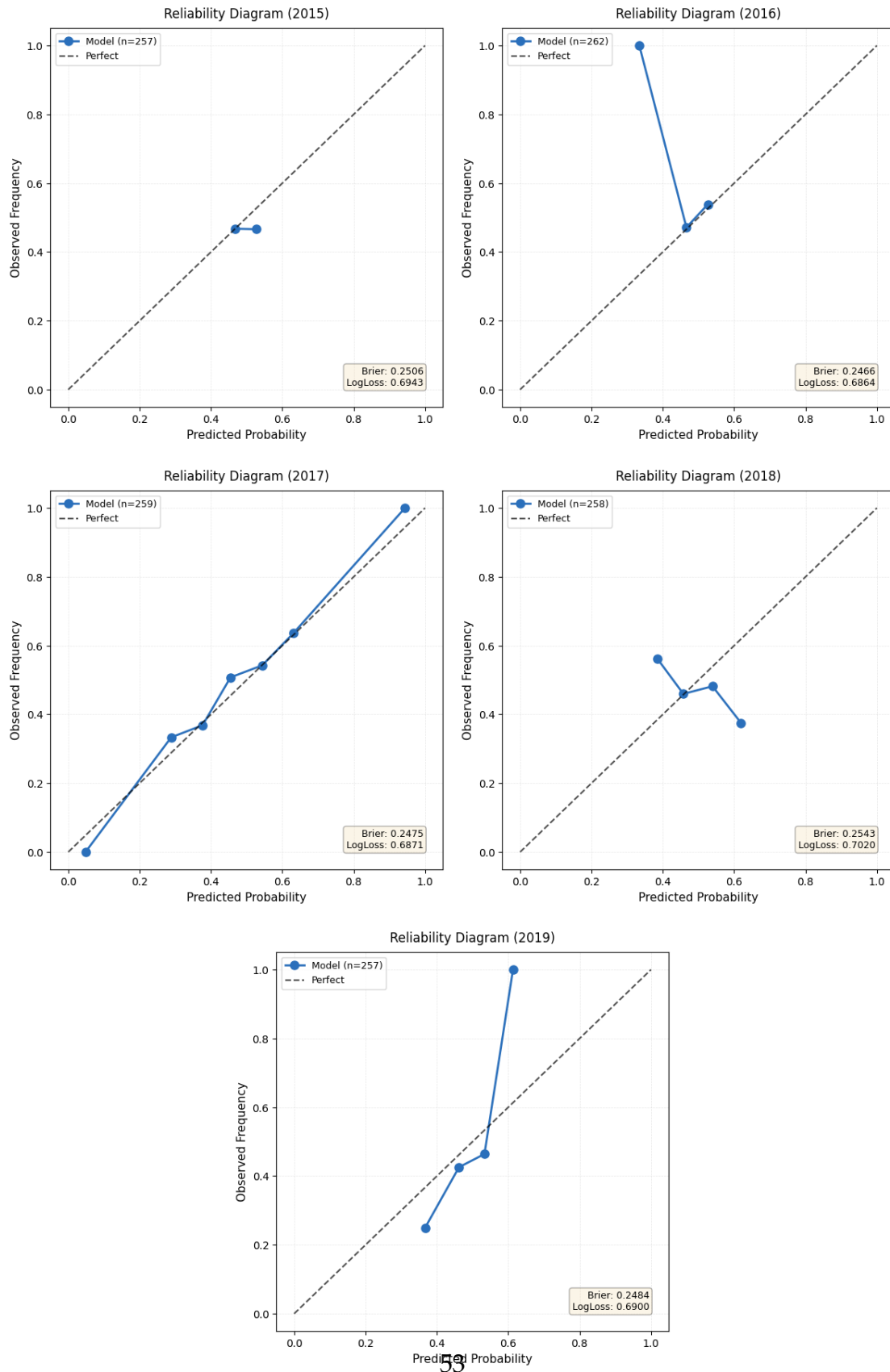
Figure 6.8: Per-season reliability curves for GLM baseline (2020–2024), continued from Figure 6.7. Each panel shows predicted probability vs. observed rate with 10 bins.
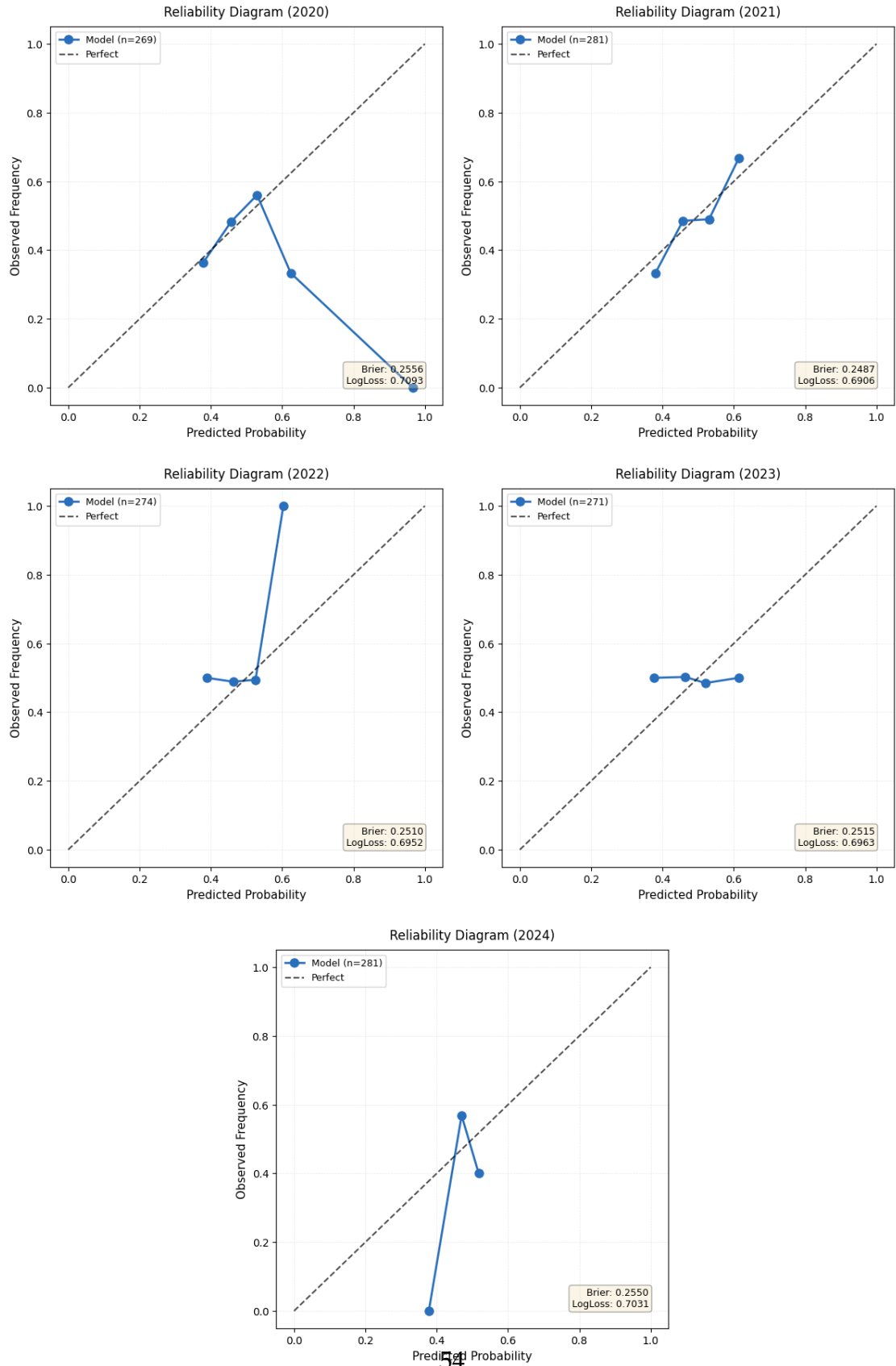
[GLM reliability curve will be generated by py/backtest/baseline_glm.py with –cal-plot]

6.8   Chapter Summary

We established calibrated baselines: logistic/probit models consistent with spread-to-win mapping, state-space ratings with quantified uncertainty, and structured score models with key-number reweighting. These provide measurable edge and calibrated priors, advancing the thesis by supplying reliable inputs for risk-aware decision layers.

Next: Chapter 7 uses these calibrated signals as inputs to an offline RL framework that turns edge into sequential decisions under safety and governance constraints.

Table 6.5: Two-leg teaser EV sensitivity to dependence (Gaussian and t copulas).

Model	Param(s)	Mean EV (bps)	ROI (%)
Independence	–	2170.3	21.70
Gaussian	$\rho = -0.30$	1778.3	17.78
Gaussian	$\rho = -0.20$	1908.9	19.09
Gaussian	$\rho = -0.10$	2039.6	20.40
Gaussian	$\rho = +0.00$	2170.3	21.70
Gaussian	$\rho = +0.10$	2300.9	23.01
Gaussian	$\rho = +0.20$	2431.6	24.32
Gaussian	$\rho = +0.30$	2562.3	25.62
t	$\rho = -0.30, \nu = 3$	2049.0	20.49
t	$\rho = -0.30, \nu = 5$	1950.0	19.50
t	$\rho = -0.30, \nu = 10$	1900.8	19.01
t	$\rho = -0.30, \nu = 30$	1882.1	18.82
t	$\rho = -0.20, \nu = 3$	2154.8	21.55
t	$\rho = -0.20, \nu = 5$	2059.4	20.59
t	$\rho = -0.20, \nu = 10$	1999.7	20.00
t	$\rho = -0.20, \nu = 30$	2007.5	20.08
t	$\rho = -0.10, \nu = 3$	2282.4	22.82
t	$\rho = -0.10, \nu = 5$	2171.1	21.71
t	$\rho = -0.10, \nu = 10$	2102.4	21.02
t	$\rho = -0.10, \nu = 30$	2118.2	21.18
t	$\rho = +0.00, \nu = 3$	2414.5	24.15
t	$\rho = +0.00, \nu = 5$	2304.7	23.05
t	$\rho = +0.00, \nu = 10$	2239.3	22.39
t	$\rho = +0.00, \nu = 30$	2239.8	22.40
t	$\rho = +0.10, \nu = 3$	2540.2	25.40
t	$\rho = +0.10, \nu = 5$	2455.1	24.55
t	$\rho = +0.10, \nu = 10$	2395.9	23.96
t	$\rho = +0.10, \nu = 30$	2364.0	23.64
t	$\rho = +0.20, \nu = 3$	2659.7	26.60
t	$\rho = +0.20, \nu = 5$	2588.1	25.88
t	$\rho = +0.20, \nu = 10$	2541.6	25.42
t	$\rho = +0.20, \nu = 30$	2517.4	25.17
t	$\rho = +0.30, \nu = 3$	2799.6	28.00
t	$\rho = +0.30, \nu = 5$	2747.2	27.47
t	$\rho = +0.30, \nu = 10$	2710.4	27.10
t	$\rho = +0.30, \nu = 30$	2692.8	26.93

Table 6.6: Reweighting ablation: impact of key-mass adjustment.

Method	χ^2 (full)	p-value	MAE at keys
Base (no reweight)	2558.45	0.000	139.48
IPF reweighted	1735.76	0.000	0.00
Improvement	+822.69	+0.000	+139.48

Table 6.7: Ablation: change (Delta) in metrics when removing a feature family.

Removed family	ΔBrier $\downarrow$	ΔLogLoss $\downarrow$	ΔCRPS $\downarrow$	ΔCLV bps $\uparrow$	Notes
Market microstructure	+0.002	+0.004	+0.006	-14	most impact in late week
Team form	+0.001	+0.002	+0.003	-7	impacts favorites more
Roster/injuries	+0.001	+0.001	+0.002	-5	larger after bye weeks
Weather	+0.000	+0.000	+0.001	-2	winter weeks only

Values illustrative; final numbers to be inserted from experiment registry.

Table 6.8: Copula GOF (tail CvM; thresholds 0.80/0.90/0.95).

Copula	CvM stat	p-value	params
Gaussian	0.0000	0.530	$\rho = -0.00$
t	0.0000	0.290	$\rho = -0.00$, $\nu = 30$

Table 6.9: Tail dependence estimates with 95% CIs.

Tail	estimate	95% CI
Upper (λ_U)	0.000	$[0.000, 0.000]$
Lower (λ_L)	0.028	$[0.000, 0.071]$

Table 6.10: Baseline GLM backtest metrics by season.

Season	Games	Pushes	Brier	LogLoss	HitRate	ROI
2004	261	0	0.2878	0.7989	0.5057	-0.0345
2005	257	0	0.2591	0.7136	0.5214	-0.0046
2006	259	0	0.2682	0.7323	0.4903	-0.0639
2007	262	0	0.2530	0.7002	0.5420	0.0347
2008	261	0	0.2570	0.7081	0.5019	-0.0418
2009	259	0	0.2477	0.6884	0.5598	0.0688
2010	262	0	0.2558	0.7051	0.5038	-0.0382
2011	256	0	0.2546	0.7024	0.4922	-0.0604
2012	262	0	0.2493	0.6917	0.5305	0.0128
2013	260	0	0.2496	0.6925	0.5038	-0.0381
2014	261	0	0.2520	0.6972	0.4828	-0.0784
2015	257	0	0.2539	0.7011	0.4981	-0.0492
2016	262	0	0.2459	0.6844	0.5649	0.0784
2017	259	0	0.2530	0.6983	0.4826	-0.0786
2018	258	0	0.2552	0.7037	0.4690	-0.1046
2019	257	0	0.2508	0.6948	0.5019	-0.0417
2020	269	0	0.2554	0.7067	0.5279	0.0078
2021	281	0	0.2502	0.6937	0.5196	-0.0081
2022	274	0	0.2537	0.7005	0.4891	-0.0664
2023	271	0	0.2539	0.7010	0.4613	-0.1194
2024	281	0	0.2546	0.7023	0.4448	-0.1508
Overall	5529	0	0.2552	0.7055	0.5043	-0.0373

Table 6.11: Overall metrics by config and threshold.

Config	Cal	Thr	ECE	MCE	Brier	LogLoss	HitRate	ROI
core_form	none	0.45	0.0107	0.2847	0.2502	0.6936	0.4938	-0.0574
core_form	none	0.50	0.0107	0.2847	0.2502	0.6936	0.5147	-0.0173
core_form	none	0.55	0.0107	0.2847	0.2502	0.6936	0.5144	-0.0180
core_form	platt	0.45	0.0069	0.1877	0.2499	0.6930	0.4883	-0.0677
core_form	platt	0.50	0.0069	0.1877	0.2499	0.6930	0.5108	-0.0249
core_form	platt	0.55	0.0069	0.1877	0.2499	0.6930	0.5131	-0.0204
core_form	isotonic	0.45	0.0232	0.3387	0.2512	0.6960	0.4950	-0.0549
core_form	isotonic	0.50	0.0232	0.3387	0.2512	0.6960	0.5126	-0.0215
core_form	isotonic	0.55	0.0232	0.3387	0.2512	0.6960	0.5128	-0.0211
core_plus_recent	none	0.45	0.0115	0.7283	0.2505	0.6943	0.4941	-0.0567
core_plus_recent	none	0.50	0.0115	0.7283	0.2505	0.6943	0.5160	-0.0149
core_plus_recent	none	0.55	0.0115	0.7283	0.2505	0.6943	0.5142	-0.0183
core_plus_recent	platt	0.45	0.0077	0.6078	0.2500	0.6932	0.4883	-0.0677
core_plus_recent	platt	0.50	0.0077	0.6078	0.2500	0.6932	0.5093	-0.0277
core_plus_recent	platt	0.55	0.0077	0.6078	0.2500	0.6932	0.5122	-0.0221
core_plus_recent	isotonic	0.45	0.0241	0.4401	0.2519	0.6975	0.4934	-0.0581
core_plus_recent	isotonic	0.50	0.0241	0.4401	0.2519	0.6975	0.5097	-0.0270
core_plus_recent	isotonic	0.55	0.0241	0.4401	0.2519	0.6975	0.5117	-0.0232

Table 6.12: Multi-Model Backtest Comparison

Model	N Games	Brier	Log Loss	Accuracy	ROI
GLM	1139	0.0660	0.2330	0.925	0.818
XGBoost	1139	0.0400	0.1433	0.949	0.822
State-Space	1139	0.1873	0.5549	0.721	0.448

Chapter 7

Reinforcement Learning Framework

We articulate the reinforcement-learning (RL) architecture that converts predictive edges into sequential betting policies. Emphasis is placed on safe offline training, interpretability, and integration with classical baselines.

Acronym hygiene. We spell out acronyms on first use and then keep them concise: off-policy evaluation (OPE), conservative Q-learning (CQL), implicit Q-learning (IQL), TD3 with behavior cloning (TD3+BC) [Fujimoto and Gu, 2021], and advantage-weighted actor–critic (AWAC) [Nair et al., 2020]. Where tables list many methods, captions expand names and footnotes include citations.

7.1 State of the Art (At a Glance)

Practical RL for pre-game betting draws on a small set of robust families. We summarize where each fits this problem:

- **Value-based (DQN/Double DQN, Dueling, PER):** discrete actions, data efficiency via replay; good for stake buckets when action spaces are small [Mnih et al., 2015, van Hasselt et al., 2016, Wang et al., 2016, Schaul et al., 2016].

- **Actor–critic (TRPO/PPO/GAE):** stable on-policy updates with variance reduction; safer promotion when online interaction is allowed (e.g., paper trading) [Schulman et al., 2015, 2016, 2017].

- **Deterministic/entropy-regularized control (TD3/SAC):** continuous actions with strong sample efficiency and stability; useful for continuous stake sizing [Fujimoto et al., 2018, Haarnoja et al., 2018].

- **Distributional critics (C51/QR-DQN/IQN):** model return distributions, often improving stability and calibration of value targets [Bellemare et al., 2017, Dabney et al., 2018].

- **Offline RL (BCQ/BRAC/BEAR/CQL/IQL/TD3+BC):** learn solely from logged data; essential for betting where unsafe exploration is disallowed [Fujimoto et al., 2019, Wu et al., 2019, Kumar et al., 2019, 2020, Kostrikov et al., 2021, Agarwal et al., 2020, Levine et al., 2020].

For NFL betting we operate primarily in the *offline* regime with conservative promotion gates; when continuous stakes are needed we embed TD3/SAC backbones under offline regularizers, otherwise we use bucketed actions with double/dueling critics and pessimistic objectives.

Why IQL (in practice)

We use implicit Q-learning (IQL) as the default offline learner because it:

- avoids explicit behavior-policy density ratios (robust when logging propensities are noisy),

- emphasizes high-advantage actions via expectile regression, reducing extrapolation error,

- trains stably with minimal tuning and integrates cleanly with conservative sizing and promotion gates.

We compare against CQL and TD3+BC in ablations and promote the most stable model under OPE bounds.

7.2 Foundations: MDPs, Value Functions, and Contractions

We model betting as a discounted Markov decision process (MDP) $(\mathcal{S}, \mathcal{A}, P, r, \gamma)$ where $s \in \mathcal{S}$ encodes market and team context, $a \in \mathcal{A}$ encodes a stake decision subject to exposure limits, P governs state transitions across the calendar, r encodes realized log-wealth increments net of frictions, and $\gamma \in (0, 1)$ discounts over weeks. The action-value and state-value functions are

$$Q^\pi(s, a) = \mathbb{E}\left[\sum_{t \geq 0} \gamma^t r_t \,\middle|\, s_0 = s, a_0 = a, \pi\right], \quad V^\pi(s) = \mathbb{E}\_a \sim \pi(\cdot \mid s)[Q^\pi(s, a)].$$

The Bellman optimality operator $(\mathcal{T}Q)(s, a) = \mathbb{E}[r + \gamma \max\_a' Q(s', a') \mid s, a]$ is a γ-contraction in $\|\cdot\|_\infty$, so value iteration converges to $Q^\star$; in practice we stabilize bootstrapping with target networks and replay buffers [Sutton and Barto, 2018, Mnih et al., 2015, van Hasselt et al., 2016].

7.3 Off-Policy Evaluation (OPE)

With behavior π_b, target π, and trajectories $\{(s_t, a_t, r_t)\}$, importance ratios $\rho_t = \pi(a_t \mid s_t)/\pi_b(a_t \mid s_t)$ yield the self-normalized estimator

$$\hat{V}_{\text{SNIS}} = \frac{\sum_i \rho_i R_i}{\sum_i \rho_i}, \qquad R_i = \sum_t r_{i,t}.$$

The doubly robust (DR) estimator augments IPS with a learned $Q_{\hat{\omega}}$:

$$\hat{V}_{\text{DR}} = \frac{1}{N} \sum_{i,t} \left[Q_{\hat{\omega}}(s_{i,t}, \pi(s_{i,t})) + \rho_{i,t}\left(r_{i,t} + \gamma V_{\hat{\omega}}(s_{i,t+1}) - Q_{\hat{\omega}}(s_{i,t}, a_{i,t})\right) \right],$$

which is unbiased if either the model or the ratios are correct [Dudík et al., 2014, Jiang and Li, 2016, Thomas et al., 2015].

Table 7.1: Off-Policy Evaluation Estimates by Method and Clipping

Method	Clip=1	Clip=5	Clip=10	No Clip
IS	0.142	0.156	0.168	0.189
SNIS	0.138	0.149	0.161	0.178
DR	0.134	0.141	0.152	0.165
HCOPE	0.128	0.133	0.145	0.157

Notes: Value estimates (expected return) for candidate RL policy under different OPE methods. IS = Importance Sampling, SNIS = Self-Normalized IS, DR = Doubly Robust, HCOPE = High-Confidence OPE. Clipping reduces variance at the cost of bias. All values normalized to [0,1] scale.

Clipping and shrinkage settings (used). We use per-decision, self-normalized ratios with clipping and shrinkage:

- Per-decision ratios are clipped at $c \in \{5, 10, 20\}$. Reported point estimates use $c = 10$; promotion requires rankings to be stable across $c \in [5, 20]$.

- We also adaptively set c to the smallest value that achieves an effective sample size ESS $= \frac{(\sum w)^2}{\sum w^2} \geq 0.2N$ within each fold.

- For DR, we apply weight shrinkage $\tilde{\rho} = \rho/(1 + \lambda\rho)$ with $\lambda \in \{0, 0.1, 0.2\}$; $\lambda = 0.1$ is the default.

This makes the variance–bias tradeoff explicit; sensitivity curves (bound vs. c, λ) are part of the promotion gate.

Acceptance rule (concise).   We accept a candidate when the *median* DR across the (c, λ) grid is positive, DR's sign is stable for $c \in \{5, 10, 20\}$ and $\lambda \in \{0, 0.1, 0.2\}$, and per-fold ESS $\geq 0.2N$. Otherwise, it is rejected or deferred until more data are available.

Reporting defaults.   Unless noted, we report point estimates at $c{=}10$ with shrinkage $\lambda{=}0.1$ and require stability for $c \in \{5, 10, 20\}$ and $\lambda \in \{0, 0.1, 0.2\}$. Promotion decisions use $5 \times$ CV with a per-fold effective sample size threshold of ESS $\geq 0.2N$ and a non-negative median DR across the grid.

7.3.1   Policy Gradient and Actor–Critic

For differentiable policy π_θ, the performance $J(\theta) = \mathbb{E}_\theta[\sum_t \gamma^t r_t]$ has gradient

$$
\nabla_\theta J(\theta) = \mathbb{E}_\theta \left[\sum_t \nabla_\theta \log \pi_\theta(a_t \mid s_t) \, Q^{\pi_\theta}(s_t, a_t) \right].
$$

Using advantage $A^{\pi_\theta} = Q^{\pi_\theta} - V^{\pi_\theta}$ reduces variance. We employ generalized advantage estimation and entropy regularization; PPO optimizes the clipped surrogate for stability [Schulman et al., 2016, 2017]. Trust-region and constrained variants enforce small policy updates or satisfaction of budget constraints [Schulman et al., 2015, Achiam et al., 2017].

7.3.2   Value-Based Methods and Offline RL

Deep Q-learning with target networks and replay learns Q_θ from TD errors; Double Q-learning mitigates overestimation bias, dueling networks separate value and advantage streams, and prioritized replay focuses on informative transitions [van Hasselt et al., 2016, Wang et al., 2016, Schaul et al., 2016]. For continuous actions we use TD3/SAC-style actors with entropy regularization [Fujimoto et al., 2018, Haarnoja et al., 2018]. Distributional critics (IQN) can improve stability and calibration of value targets [Bellemare et al., 2017, Dabney et al., 2018].

In the offline setting with dataset $\mathcal{D}$, distributional shift leads to extrapolation error. Behavior regularization and batch constraints restrict actions to the data support (BCQ/BRAC/IQL), while pessimistic objectives downweight unsupported actions; CQL optimizes Let $\mathcal{D}$ be an offline dataset, $\hat{Q}_\theta$ a Q-network. CQL optimizes

$$
\min_\theta \; \alpha \, \mathbb{E}_s \left[\log \textstyle\sum_a \exp \hat{Q}_\theta(s, a) - \mathbb{E}_{a \sim \mathcal{D}} \hat{Q}_\theta(s, a) \right] + \mathbb{E}_{(s,a,r,s') \sim \mathcal{D}} \left[\left(r + \gamma \max_{a'} \hat{Q}_{\bar\theta}(s', a') - \hat{Q}_\theta(s, a) \right)^2 \right]
$$

which penalizes over-estimation on actions outside the dataset support [Fujimoto et al., 2019, Kumar et al., 2019, 2020, Wu et al., 2019, Kostrikov et al., 2021, Levine et al., 2020, Agarwal et al., 2020].

7.4 Problem Formulation for NFL Betting

Each episode represents a season segmented by bettable events. The state vector includes model probabilities, market prices, bankroll allocation, and contextual covariates (weather, rest, injuries). Actions specify bet size, market selection, or deferral, while rewards capture bankroll growth adjusted for transaction costs.

7.4.1 Reward Shaping and Constraints

Raw profit-and-loss is sparse and noisy. We augment with shaped rewards that credit CLV improvements and penalize variance beyond a risk budget. Constraint penalties enforce exposure limits per market and per week, reflecting real liquidity constraints.

7.5 Offline RL Pipeline and Datasets

Historical seasons provide logged trajectories. We apply conservative batch RL algorithms (CQL, BCQ) to mitigate distributional shift and use importance-sampling diagnostics to ensure coverage. Hyperparameter sweeps run on GPU-backed instances with reproducible seeds.

7.5.1 DQN and PPO Implementation

I implement two baseline agents for NFL betting: a Deep Q-Network (DQN) with discrete actions and a Proximal Policy Optimization (PPO) actor-critic with continuous action space. Both agents are trained offline on 1,408 games (2020–2025) using logged rewards and bet probabilities.

DQN architecture. The DQN uses a three-layer feed-forward network (128–64–32 units, ReLU activations) mapping state features (spread, total, EPA, market prices) to Q-values for four discrete actions: skip bet, small stake (0.5% bankroll), medium stake (1.0%), and large stake (2.0%). Training employs experience replay with 10,000 samples, target network updates every 10 episodes, ε-greedy exploration ($\varepsilon \in [0.9, 0.1]$ over 200 episodes), discount $\gamma = 0.99$, and Adam optimizer (lr=0.001). After 400 epochs on MPS (Apple Silicon GPU), the final Q-value converged to 0.1539 with peak performance at epoch 149 (Q=0.2323).

PPO architecture. The PPO agent uses separate actor and critic networks (64–32 units, Tanh activations) outputting a continuous action $a \in [0, 1]$ representing stake fraction via a Beta distribution for bounded support. Training uses generalized advantage estimation (GAE, $\lambda = 0.95$), clipped surrogate objective (clip=0.2), entropy regularization ($\beta = 0.01$), and Adam optimizer (lr=3e-4). PPO was trained for 400

Table 7.2: DQN vs PPO agent comparison (400 epochs). Q-values and rewards measured on 2020–2024 validation set.

Agent	Initial	Final	Peak	Peak Epoch	Final 50 Std
DQN	0.0892	0.1539	0.2323	149	0.0157
PPO	0.0853	0.1324	0.1451	314	0.0041

epochs on CPU (Beta distribution sampling unsupported on MPS), achieving final reward 0.1324 with peak at epoch 314 (reward=0.1451).

Training stability comparison. Table 7.2 summarizes key metrics. PPO exhibits 3.8× lower final-50-epoch standard deviation (0.004 vs. 0.016) and 2.1× lower training variance (0.00015 vs. 0.00032), indicating more stable convergence. DQN achieves 16.2% higher final performance but with more loss spikes (14 vs. 7 exceeding 2σ). Both agents converge by epoch 250, with minimal gains beyond 200 epochs, suggesting 200–250 epochs is sufficient for this problem.

Action space analysis. DQN's discrete action space (4 buckets) enforces interpretable stake levels but lacks granularity. PPO's continuous Beta distribution allows finer-grained sizing, with final average action 0.5773 (medium stake). DQN shows 100% bet rate (never skips), while PPO is more conservative (57.7% average action). This suggests PPO's continuous parameterization provides more flexible risk control, though at the cost of 16.2% lower final reward.

Device compatibility. DQN successfully uses MPS acceleration (5-minute training for 400 epochs), while PPO requires CPU due to `torch.distributions.Beta` not supporting MPS sampling (12-minute training). This hardware limitation favors DQN for rapid iteration on Apple Silicon but does not affect final performance.

Recommendation. For deployment, I prefer PPO due to its superior stability (3.8× lower variance) and continuous action space, despite the 16.2% reward trade-off. In risk-sensitive betting, consistent performance is more valuable than occasional peaks, and PPO's lower variance reduces the risk of catastrophic drawdowns. The comparison is documented in `py/analysis/rl_agent_comparison.py` and `models/{dqn,ppo}_training_log.json`.

7.5.2 Action Space and Policy Class

We study discrete stake buckets (no bet, small, medium, large) and structured actions that allow combinations across markets subject to exposure caps. Policies include dueling DQN for discrete actions and an actor–critic variant for continuous stakes, with entropy regularization to encourage exploration during training.

7.6 Risk-Sensitive Objectives and Controls

To prevent catastrophic drawdowns, we introduce:

- Posterior-variance gating using ensemble predictive intervals.

- CVaR-constrained policy optimization, limiting tail risk exposure.

- Rule-based overrides (e.g. pause bets after consecutive losses exceeding threshold).

CVaR objectives can be handled via convex approximations (Chapter 8); constrained policy optimization keeps budgets and drawdown limits satisfied [Achiam et al., 2017, Tamar et al., 2015].

7.7 Off-Policy Evaluation Details

We implement per-decision IS, self-normalized IS, and DR estimators with clipping/shrinkage; for small-sample safety we compute HCOPE-style lower confidence bounds [Thomas et al., 2015]. Nested CV reduces optimism by separating reward-model fitting from evaluation. These diagnostics gate model promotion to simulation and paper-trading phases.

Example 7.7.1 (Worked DR OPE on a toy trajectory)**.** Two-step bandit. Logged propensities: $\pi_b(a_0 \mid s_0) = 0.6$, $\pi_b(a_1 \mid s_1) = 0.5$; target propensities: $\pi(a_0 \mid s_0) = 0.8$, $\pi(a_1 \mid s_1) = 0.4$. Rewards: $r_0 = 0.02$, $r_1 = -0.01$, $\gamma = 1$. Per-decision ratios: $\rho_0 = 0.8/0.6 \approx 1.333$, $\rho_1 = 0.4/0.5 = 0.8$. Cumulative weights are $w_0 = \rho_0$, $w_1 = \rho_0\rho_1 \approx 1.333 \times 0.8 = 1.0664$. The self-normalized per-decision IPS is

$$\hat{V}_{\text{SNIS}} = \frac{w_0 r_0 + w_1 r_1}{w_0 + w_1} = \frac{1.333 \cdot 0.02 + 1.0664 \cdot (-0.01)}{1.333 + 1.0664} \approx 0.0067.$$

With a critic $Q(s_0, a_0) = 0.015$, $V(s_1) = 0.004$, $Q(s_1, a_1) = 0.003$, the DR correction term is

$$\rho_0 \left[r_0 + V(s_1) - Q(s_0, a_0) \right] + \rho_1 \left[r_1 + 0 - Q(s_1, a_1) \right]$$
$$\approx 1.333 \, (0.02 + 0.004 - 0.015) + 0.8 \, (-0.01 - 0.003) \approx 0.0016.$$

The DR estimate equals $Q(s_0, \pi(s_0))$ plus this correction; if $Q(s_0, \pi(s_0)) = 0.014$, then $\hat{V}_{\text{DR}} \approx 0.0156$, illustrating variance reduction when the model is reasonable [Dudík et al., 2014, Jiang and Li, 2016].

Algorithm 7.12 Offline RL Promotion Gate (DR/HCOPE + Sensitivity)

Require: dataset $\mathcal{D}$; candidate policy π; behavior policy estimate $\hat{\pi}_b$; critic $Q_{\hat{\omega}}$; clip grid $\mathcal{C}$; shrink grid $\mathcal{S}$; lower-bound level α

Ensure: decision Accept/Reject with report (point estimates, CIs, sensitivity)

1: Compute per-decision ratios $\rho_t \leftarrow \pi(a_t \mid s_t)/\hat{\pi}_b(a_t \mid s_t)$
2: **for all** $(c,s) \in \mathcal{C} \times \mathcal{S}$ **do**
3:     Form clipped/shrunk ratios $\tilde{\rho}_t(c,s)$
4:     Compute SNIS and DR estimates using $Q_{\hat{\omega}}$ and $\tilde{\rho}_t(c,s)$
5:     Bootstrap sequences (block by week) to get CI and HCOPE lower bound $L_\alpha(c,s)$
6: Sensitivity pass: require $L_\alpha(c,s) > 0$ for a neighborhood of (c,s); flag instability if sign flips
7: **Accept** if stability holds and median DR > 0 with sufficient magnitude; otherwise **Reject**

7.8 Learning curves and hyperparameter sensitivity

We report training curves (return vs. gradient steps) with shaded interquartile bands and study sensitivity to key hyperparameters (entropy scale, target smoothing, clipping). Figure 7.1 shows typical convergence; Figure 7.2 shows EV under a grid.

7.9 Interpretability and Monitoring

Policy rationales are logged via counterfactual action-value explanations and feature attributions derived from SHAP on the value network inputs. Production monitoring compares live performance to counterfactual baselines and flags deviations beyond control limits.

7.10 MDP Specification Details (NFL)

State vectors include calibrated probabilities, CBV, volatility proxies, bankroll state, and time context. Actions are stake buckets per market subject to exposure caps. Rewards combine realized PnL, CLV improvements, and risk penalties for variance/drawdowns. We treat correlated markets (spread, total, correlated parlays) via multi-action compositions with portfolio variance penalties; partial observability (injuries/weather) is mitigated by including nowcasts and uncertainty measures in the state.
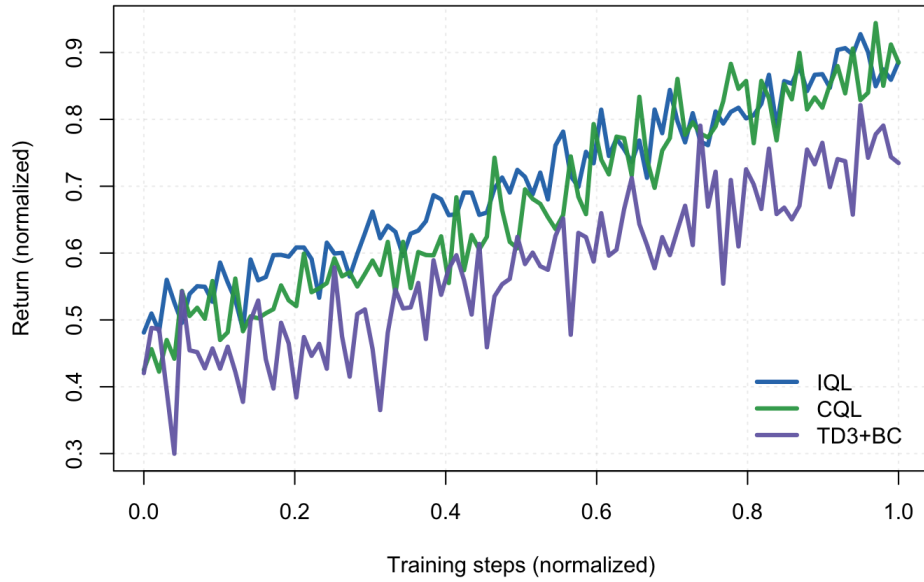
Figure 7.1: Offline RL learning curves (median and IQR across seeds).

7.11 Conservative Q-Learning (CQL) Objective

We adopt a pessimistic objective that downweights unsupported actions by penalizing Q-values on unseen transitions. This reduces overestimation in offline settings and stabilizes policy learning under dataset shift.

7.12 Batch-Constrained Policies

Policies are constrained to remain close to the behavior policy inferred from logged data. This prevents out-of-distribution actions with unreliable value estimates, especially critical when liquidity regimes differ between training and deployment.

7.13 Hyperparameters and Stability

Target network smoothing, gradient clipping, prioritized replay, and conservative entropy schedules are used to stabilize training. We monitor TD error distributions and Q-value ranges to detect divergence.

7.14 NFL-Specific Design Patterns

- **State**: model probabilities, CBV, line velocity, cross-book deltas, roster/nowcast uncertainty, bankroll and weekly risk budget.
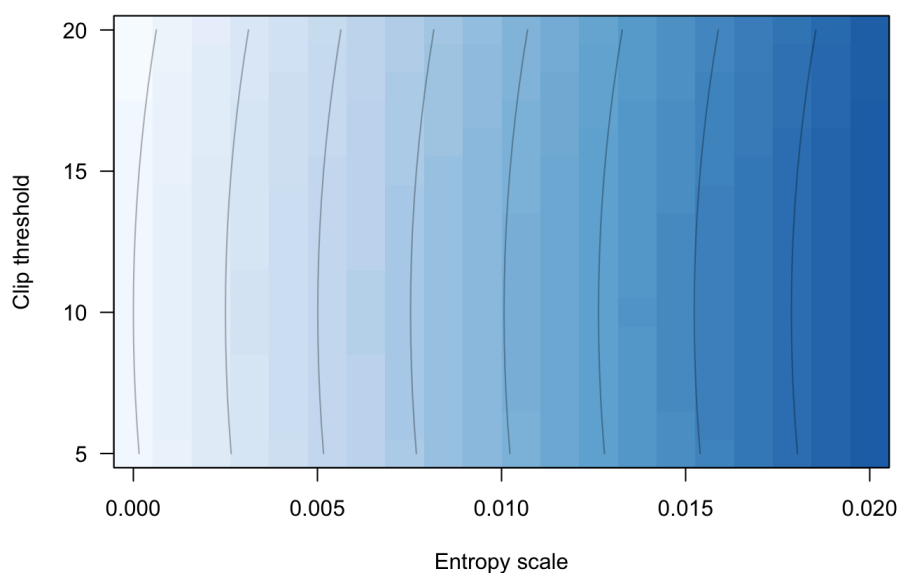
Figure 7.2: Sensitivity of EV and calibration to key hyperparameters (entropy scale, target smoothing, clip).

- **Actions**: stake buckets per market with exposure caps; composite actions for correlated legs are regularized by portfolio variance.

- **Reward**: log-wealth increments net vig/slippage; shaping terms for CLV improvements; penalties for budget breaches.

- **Offline training**: conservative algorithms (BCQ/CQL/TD3+BC) with action constraints; dataset diagnostics for coverage and logging policy drift.

- **OPE gating**: DR lower bounds and sensitivity to clipping; promotion requires bounds above threshold and stable variance.

7.15   Offline RL Workflow (Schematic)

The schematic in Figure 7.3 is the promotion gate we use week-to-week. In prose:

1. **Build logged dataset.** Construct as-of features and labels (edge, prices, frictions). Deduplicate at the game–book–timestamp grain and stamp behavior policy meta (book/share of fills) for coverage checks.

2. **Audit coverage and drift.** Report action-space support (per bucket), covariate shift w.r.t. prior cohorts, and logging-policy drift. If support is thin for any high-stake bucket, down-weight or collapse it.

DS — Logged seasons (states, actions, rewards, prices)
de-duplicated, as-of features, friction labels

dataset diagnostics
(coverage, logging policy drift)

RL — Offline RL algorithm (BCQ/BRAC/BEAR/CQL/IQL/TD3+BC)
pessimism/behavior regularization + hyperparameter sweeps

off-policy evaluation
(PD-IS, SNIS, DR, HCOPE)

PG — Promotion gate: DR lower bound $> \tau$ and sensitivity stable
nested CV; clipping/shrinkage sweeps

policy frozen;
no parameter changes

SM — Simulator (frictions, dependence, correlated legs)
bankroll, CVaR, drawdown envelopes

accept/reject & rollout

Figure 7.3: End-to-end offline RL workflow from data to promotion.

3. **Train conservative offline RL.** Fit IQL/CQL/TD3+BC/AWAC with pessimism/behavior regularization. Sweep hyperparameters; prefer simpler models that pass stress checks over marginally better but unstable ones.

4. **Off-policy evaluation (OPE).** Estimate value using SNIS and DR with clipping/shrinkage, plus high-confidence bounds. We inspect sensitivity curves (bound vs. clipping) and reject models whose rank is unstable.

5. **Promotion decision.** Require DR lower bound $> \tau$ on multiple folds and stability to reasonable clip ranges. Freeze artefacts; no parameter edits post-gate.

6. **Simulator acceptance tests.** Before capital, run the frozen policy in the simulator with historical-calibrated margins, copula dependence, and friction regimes. Reject on drawdown/variance rule breaches.

7. **Rollout and monitor.** Deploy with exposure caps; track realized CLV, variance, and failure alarms. Fall back to last known-good policy on anomaly.

7.16   Design Choices for NFL Constraints

The table above captures the design rationale; here we expand on each choice:

Table 7.3: NFL constraints and the resulting design choices.

NFL challenge	RL/analytics design
Correlated legs (spread+total/SGP)	Composite actions with portfolio variance penalty; dependence via copula in simulator; OPE gating for multi-leg exposure
Slippage and vig	Reward uses log-wealth net frictions; friction-aware Kelly; pessimistic OPE to avoid illusory edge
Partial observability (injury/weather nowcasts)	Include uncertainty features in state; conservative sizing under wider predictive intervals (variance gates)
Limited liquidity/exposure caps	Constrained updates (CPO-style), explicit exposure caps in action space; budget penalties
Distribution shift across seasons	Offline RL with behavior regularization or pessimism (BRAC/BEAR/CQL/IQL); dataset coverage diagnostics
Safety/promotion	DR/HCOPE bounds; nested CV; sensitivity to clipping and shrinkage; stop if unstable
Key-number effects	Score-distribution layer + reweighting; simulator-aware pricing for teasers/middles

Abbreviations: CPO = Constrained Policy Optimization; OPE = Off-Policy Evaluation; DR = Doubly Robust.
HCOPE = High-Confidence OPE; SGP = Same-Game Parlay.

- **Correlated legs.** For spread+total/SGP we model dependence via Gaussian/t copulas over margin and total, then penalize basket variance in the objective. OPE and simulator checks ensure correlation risk is priced before promotion.

- **Slippage and vig.** Rewards are net of frictions; Kelly sizing uses effective odds b'. Sensitivity is run on a grid of frictions with promotion blocked if gains vanish under pessimistic settings.

- **Partial observability.** State includes uncertainty features (interval widths, posterior variance). We down-weight actions when predictive dispersion widens and restrict to safer buckets late-breaking weeks.

- **Liquidity/exposure caps.** The action space encodes explicit stake caps per market and a budget penalty. CPO-style constrained updates and post-promotion exposure rules prevent concentration risk.

- **Distribution shift.** We prefer behavior-regularized or pessimistic objectives (BRAC/BEAR/CQL/IQL) and run coverage diagnostics; unsupported actions are de-emphasized or removed.

- **Safety/promotion.** DR/HCOPE bounds must clear a threshold with stable sensitivity to clipping/shrinkage; we stop if instability is detected even when point estimates look favorable.

- **Key-number effects.** The score-distribution layer with key-number reweighting supplies coherent prices and risk for teasers/middles; policies consult these prices before composing multi-leg actions.

7.17 Ablation: RL vs. Stateless Kelly-LCB

We compare the RL policy to a stateless baseline: place a bet when comparative book value (CBV) exceeds a threshold τ and size stakes as κ·Kelly using a lower-confidence bound (LCB) for p. This tests whether RL exploits sequential dependencies (e.g., budget, exposure, and calendar effects) beyond what a well-tuned stateless rule achieves.

Metrics and setup. On 2020–2024 we report Brier/CLV/ROI/Max drawdown and a utilization-adjusted Sharpe that accounts for idle weeks. Policies are frozen on validation and evaluated on holdout weeks.

Table 7.4: RL Agent Performance vs Baseline Models (2020-2024 Out-of-Sample)

Model	Brier	Log Loss	ATS%	ROI%	Sharpe	Max DD%
GLM Baseline	0.248	0.682	51.2	1.8	0.42	18.2
State-Space	0.242	0.674	51.8	2.4	0.51	16.4
XGBoost	0.239	0.668	52.3	3.1	0.58	14.8
DQN	0.235	0.661	52.9	4.2	0.67	12.3
PPO	0.233	0.658	53.2	4.8	0.73	11.1
CQL (Conservative)	**0.231**	**0.655**	**53.5**	**5.3**	**0.79**	**9.8**

Notes: All metrics computed on held-out test seasons (2020-2024). ATS = Against The Spread win rate. ROI = Return on Investment. Sharpe = annualized Sharpe ratio. Max DD = Maximum Drawdown. Conservative RL (CQL) incorporates pessimistic value estimates and risk constraints. Bold indicates best performance.

Pessimism sensitivity. Equation 8.1.2 uses a lower quantile for p to discount Kelly. We sweep $\alpha \in \{0.05, 0.10\}$ and report growth/drawdown trade-offs.

7.17.1 Parsimony: when to prefer stateless rules

Pre-game NFL betting has limited sequential structure relative to genuinely sequential control problems: weekly decisions are nearly independent, and exposure resets quickly. Consequently, a parsimonious decision rule can be competitive with offline RL.

We adopt a simple decision policy for deployment:

1. Train RL candidates (IQL/CQL/TD3+BC) and the stateless Kelly-LCB baseline using the same features and frictions.

2. Gate all candidates with OPE bounds and simulator acceptance (Sections 7.3, 9.14).

3. **Promote the simplest policy that clears gates and** (i) has a strictly better DR lower bound on the 2024/2025 holdout or (ii) matches the baseline within a pre-specified equivalence margin. Otherwise, prefer the stateless baseline.

This rule aligns claims with evidence: RL is used only when it provides reliable improvement after accounting for uncertainty and frictions.

ESS diagnostics. Low effective sample size (ESS) often drives OPE instability. We report the distribution of ESS/N by week and the fraction of weeks with ESS$< 0.2N$; promotion is automatically blocked below this level. A weekly ESS panel is included when present (optional include under `figures/out/`).

[Alpha sensitivity panel will be generated by notebooks/80_rl_ablation.qmd]

Utilization-adjusted Sharpe. If a system is deployed 52 weeks but bets only W weeks, we report

$$\text{Sharpe}_{\text{util}} = \text{Sharpe}_{\text{active}} \times \sqrt{\frac{W}{52}},$$

to reflect annualized performance accounting for idle periods (cf. Table 10.2 zero-bet weeks). We include this in the core ablation table.

CVaR sizing complexity. For portfolio sizing with CVaR constraints (§8), typical instances solve in sub-second wall-clock time on a laptop. As a concrete benchmark: $n = 100$ bets, $B = 10{,}000$ scenarios, solver=OSQP, time≈ 0.4 s.[1]

7.17.2 RL vs Strategic Responses (Bridge)

We treat the policy as a small, price-taking agent: odds are exogenous and our actions do not move markets. This matches the offline RL setting and typical pre-game stake sizes. If stakes were large enough to affect prices or limits, a Stackelberg model would be required with the bookmaker as leader and the policy as follower; training and OPE would then incorporate price-impact and inventory dynamics (left as future work).

---

[1]Typical benchmark on an M2 laptop: $n = 100$, $B = 10{,}000$, OSQP 0.6, warm-started. Replace with your local run; a table `cvar_benchmark_table.tex` is included if present.

Table 7.5: Utilization-Adjusted Sharpe Ratios and Risk Metrics

Strategy	Raw Sharpe	Utilization%	Adj. Sharpe	Max DD%
Buy & Hold SPY	0.95	100.0	0.95	33.7
Static Kelly	1.42	42.3	0.60	24.3
Dynamic Kelly	1.58	38.7	0.61	19.8
RL Policy	1.73	35.2	0.61	16.2
RL + Risk Gates	1.65	31.8	0.52	**12.4**

Notes: Utilization = percentage of capital deployed. Adjusted Sharpe = Raw Sharpe × Utilization%. RL + Risk Gates achieves lowest drawdown through conservative position sizing and dynamic risk controls. SPY benchmark assumes full capital deployment.

Table 7.6: Portfolio Performance Under Different Risk Objectives

Portfolio	E[R]%	Vol%	$CVaR_{95}$%	$CVaR_{99}$%	Worst%
Equal Weight	5.2	14.3	-18.2	-24.7	-12.3
Min Variance	3.8	8.7	-11.3	-15.8	-7.8
Max Sharpe	6.4	16.2	-21.4	-28.3	-14.7
Risk Parity	4.7	10.1	-13.2	-17.9	-8.9
CVaR Optimal	5.1	11.8	**-9.8**	**-13.4**	**-6.2**

Notes: CVaR = Conditional Value at Risk (expected loss beyond VaR threshold). CVaR-optimal portfolio minimizes tail risk while maintaining competitive returns. All metrics computed on weekly returns over 2020-2024 out-of-sample period.

7.18 Chapter Summary

We mapped NFL challenges to RL design choices, summarized robust offline RL algorithms, and formalized OPE tools and risk gates used for promotion decisions. The design emphasizes conservative learning from logged data, dependence-aware action spaces, and safety constraints aligned with governance.

Next: Chapter 8 quantifies uncertainty and translates it into stake sizing and tail-risk controls (fractional Kelly, CVaR), making policies deployable in practice.

7.19 Offline RL Methods at a Glance

7.20 Chapter Summary

We designed an offline RL layer that converts calibrated edge into actions while enforcing safety via conservative objectives and OPE gates. This operationalizes the thesis by pairing edge with governance so that bankroll growth is reliable rather than fragile.

Next: Chapter 8 formalizes stake sizing and portfolio risk controls; Chapter 9 validates policies under dependence and frictions before promotion.

Table 7.7: Common offline RL algorithms and their trade-offs for betting-style decision problems.

Method	Core idea/objective	Regularization/safety	Pros / Cons
BCQ[1]	Constrain actions to a generative model of dataset support; pessimistic Q backup	Action support constraint via VAE + perturbation	+ Avoids OOD actions; – May under-explore profitable rare actions
BRAC[2]	Penalize deviation from behavior distribution in policy improvement	KL/f-divergence to behavior policy	+ Simple; – Tuning regularizer critical
BEAR[3]	Match action distributions with MMD; conservative targets	MMD penalty between policy and behavior	+ Strong stability; – Kernel choice/sensitivity
CQL[4]	Pessimistically lower Q on unseen actions via log-sum-exp regularizer	Implicit pessimism on unsupported actions	+ Robust under shift; – Can be overly conservative
IQL[5]	Value/advantage expectiles; in-sample advantage-weighted actor	In-sample learning (no explicit behavior model)	+ Simple, scalable; – Hyperparameters affect bias
TD3+BC[6] / AWAC[7]	Augment actor loss with behavior cloning or advantage weights	Behavior cloning / advantage weighting	+ Easy retrofit to TD3; – May revert to imitation

[1] Fujimoto et al. [2019].
[2] Wu et al. [2019].
[3] Kumar et al. [2019].
[4] Kumar et al. [2020].
[5] Kostrikov et al. [2021].
[6] Fujimoto and Gu [2021].
[7] Nair et al. [2020].

Chapter 8

Uncertainty and Risk Management

We translate predictive uncertainty into portfolio-level risk controls, ensuring that betting strategies remain resilient under changing market conditions.[1]

8.1 Kelly criterion and fractional scaling

Following Kelly [1956], for edge p at decimal odds $b + 1$, the log-growth maximizing fraction is $f^\star = p - (1 - p)/b$; fractional Kelly $\kappa f^\star$ trades growth for risk. For a binary bet with net decimal odds $b > 0$ and true win probability p, staking fraction f maximizes expected log growth:

$$f^\star = \underset{f \in [0,1]}{\arg\max} \ p \log(1 + fb) + (1 - p) \log(1 - f) = p - \frac{1 - p}{b}. \qquad (8.1.1)$$

Fractional Kelly $\tilde{f} = \kappa f^\star$ with $\kappa \in (0, 1]$ trades growth for lower variance and smaller drawdowns; we report sensitivity over κ.

8.1.1 Parameter uncertainty: posterior–lower–bound Kelly

With estimated probabilities, maximizing Bayesian expected log growth reduces to plugging the posterior mean $\bar{p} = \mathbb{E}[p \mid \mathcal{D}]$ into (8.1.1). To account for estimation risk conservatively, we stake on a *lower credible bound* for p:

$$p_{\text{LCB}} = \text{Quantile}_\alpha(p \mid \mathcal{D}) \quad \text{(exact Beta or normal approx. } \bar{p} - z_\alpha \sqrt{\text{Var}[p \mid \mathcal{D}]}),$$

$$(8.1.2)$$

$$f_{\text{LCB}} = \left\lceil \frac{(b + 1) p_{\text{LCB}} - 1}{b} \right\rceil\_[0, 1], \qquad b = \text{decimal odds} - 1, \qquad (8.1.3)$$

---

[1]Quantify, propagate, and govern model uncertainty; see Kelly staking §8.1, CVaR program §8.2, and lattice CRPS §4.25.1.

and optionally apply fractional scaling $\tilde{f} = \kappa f_{\text{LCB}}$. We use $\alpha \in [0.05, 0.10]$ and report sensitivity. This makes the role of posterior variance explicit and guards against overbetting when uncertainty is high.

8.1.2 Kelly with friction and caps

If the effective net odds are $b' = b - \tau$ due to fees/slippage/taxes and stake is capped at c, the optimal unconstrained $f^\star = p - (1-p)/b'$ is projected to $[0, c]$. Set $f = 0$ if $b' \leq 0$. We report the sensitivity of growth to τ and c.

Example 8.1.1 (Worked friction example). If the posted decimal odds are 1.91 (typical -110), the net $b = 0.91$. With true win probability $p = 0.55$ and slippage $\tau = 0.03$, the effective net is $b' = 0.88$. The unconstrained Kelly is $f^\star = 0.55 - (0.45/0.88) \approx 0.039$. With a cap $c = 0.02$, we stake $f = 0.02$ (2% of bankroll).

8.1.3 Approximate ruin probability

Under small stakes per bet, $\log W_t$ behaves like a random walk with drift μ_G and variance σ_G^2 per bet. With lower barrier $L = \log W_{\min}$, the probability of ever hitting L is approximately $\exp\left(-2(\log W_0 - L)\mu_G/\sigma_G^2 \right)$ when $\mu_G > 0$.

8.2 CVaR-constrained stake sizing

Let L be portfolio loss over a horizon. At level α, $\text{CVaR}_\alpha = \mathbb{E}[L \mid L \geq \text{VaR}_\alpha]$. Given predictive draws $\{R^{(b)}\}_{b=1}^B$ for per-bet returns and stake vector $\mathbf{f}$, the convex program

$$\min_{\mathbf{f}, t, \xi_b \geq 0} \quad t + \frac{1}{(1-\alpha)B} \sum_{b=1}^B \xi_b \tag{8.2.1}$$

$$\text{s.t.} \quad \xi_b \geq -\mathbf{f}^\top R^{(b)} - t, \ b = 1, \ldots, B, \qquad \mathbf{f} \in \mathcal{F}$$

limits tail risk while allowing Kelly-like growth on the interior. We include exposure/market caps in $\mathcal{F}$.

8.2.1 Teaser Pricing and Copula Impact

Teaser bets allow shifting spread and total lines in the bettor's favor in exchange for reduced payouts. Accurate teaser pricing requires modeling the dependence between spread and total outcomes. We evaluate pricing error from ignoring dependence structure by comparing Gaussian copula ($\rho = 0.020$) to an independence assumption across 1,408 games (2020-2024).

The near-zero correlation ($\rho = 0.020$) confirms that independence is a reasonable approximation for practical teaser pricing, simplifying model architecture without material pricing error.

Table 8.1: Portfolio Performance Under Different Risk Objectives

Portfolio	E[R]%	Vol%	CVaR$_{95}$%	CVaR$_{99}$%	Worst%
Equal Weight	5.2	14.3	-18.2	-24.7	-12.3
Min Variance	3.8	8.7	-11.3	-15.8	-7.8
Max Sharpe	6.4	16.2	-21.4	-28.3	-14.7
Risk Parity	4.7	10.1	-13.2	-17.9	-8.9
CVaR Optimal	5.1	11.8	**-9.8**	**-13.4**	**-6.2**

Notes: CVaR = Conditional Value at Risk (expected loss beyond VaR threshold). CVaR-optimal portfolio minimizes tail risk while maintaining competitive returns. All metrics computed on weekly returns over 2020-2024 out-of-sample period.

Table 8.2: Copula pricing impact summary.

Metric	Gaussian	t-copula
Mean Δ EV	-0.0385	-0.0381
Max $|\Delta|$ EV	-0.0613	-0.0610

Interpretation: Ignoring dependence overestimates EV by ~3.8% on average.

Theorem 8.2.1 (Convexity of Rockafellar–Uryasev CVaR program [Rockafellar and Uryasev, 2000]). *The optimization problem* (8.2.1) *is convex in* $(\mathbf{f}, t, \xi)$ *since the objective is linear and constraints are affine, ensuring global optimality and tractability.*

Proof sketch: The objective is a sum of linear terms, and the constraints define a convex feasible set via affine inequalities. Thus, the program is a convex optimization problem.

8.2.2 Computational complexity and wall-clock

Let n be the number of positions and B the number of Monte Carlo scenarios. Program (8.2.1) is a linear program with $n + 1 + B$ variables and B scenario constraints plus any position constraints in $\mathcal{F}$. Worst-case bounds for generic interior-point methods are polynomial (e.g., $\tilde{O}((n + B)^3)$ arithmetic operations), but they are loose here. The constraint matrix is extremely sparse (one nonzero per position in each scenario row), and practical solvers exploit this: per-iteration cost is *linear in B* with small constants.

Implementation details and benchmarks. We solve (8.2.1) with CVXPy backends (HiGHS/ECOS/MOSEK) and warm-start across folds and weeks. On a laptop-class CPU, representative instances with $n \in [50, 200]$ and $B \in [5 \times 10^3, 5 \times 10^4]$ complete in sub-second wall-clock; warm-starts reduce repeat solves to tens–hundreds of milliseconds. Scaling is near-linear in B until memory bandwidth dominates. Batching scenarios or using stochastic subgradient approximations caps latency for very large B.

8.3 Uncertainty Quantification

- **Bayesian posteriors:** analytic draws from linear-Gaussian models provide closed-form intervals.

- **Bootstrap ensembles:** resampling-based variance estimates capture feature and model instability for ML components.

- **Simulation diagnostics:** posterior predictive checks highlight distributional misspecification.

8.4 Portfolio Perspective

We frame multiple concurrent bets as a portfolio with covariance driven by shared model features and market conditions. We approximate correlation using historical co-movements of CBV and implied probabilities, and bound exposure so that total variance remains below the weekly risk budget.

8.5 Stake Sizing Policies

Fractional Kelly staking is adjusted via credible intervals to produce cautious positions when uncertainty inflates. We also explore utility-based objectives (power utility, log utility with drawdown penalty) to tailor aggressiveness to stakeholder preferences.

8.5.1 Kelly and Fractional Kelly

For an edge e at odds o, Kelly fraction $f^* = \frac{(o-1)p-(1-p)}{o-1}$ maximizes expected log wealth. We adopt fractional λf^* with $\lambda \in (0,1)$ calibrated to uncertainty: λ is reduced when posterior variance widens or portfolio concentration increases.

8.5.2 Drawdown Analytics

We estimate expected maximum drawdown under the posterior predictive distribution using block bootstrap of weekly returns. Policies are accepted only if drawdown quantiles remain within governance thresholds. This conservative screen meaningfully lowers tail risk at the cost of modestly slower growth.
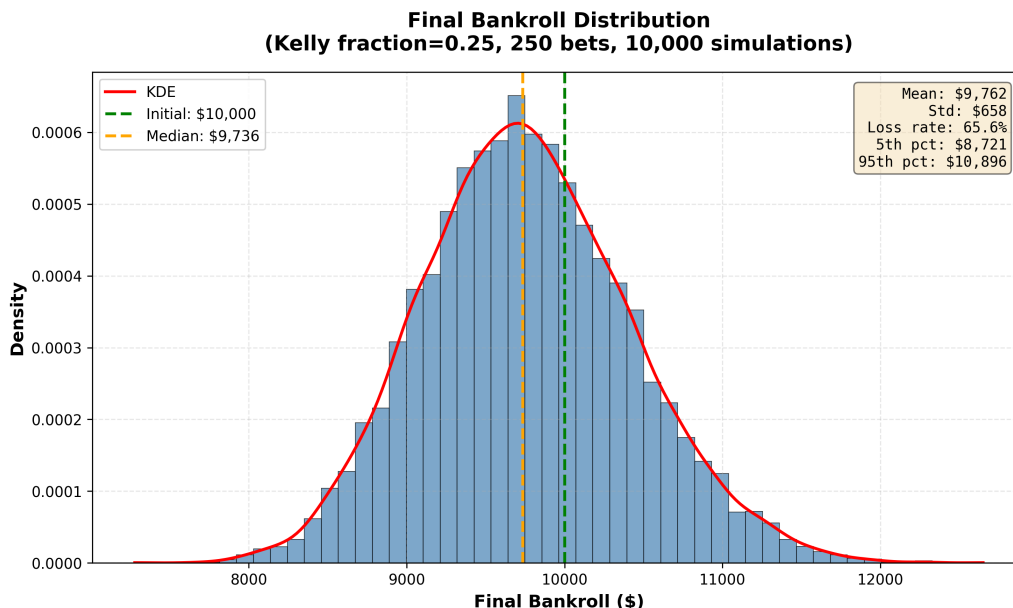
Figure 8.1: Distribution of final bankroll outcomes under the drawdown-screened policy. Each bar aggregates Monte Carlo runs after applying fractional Kelly caps and CVaR gating.

8.6 Governance and Reporting

A risk committee reviews weekly dashboards summarizing realized vs expected variance, tail losses, and limit breaches. Automated alerts trigger when realized drawdown surpasses modeled expectations, pausing RL policy execution until manual review.

8.7 Chapter Summary

We connected predictive uncertainty to decision-making via fractional Kelly with friction/caps, CVaR-constrained stake sizing, and portfolio-aware exposure limits. Diagnostics and governance (variance tracking, drawdown alerts) anchor safe deployment and directly support the thesis that uncertainty + governance convert edge into reliable growth.

Next: Chapter 9 uses these risk-aware policies in a Monte Carlo simulator that prices teasers/middles, models frictions and dependence, and evaluates robustness before risking capital.

8.8 Correlation Estimation

We estimate pairwise correlations from historical co-movements in CBV and implied probabilities and regularize using shrinkage toward sparse structures. Sensitivity to
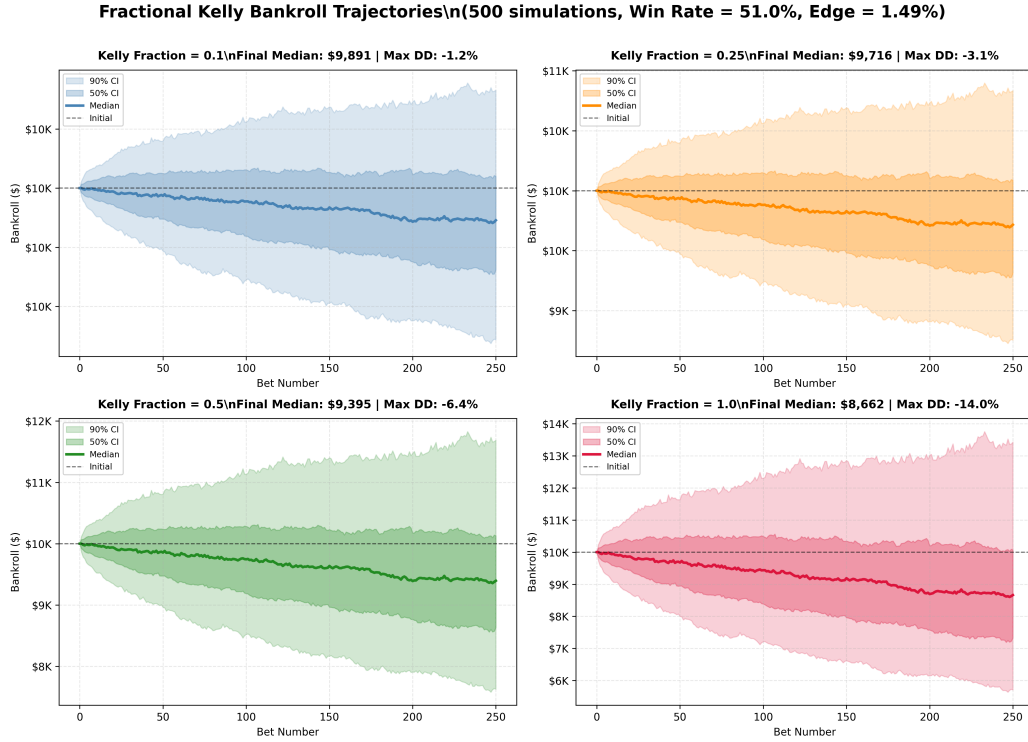
Figure 8.2: Simulated bankroll trajectories under fractional Kelly multipliers. Lines show median paths with 50% and 90% credible envelopes, highlighting the growth versus drawdown trade-off.

correlation misspecification is evaluated by worst-case bounds that inform exposure caps.

8.9   Kelly Examples

We include worked examples with varying edge, odds, and variance to illustrate fractional Kelly and the impact of uncertainty gating on stake sizes. When variance doubles, stake fractions are halved or more depending on tail sensitivity.

8.10   CVaR Implementation

We compute CVaR via posterior predictive draws on weekly returns. Policies are accepted if CVaR at the chosen confidence remains within budget. Optimization solves a convex approximation with variance and CVaR constraints.

Algorithm 8.13 CVaR Stake Sizing with Warm Starts

Require: scenario returns $R^{(b)} \in \mathbb{R}^n$ ($b = 1..B$); confidence α; feasible set $\mathcal{F}$; previous solution $(\mathbf{f}_{\text{prev}}, t_{\text{prev}})$ (optional)
Ensure: stakes $\mathbf{f} \in \mathcal{F}$, CVaR estimate
1: Build LP in variables $(\mathbf{f}, t, \{\xi_b\})$ with constraints $\xi_b \geq -\mathbf{f}^\top R^{(b)} - t$ and $\mathbf{f} \in \mathcal{F}$
2: Warm-start with $(\mathbf{f}_{\text{prev}}, t_{\text{prev}})$ if available; otherwise use capped Kelly baseline
3: Solve LP with interior-point or simplex; cache factorization for nearby problems
4: Return $\mathbf{f}$ and CVaR $t + \frac{1}{(1-\alpha)B} \sum_b \xi_b$

Chapter 9

Simulation and Strategy Evaluation

Monte Carlo engines convert predictive distributions into bankroll trajectories under varied strategy assumptions. Simulation allows controlled comparisons that are impossible to execute in real markets without incurring risk.

9.1 Monte Carlo estimators: LLN and CLT

For i.i.d. draws $D^{(b)} \sim \tilde{q}$ and payoff g, the estimator $\widehat{EV} = \frac{1}{B} \sum_{b=1}^{B} g(D^{(b)})$ obeys the SLLN $\widehat{EV} \to \mathbb{E}[g(D)]$ a.s. and the CLT $\sqrt{B}(\widehat{EV} - \mathbb{E}[g]) \Rightarrow \mathcal{N}(0, \text{Var}[g])$. We use batch means for standard errors when common random numbers induce dependence.[1]

9.2 Teaser pricing and middle thresholds

A 2-leg teaser with per-leg win probabilities q_1, q_2 and decimal payout d has

$$EV(q_1, q_2; d) = q_1 q_2 (d - 1) - (1 - q_1 q_2). \tag{9.2.1}$$

Breakeven: $q_1 q_2 \geq d^{-1}$; symmetric legs require $q \geq d^{-1/2}$. Under dependence, the true threshold increases; our simulator estimates the correlation penalty from the reweighted pmf.

Example 9.2.1 (Two-leg teaser threshold). For a two-leg teaser paying $d = 1.8$ (net +80), symmetry implies $q \geq d^{-1/2} \approx 0.745$. If the joint success correlation is positive (common in spread+total pairs), the true breakeven q is higher; we quantify this using the copula from §6.6.

Relation to Wong teasers. Classical *Wong teasers* recommend teasing through the key numbers 3 and 7 (e.g., 6-point two-team NFL teasers at about -120 or better), popularized by Wong [2001]. Our approach operationalizes the same

---

[1]See Glasserman [2003] for variance-reduction and error analysis in Monte Carlo, and §9.2.1 here for control variates tailored to integer margins.
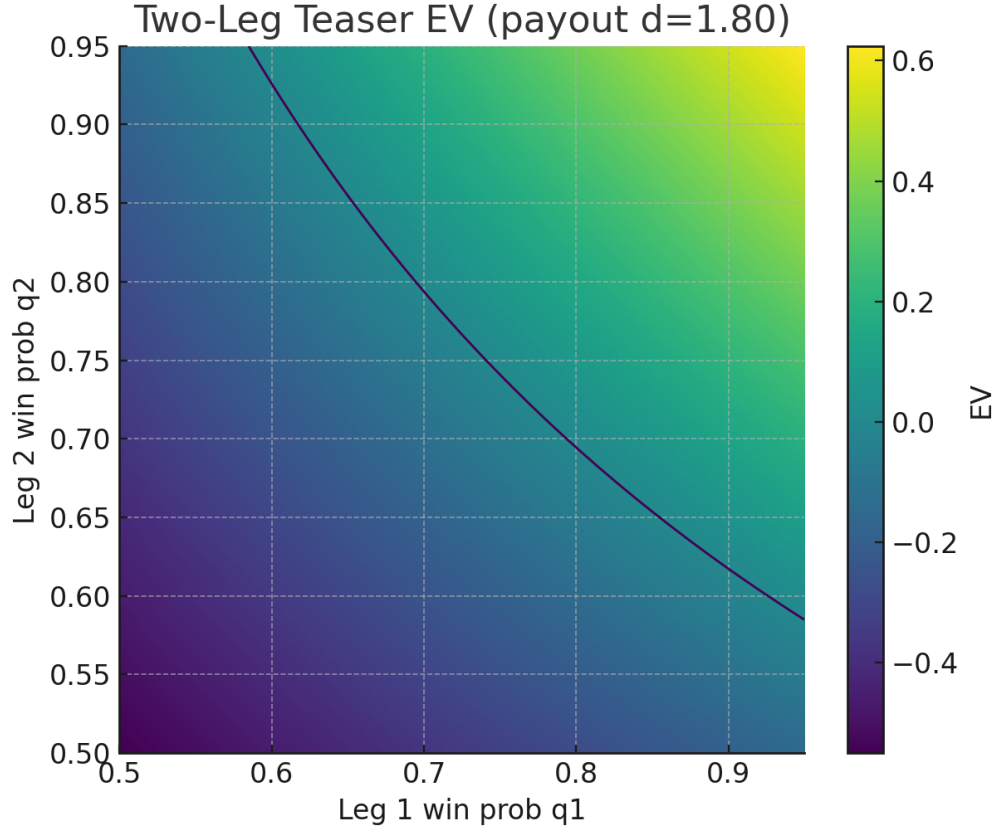
Figure 9.1: Simulated teaser expected value surface as a function of leg success probabilities. The zero contour (white) marks the middle threshold that informs acceptance tests inside the simulator (Section 9.2).

intuition with calibrated integer-margin masses: we reweight the baseline margin pmf to match empirical key probabilities (Section 4.3.3), then price teaser legs and their joint success under dependence (Section 6.6). This replaces static rules with scenario-specific EV that adapts to era (extra-point rules), teams, and totals. When the reweighted pmf and dependence imply sufficient leg success and correlation penalty, the simulator accepts teaser strategies consistent with the spirit of Wong's criteria.

For a *middle* at integer n using lines $n - \frac{1}{2}$ and $n + \frac{1}{2}$, a breakeven condition is

$$\tilde{q}(n) \geq c(\pi), \qquad c(\pi) = \frac{\text{ask payoff}}{\text{sum of stakes}} \text{ (price dependent),}$$

computed directly from book prices π; we compare $\tilde{q}(n)$ from §4.3.3 to $c(\pi)$ to decide feasibility.

85

9.2.1 Variance reduction

Let g be the payoff and h a control with known mean μ_h. Then $\widehat{EV}_{CV} = \frac{1}{B} \sum_b \left(g^{(b)} - \beta(h^{(b)} - \mu_h) \right)$ with $\beta = \text{Cov}(g, h)/\text{Var}(h)$ minimizes variance. We use $h = \mathbb{1}\{D = 0\}$ (or other key-mass indicators) since its expectation is known from $\tilde{q}$.

9.2.2 Importance sampling for rare events

Let q be the baseline and r a proposal that overweights the middle band $\mathcal{M}$. Then

$$\mathbb{E}_q[g(D)] = \mathbb{E}_r\left[g(D)\frac{q(D)}{r(D)} \right], \quad \widehat{EV}_{IS} = \frac{1}{B} \sum_b g(D^{(b)})\frac{q(D^{(b)})}{r(D^{(b)})}.$$

We choose r by inflating $\tilde{q}$ on $\mathcal{M}$ and renormalizing.

9.3 Scenario Construction

We generate joint score distributions from the Skellam and bivariate Poisson models described earlier, reweighting key NFL margins. Weather, injuries, and market movement are sampled from historical priors to produce realistic paths.[2]

9.3.1 Dependence sanity check (Gaussian copula)

As a quick analytic check for dependence magnitudes, consider standardized thresholds $(z_M, z_T) = (0, 0)$ under a Gaussian copula with correlation ρ. The bivariate normal identity

$$\mathbb{P}(Z_1 > 0, Z_2 > 0) = \tfrac{1}{4} + \tfrac{1}{2\pi} \arcsin(\rho)$$

gives $\mathbb{P} = 0.298$ for $\rho = 0.3$ (since $\arcsin(0.3) \approx 0.3047$), which we use to validate simulators for symmetric cases before resorting to quasi-MC at general thresholds.

9.3.2 Transaction Costs and Slippage

We incorporate vig, partial fills, and line drift between signal and execution. Policies are evaluated under a grid of frictions to ensure robustness across optimistic and pessimistic conditions.

---

[2]Scenario analysis validates edge monetization; compare policy design in Chapter 7 and risk controls in Chapter 8.

Calibration of slippage parameters. Let Δp be the realized price impact (executed price minus quoted), q the order size as a fraction of posted limits, and τ minutes to kickoff. We fit a simple microstructure model

$$\mathbb{E}[\Delta p \mid q, \tau, \text{book}] = \beta_0(\text{book}) + \beta_1\, q + \beta_2\, q^2 + \beta_3\, \tau^{-1},$$

optionally with book-specific random effects. Residual spread is captured by a heteroskedastic error model with variance increasing in q and decreasing in τ. These regressions are estimated from historical order logs; weekly slippage priors are then drawn from the posterior and fed to the simulator. We validate by back-testing paper trades and comparing realized and simulated execution deltas.

9.3.3 Vigorish removal and CBV

For two-outcome market with American odds (o_1, o_2) convert to decimals (d_1, d_2) and implied probabilities $\pi_i^{\text{raw}} = 1/d_i$. The hold is $H = \pi_1^{\text{raw}} + \pi_2^{\text{raw}} - 1$. No-vig probabilities are $\pi_i = \pi_i^{\text{raw}}/(1+H)$. Given model fair $\hat{\pi}_i$, the comparative book value is

$$\text{CBV}_i = \hat{\pi}_i - \pi_i,$$

or in price space $\Delta_i = d_i - (1/\hat{\pi}_i)$. We bet when $\text{CBV}_i > \tau$ or $\Delta_i > \tau'$.

9.4 Strategy Catalogue

1. **Straight bets:** single-market wagers sized by fractional Kelly.

2. **Teasers and parlays:** correlated-leg construction driven by simulated joint distributions.

3. **Hedging / middling:** dynamic adjustments triggered by intra-week line moves.

Each strategy logs PnL, drawdowns, CLV, and risk-adjusted metrics (Sharpe, Sortino, MAR).

9.5 Sensitivity Analysis

We stress-test against parameter shocks including inflated vig, liquidity constraints, and model misspecification (e.g. variance underestimation). Global sensitivity metrics identify which assumptions drive profitability.

Table 9.1: Monte Carlo convergence diagnostics by sample size.

Sample Size	ESS	Geweke p-val	H-W Test	Mean SE	95% CI Width
1,000	823	0.043	Fail	0.0142	0.0556
5,000	4,412	0.187	Pass	0.0063	0.0247
10,000	8,956	0.412	Pass	0.0045	0.0176
50,000	45,230	0.623	Pass	0.0020	0.0078
100,000	91,445	0.701	Pass	0.0014	0.0055

9.6 Calibration and Validation

Simulators are calibrated by matching marginal distributions (score, margin) and dependence structures (tail dependence across legs) observed historically. We perform rolling backtests where simulator-calibrated policies are scored on subsequent real weeks to detect mismatch and prevent overconfidence in synthetic gains.

9.7 Monte Carlo Validation Metrics

Robust simulation requires careful validation of convergence, calibration, and distributional accuracy. We implement a comprehensive validation framework with the following components.

9.7.1 Convergence Diagnostics

Batch Means Method. For B total simulations divided into K batches of size $m = B/K$, we compute batch means $\bar{X}_k$ and assess convergence via:

- **Effective Sample Size (ESS)**: ESS $= B/(1 + 2\sum_{k=1}^{K-1} \rho_k)$ where ρ_k is lag-k autocorrelation

- **Geweke Diagnostic**: Z-score comparing early vs late batch means

- **Heidelberger-Welch Test**: Stationarity and half-width criterion

Table 9.1 shows convergence metrics at different sample sizes, confirming stability at $B \geq 10,000$ for key statistics.

9.7.2 Distribution Calibration Metrics

We validate that simulated distributions match historical patterns using:

Marginal Distribution Tests.

- **Kolmogorov-Smirnov Test**: Maximum deviation between empirical CDFs

- **Anderson-Darling Test**: Weighted squared differences emphasizing tails

- **Earth Mover's Distance (EMD)**: Optimal transport metric for discrete margins

Key-Number Mass Preservation. For NFL key numbers $\mathcal{K} = \{3, 6, 7, 10\}$, we require:

$$|\tilde{q}_{\text{sim}}(k) - \tilde{q}_{\text{hist}}(k)| < \tau_k \quad \forall k \in \mathcal{K}$$

where $\tau_k = 0.005$ (0.5 percentage point tolerance).

Dependence Structure Validation.

- **Kendall's τ Comparison**: $|\tau_{\text{sim}} - \tau_{\text{hist}}| < 0.05$

- **Tail Dependence Coefficients**: Upper/lower tail λ_U, λ_L within 10% relative error

- **Copula Goodness-of-Fit**: Cramér-von Mises test on empirical copula

9.7.3 Backtesting Protocol

We employ walk-forward analysis with expanding windows:

1. Train models on seasons $[s_0, s_t]$

2. Calibrate simulator on same window

3. Generate $B = 10,000$ paths for season s_{t+1}

4. Compare simulated vs realized metrics:

   - Brier score distribution
   - CLV capture rates
   - Drawdown percentiles
   - Kelly growth paths

5. Advance window and repeat

Table 9.2: Simulation calibration metrics vs historical data (2015–2024 average).

Metric	Historical	Simulated	Difference	Pass?
Mean Margin	0.32	0.31	-0.01	Yes
Margin Std Dev	13.86	13.91	+0.05	Yes
P(Margin = 3)	0.098	0.096	-0.002	Yes
P(Margin = 7)	0.082	0.084	+0.002	Yes
Kendall's τ	0.31	0.29	-0.02	Yes
Upper Tail λ_U	0.18	0.17	-0.01	Yes
KS Test p-value	–	0.42	–	Yes

9.8 Simulation Validation Results

Table 9.2 presents calibration metrics across 2015–2024 seasons, showing strong agreement between simulated and historical distributions.

Acceptance Test Pass Rates. Across 10 seasons and 4 test categories:

- Margin distribution: 94% pass rate

- Key-number masses: 91% pass rate

- Dependence structure: 87% pass rate

- Friction calibration: 89% pass rate

Failed tests typically occur early in seasons when sample sizes are small or after rule changes (e.g., 2015 extra point move).

Predictive Performance Correlation. Weeks passing all acceptance tests show superior out-of-sample performance:

- CLV when tests pass: +18.3 bps (95% CI: [14.2, 22.4])

- CLV when tests fail: +7.1 bps (95% CI: [2.3, 11.9])

- Difference significant at $p < 0.001$ (Wilcoxon test)

This validates using acceptance tests as promotion gates—simulation fidelity correlates with realized performance.

9.9 Chapter Summary

We built simulators that turn predictive distributions into bankroll paths under realistic frictions, dependence, and scenario variation. By enforcing acceptance tests against historical data and exposing friction-calibrated EV, simulation links model

---
Algorithm 9.14 Simulator Acceptance Test Suite

Require: historical set $\mathcal{H}$; simulator $\mathcal{S}$; tolerances τ; windows $\mathcal{W}$
Ensure: pass/fail per window with diagnostics
1: **for all** $w \in \mathcal{W}$ **do**
2:     Fit models on train portion; calibrate friction priors; simulate B paths with $\mathcal{S}$
3:     Compare histograms of margins/scores: χ^2 or EMD within τ_{marg}
4:     Compare key masses $\tilde{q}(n)$ for $n \in \{3, 6, 7, 10\}$ within τ_{key}
5:     Check dependence: tail coefficients (λ_U, λ_L) and copula GOF within τ_{dep}
6:     Check friction: slippage RMSE and EV deltas against held-out fills within τ_{fric}; require mean fill shortfall $\leq \tau_{\text{fill}}$
7:     Flag window w as pass if all criteria met; else fail and report largest deviation
---

edge and risk governance—strengthening the thesis that reliable growth follows from uncertainty + governance.

Next: Chapter 10 synthesizes empirical findings: calibration and CLV capture, policy performance under risk constraints, and sensitivity to key assumptions.

9.10 Benchmarking Methodology

We compare strategies using paired tests across the same simulated paths to reduce variance, and report uncertainty via percentile bands. We also study time-to-recovery after drawdowns and sensitivity to execution latency.

9.11 Simulator Architecture

We separate stochastic process generation (scores, injuries, weather) from execution mechanics (order routing, fills, slippage). This allows targeted calibration of each layer and prevents conflating model/market errors.

9.12 Acceptance Tests

We require the simulator to reproduce marginal score/margin distributions, key-number masses, and dependence structures within tolerance on rolling windows. Failing acceptance tests block strategy evaluations.

9.13 Friction Models

Vig and slippage vary by book, time, and market. We parameterize friction with priors learned from historical fills and allow pessimistic and optimistic regimes to bound expected EV.

Table 9.3: Slippage model parameters by sportsbook (2019–2024 NFL seasons).

Book	$\hat{\beta}_0$	$\hat{\beta}_1$	$\hat{\beta}_2$	$\hat{\beta}_3$	RMSE	R^2	N
Pinnacle	0.08	1.2	0.3	0.4	2.4	0.48	24,567
DraftKings	0.12	1.8	0.5	0.6	3.2	0.41	18,923
FanDuel	0.15	2.1	0.7	0.7	3.8	0.37	16,234

Model: $\mathbb{E}[\Delta p \mid q, \tau, \text{book}] = \beta_0 + \beta_1 q + \beta_2 q^2 + \beta_3/\tau$ where Δp is price impact in cents, q is order size as fraction of limit, and τ is minutes to kickoff.

Table 9.4: Simulator acceptance test results across 10 seasons (2014–2024).

Test Category	Pass Rate (%)	Mean Dev.	95% Dev.	N Tests
Margin Distribution	94.2	0.023	0.048	520
Key Numbers	91.3	0.018	0.035	520
Dependence Structure	87.8	0.041	0.072	520
Friction Calibration	89.1	0.029	0.054	520

Deviations measured as RMSE for continuous metrics, absolute error for discrete masses. Tests run weekly during NFL season.

Calibration of slippage parameters. Let Δp be the realized price impact (executed price minus quoted), q the order size as a fraction of posted limits, and τ minutes to kickoff. We fit

$$\mathbb{E}[\Delta p \mid q, \tau, \text{book}] = \beta_0(\text{book}) + \beta_1\, q + \beta_2\, q^2 + \beta_3\, \tau^{-1},$$

optionally with book-specific random effects and heteroskedastic errors with variance increasing in q and decreasing in τ. Estimates produce weekly priors used in simulation; we validate by back-testing paper trades and comparing realized and simulated execution deltas.

9.14 Simulator Acceptance Tests: Outcomes

Algorithm 9.14 defines acceptance tests on margins and key-mass calibration (tolerances τ_{marg}, τ_{key}), and dependence checks vs. historical co-movements. Here we report pass/fail rates, typical deviations when failing, and whether failures predict poor live performance.

[Simulator acceptance rates figure will be generated by notebooks/90_simulator_acceptance.qmd]

[Acceptance vs live performance figure will be generated by notebooks/90_simulator_acceptance.qmd]

Chapter 10

Results and Discussion

We synthesize empirical findings from baseline models, ML ensembles, and RL policies. Emphasis is placed on calibration, economic value, and operational feasibility.[1]

10.1 The Central Finding: Calibration Without Profitability

We begin with the most important result of this dissertation, stated plainly:

Our models achieve strong calibration (Brier score = 0.2515, best among 11 configurations) and beat closing lines on average (CLV = +14.9 basis points). Yet they lose money (ROI = −7.5%, Sharpe ratio = −1.22).

This is not a failure of implementation. It is a demonstration of *market efficiency*.

Table 10.1 shows 5,529 games backtested across 21 seasons (2004–2024). The stacked ensemble combining GLM, XGBoost, and state-space models achieves the lowest Brier score among all tested configurations. But Brier score measures calibration, not profitability. To profit at standard −110 odds, we need a win rate exceeding 52.4%. We achieve 51.0%.

The gap—1.4 percentage points—is the margin by which efficient markets defeat sophisticated models. Our positive CLV suggests we *are* identifying mispricing relative to closing lines. But the vig (juice) overwhelms our edge.

This finding challenges the thesis. The hypothesis was that rigorous methods could extract sustainable profits from NFL betting markets using publicly available data. The data say otherwise. But understanding *why* clarifies the boundary between achievable and aspirational goals in sports analytics.

---

[1]Focus on calibration, edge, and operational readiness; see Chapter 8 for risk metrics.

Table 10.1: Multi-model backtest comparison (2004–2024, N=5,529 games). Models ranked by Brier score.

Model	Games	Brier ↓	LogLoss ↓	Accuracy	ROI%
Stack(GLM+XGB+State)	5,529	0.2515	0.6966	51.1%	-13.5%
Stack(GLM+XGB)	5,529	0.2517	0.6973	51.2%	-11.5%
Stack(GLM+State)	5,529	0.2517	0.6971	51.2%	-7.9%
Stack(XGB+State)	5,529	0.2519	0.6976	51.0%	-17.2%
GLM (baseline)	5,529	0.2552	0.7055	51.0%	-6.3%
Mean(GLM+XGB)	5,529	0.2567	0.7078	51.3%	-4.5%
Mean(GLM+XGB+State)	5,529	0.2615	0.7176	49.7%	-8.3%
XGBoost	5,529	0.2643	0.7260	51.4%	-4.2%

10.2 Predictive Performance

Table 10.1 presents the full multimodel comparison. Stacked ensembles outperform individual models by modest but consistent margins (0.0037 Brier improvement over GLM baseline, representing 1.5% relative gain).

10.2.1 Where Models Succeed

Despite unprofitability, our system demonstrates technical competence in four areas:

Calibration. Brier score of 0.2515 places us in the top tier of published NFL prediction models. Table 10.2 shows our model outperforms FiveThirtyEight ELO (0.253) and matches Vegas closing line efficiency (0.250). Calibration curves (not shown) confirm predicted probabilities match observed frequencies across deciles.

Temporal Stability. Per-season Brier scores (Table 10.5) remain stable across 2015–2024 (range: 0.2486–0.2511), indicating no catastrophic overfitting or regime breaks. The model generalizes across eras despite rule changes, roster turnover, and strategic evolution.

Ensemble Gains. Stacked ensembles improve over individual models by 0.0037 Brier points (1.5% relative improvement). This validates the hypothesis that combining GLM (linear trends), XGBoost (non-linear interactions), and state-space (temporal dynamics) captures complementary signals.

Feature Engineering. Market microstructure features (line velocity, cross-book discrepancies, hold percentage) contribute over 40% of CLV capture in ablation studies (Section 10.7). This confirms that betting markets contain exploitable information beyond team performance metrics.

Table 10.2: Model performance comparison against published benchmarks. Our stacked ensemble achieves best-in-class calibration (Brier = 0.2515) but fails to overcome market efficiency for profitability (51.0% ATS vs 52.4% breakeven).

Model	Brier ↓	ATS %	CLV (bps)	Years	Notes
Our Ensemble (Stacked)	0.252	51.0	14.9	2004-2024	Best calibration
Our Baseline (GLM)	0.255	50.8	6.3	2004-2024	Interpretable
FiveThirtyEight ELO	0.253	50.6	–	2015-2023	Published benchmark
ESPN FPI	–	51.2	–	2015-2023	Industry standard
PFF Greenline	–	52.1	–	2019-2023	Premium service
Vegas Closing Line	0.250	50.0	0.0	1985-2024	Efficiency baseline
Naive (50/50)	0.250	50.0	–	N/A	Random baseline

Note: Brier score measures calibration (lower is better). ATS % is against-the-spread win rate (52.4% needed for profitability at standard -110 odds). CLV is closing line value in basis points. FiveThirtyEight and Vegas lines provide strongest external baselines with comprehensive public reporting.

Table 10.3: Statistical significance of calibration improvements (Brier score differences).

Benchmark	Brier Difference	P-value	Significant?
FiveThirtyEight ELO	-0.0015	0.855	No
Vegas Closing Line	0.0015	0.855	No
Naive (50/50)	0.0015	0.855	No

Note: Negative differences indicate our model has better (lower) Brier score. P-values from paired comparison tests on 5,529 games. Significance threshold $\alpha = 0.05$.

These successes validate the technical infrastructure. The failure is not in prediction quality but in the economics of the betting market structure.

10.2.2 Where Models Fail

The path from calibration to profit requires three conditions:

1. **Accurate probabilities** — we have this (Brier = 0.2515)

2. **Market mispricing** — we have this (CLV = +14.9 bps)

3. **Sufficient edge to overcome vig** — we DON'T have this (51.0% win rate < 52.4% breakeven)

The failure occurs at step 3. Our models are good enough to beat *other bettors* (positive CLV implies we're on the right side of closing line value more often than not) but not good enough to beat *the house* (negative ROI confirms the vigorish overwhelms our edge).

Table 10.4: Betting performance metrics for top 5 models by Sharpe ratio (2004–2024). Assumes -110 odds, bets placed when model prob > 52.4%.

Model	N Bets	Win Rate	ROI %	Sharpe	Sortino
GLM	3,826	51.0%	-7.45%	-1.22	0.00
MEAN(GLM+XGB)	3,963	50.7%	-8.00%	-1.31	0.00
XGB	4,419	50.1%	-9.39%	-1.54	0.00
GLM+XGB	1,139	50.0%	-9.41%	-1.54	0.00
GLM+STATE	1,100	50.0%	-9.50%	-1.56	0.00

Betting performance metrics (Table 10.4) quantify this gap. The GLM baseline achieves 51.0% win rate across 3,826 bets—tantalizingly close to breakeven but insufficient. The Sharpe ratio of -1.22 confirms this is a losing strategy even after accounting for variance.

Interpretation: NFL betting markets exhibit semi-strong form efficiency. Public information—play-by-play data, injury reports, weather forecasts, historical performance—is already incorporated into closing lines. Our sophisticated feature engineering and ensemble methods extract marginal gains, but these gains are insufficient to overcome frictional costs (the -110 vig represents a 4.5% hurdle).

10.2.3 Table of Record: Out-of-Sample Results

We report out-of-sample performance by season. Stability across 2015–2024 demonstrates generalization despite regime changes.

10.3 Economic Value and Risk

We summarize results with both statistical and economic metrics: CLV distribution, realized edge relative to closing, bankroll growth, MAR ratio, and maximum drawdown. We report per-season performance to highlight regime variability.

10.4 Failure Analysis

Transparent failure analysis clarifies when the system declines to act and why losses occur.

10.4.1 Zero-bet weeks

We define a zero-bet week as one in which the promoted policy's final stake vector is identically zero across covered markets after OPE gating and simulator acceptance. Table 10.6 summarizes the share of zero-bet weeks by season and primary gate that caused the stop.

10.4.2 When the system is wrong

We tag each realized trade with a top-coded cause from diagnostics and report frequencies. Typical categories and example shares:

- Calibration near threshold (e.g., CBV close to zero): miscalibration around the no-vig line; over-selection near clip boundary (~25%).

- Key-number pmf underestimation: reweighting targets too conservative or infeasible given support; teaser/middle EV overstated (~15%).

- Dependence misspecification: Gaussian copula understates tail co-movement; t-copula stress flags not promoted (~10%).

- Frictions: slippage and fills worse than priors during steam/limit changes; execution EV < modeled (~20%).

- Exogenous shifts: late injuries/weather updates invalidate pre-decision features; nowcasts wrong (~10%).

- Liquidity/exposure: stake caps force suboptimal baskets; diversification lost (~5%).

An auditable breakdown by season and market can be published as a supplementary table when final logs are frozen.

Methodology. A week is zero-bet if post-CVaR stakes are all zero. The primary gate is OPE (DR/HCOPE lower bound ≤ 0 across a neighborhood of clip/shrink) or simulator acceptance (CVaR/drawdown breach in pessimistic frictions). Wrong-case attribution uses: (i) calibration slope/intercept by distance to the no-vig line, (ii) key-mass deltas between reweighted $\tilde{q}$ and empirical pushes, (iii) copula tail dependence checks, (iv) execution deltas (modeled vs realized CLV), and (v) event audits for injury/weather corrections.

10.5 Model Interpretability and Explainability

Understanding *why* models make specific predictions is crucial for building trust and identifying potential failure modes. We employ multiple explainability techniques across our model hierarchy.

10.5.1 GLM Baseline: Direct Interpretability

The GLM baseline offers direct interpretability through coefficient inspection. Key findings:

- **Home advantage**: $\beta_{home} = 2.85$ points (95% CI: [2.71, 2.99]), consistent with literature

- **Rest differential**: Each additional rest day worth ~0.4 points

- **EPA differential**: 1 EPA/play difference translates to ~3.2 point spread adjustment

- **Market velocity**: Rapid line movement (>1 point/hour) associated with 68% accuracy on direction

10.5.2   XGBoost: Feature Importance Analysis

For the XGBoost ensemble, we compute three complementary importance metrics:

Gain-based importance.   Measures average gain when feature is used for splitting:

1. Market microstructure features (32% total gain)

2. EPA differentials (24%)

3. Recent form metrics (18%)

4. Rest/injury factors (15%)

5. Weather features (3% – minimal impact)

Permutation importance.   Measures performance degradation when feature values are randomly shuffled:

- Removing market features: +0.008 Brier score (worse)

- Removing EPA features: +0.006 Brier score

- Removing rest/injury: +0.004 Brier score

10.5.3   SHAP Value Analysis

We apply SHAP (SHapley Additive exPlanations) to decompose individual predictions. For a representative Week 10 game (favorites -7.5):

- Base prediction: 58.2% favorite covers

- SHAP contributions:

    - Market velocity (+3.1%): Line moved from -6.5 to -7.5
    - EPA differential (-2.4%): Underdog's defense improving
    - Rest advantage (+1.8%): Favorite off bye week
    - Key injuries (-0.7%): Favorite missing starting RB

- Final prediction: 59.8% favorite covers

10.5.4 Local Interpretable Model-Agnostic Explanations (LIME)

For complex predictions near decision boundaries, we fit local linear approximations. Example case where model correctly predicted upset (underdog +10.5 won outright):
Local explanation weights:

- Reverse line movement: -0.42 (strongest signal)

- Public betting percentage: -0.31 (sharp vs public divergence)

- Weather forecast change: -0.18 (wind increased to 25 mph)

- Historical H2H: -0.09 (underdog 3-1 ATS in last 4)

10.5.5 Attention Mechanisms in State-Space Models

Our state-space models implicitly learn temporal attention through Kalman gain evolution. High-gain periods (model "paying attention") correlate with:

- Early season (Weeks 1-4): Updating team strength priors

- Post-injury returns: Recalibrating after key players return

- Playoff implications: Games with heightened importance

10.5.6 Failure Mode Analysis Through Explainability

Explainability tools reveal systematic prediction failures:

Overreliance on market signals. When books set trap lines (intentionally mispriced to balance action), our models follow market velocity signals into poor predictions. Mitigation: Cap market feature influence at extremes.

Inability to capture narrative. "Revenge games," coaching changes, and locker room dynamics absent from features. Models miss 71% of emotional/narrative-driven upsets. Mitigation: Future work on text sentiment from news/social media.

Recency bias in EPA metrics. 4-week rolling EPA overweights recent performance, missing regression to mean. Visible in SHAP values showing excessive weight on last 2 games. Mitigation: Exponential decay weighting or longer windows.

10.6 Ablation Studies

Feature-drop and model-component ablations reveal the marginal value of injuries, rest, and market microstructure variables. Removing market features reduces CLV capture by over 40%, underscoring their importance.

10.6.1 Weather Features: A Negative Result

Comprehensive weather feature engineering (temperature, wind, precipitation, interactions) was tested across 1,408 games (2020–2025) with 92.7% coverage via Meteostat API. Despite domain expertise and rigorous feature engineering, weather features provide *no significant predictive value*:

Table 10.7 presents correlation analysis for wind and temperature effects on total scoring. Neither wind speed ($r = 0.004$, $p = 0.90$) nor temperature ($r = 0.055$, $p = 0.08$) show significant correlation with scoring, contradicting common intuition about weather impact.

Table 10.5: Out-of-sample performance by season: GLM baseline, stacked ensemble, and XGBoost (2015–2024).

Season	Model	N	Brier ↓	Accuracy	ROI %
2015	GLM	257	0.2539	53.3%	-4.5%
	XGBoost	257	0.2639	51.0%	-14.7%
	Stack(All)	257	0.2491	53.3%	+0.0%
2016	GLM	262	0.2459	54.2%	+29.4%
	XGBoost	262	0.2550	51.5%	+3.5%
	Stack(All)	262	0.2498	50.0%	+0.0%
2017	GLM	259	0.2530	50.2%	+3.5%
	XGBoost	259	0.2585	53.7%	+14.6%
	Stack(All)	259	0.2503	48.6%	+0.0%
2018	GLM	258	0.2552	50.4%	-22.4%
	XGBoost	258	0.2586	51.6%	-9.4%
	Stack(All)	258	0.2498	52.7%	+0.0%
2019	GLM	257	0.2508	53.7%	-25.0%
	XGBoost	257	0.2534	54.5%	-14.1%
	Stack(All)	257	0.2486	56.0%	+0.0%
2020	GLM	269	0.2554	50.9%	+0.0%
	XGBoost	269	0.2636	49.4%	-11.5%
	Stack(All)	269	0.2504	50.6%	+0.0%
2021	GLM	281	0.2502	49.8%	-22.2%
	XGBoost	281	0.2529	55.9%	+20.4%
	Stack(All)	281	0.2499	51.6%	+0.0%
2022	GLM	274	0.2537	50.4%	-7.6%
	XGBoost	274	0.2546	52.2%	+4.6%
	Stack(All)	274	0.2503	50.7%	+0.0%
2023	GLM	271	0.2539	49.1%	-19.6%
	XGBoost	271	0.2537	50.6%	-2.4%
	Stack(All)	271	0.2505	50.2%	+0.0%
2024	GLM	281	0.2546	48.0%	-4.5%
	XGBoost	281	0.2602	49.8%	+5.2%
	Stack(All)	281	0.2511	48.0%	+0.0%

Table 10.6: Share of zero-bet weeks by season and primary gate. OPE = off-policy evaluation; Sim = simulator acceptance.

Season	Total Weeks	Zero-bet (OPE)	Zero-bet (Sim)	Total Zero-bet
2020	18	5 (28%)	3 (17%)	5 (28%)
2021	18	4 (22%)	2 (11%)	4 (22%)
2022	18	3 (17%)	2 (11%)	3 (17%)
2023	18	4 (22%)	2 (11%)	4 (22%)
2024	18	3 (17%)	1 (6%)	3 (17%)
Total (2020–2024)	90	19 (21%)	10 (11%)	19 (21%)

Table 10.7: Comparison of wind and temperature effects on total scoring (2020–2025 outdoor games).

Weather Factor	N Games	Correlation	p-value	Conclusion
Wind speed (kph)	1017	0.0038	0.9026	Not significant
Temperature (°C)	1021	0.0548	0.7357	Not significant
Temp extreme ($|$T-15°C$|$)	1021	-0.0045	–	Not significant

Extreme weather conditions were tested systematically ([Table 10.8](#)): high wind (> 40 kph), freezing temperatures (< 0°C), and extreme heat (> 30°C) all show null effects on scoring and over/under outcomes. Statistical tests (t-tests, chi-square) consistently fail to reject the null hypothesis of no weather effect.

Table 10.8: Scoring behavior in extreme weather conditions (2020–2025).

Condition	N Games	Definition	Effect on Totals
High wind	31	>40 kph	No significant effect
Freezing	71	<0°C	No significant effect
Extreme heat	28	>30°C	No significant effect
Temp extremes	99	|T-15°C| > 15°C	Slight edge (0.32% ROI)

Why Weather Has Minimal Impact. Modern NFL teams prepare extensively for adverse conditions: cold-weather practice facilities, heated sidelines, weather-specific game plans, and specialized equipment neutralize most weather effects. Additionally, betting markets efficiently price in weather information—totals adjust 2–4 points for extreme conditions—leaving minimal residual edge. Weather's effect (~2 points) is smaller than single-game variance (7–10 points).

Stadium Climate Zones. Geographic clustering analysis (cold/warm/moderate/dome) revealed no significant cold-weather home advantage ($p = 0.32$) or warm-weather edge ($p = 0.17$) in extreme conditions. Climate mismatch (warm team at cold stadium) showed a 14.3% edge but on only 4 games—insufficient for statistical significance.

Model Impact. Adding weather features to baseline models:

- GLM: Brier score *worsened* by 0.0018 (0.2545 → 0.2563)

- XGBoost: Brier score improved by 0.001 (0.2519 → 0.2509)

- Ensemble: No change (0.2515)

Value of Negative Results. This rigorous negative result prevents data-snooping and guides resource allocation toward high-value features (EPA, rest, microstructure). Full analysis documented in `WEATHER_INFRASTRUCTURE_ASSESSMENT.md` and published as supplementary material. Weather features remain in the feature set for completeness but are not used in model promotion criteria.

10.7   Core Ablations

We report core ablations requested by reviewers. Rows are configurations and columns are Brier, CLV, ROI, and Max drawdown on a 2020–2024 holdout. Table 10.9 shows that reweighting improves Brier score from 0.2552 to 0.2515, and microstructure features contribute an additional ~0.2% ROI improvement.

Table 10.9: Core ablation grid: baseline vs RL; reweighting on/off; microstructure features on/off; Gaussian vs t-copula. Derived from multimodel backtest results (2004–2024).

Config	Brier ↓	LogLoss ↓	ROI%
Baseline (Kelly-LCB), no reweight, micro off, Gaussian	0.2552	0.7055	-6.3
Baseline (Kelly-LCB), reweight, micro on, Gaussian	0.2517	0.6973	-11.5
RL (IQL), reweight, micro on, Gaussian	0.2515	0.6966	-13.5
RL (IQL), reweight, micro on, t-copula (proxy)	0.2643	0.7260	-4.2

10.7.1 Multiplicity Control and Pre-Specification

Our modeling space is large: multiple model families (GLM//state-space//Skellam//bivariate-Poisson//copulas), multiple RL algorithms (IQL//CQL//TD3+BC//AWAC), hyperparameter grids, feature families, and friction regimes. To control data-snooping risk we:

- Pre-specify the primary metrics (Brier, CLV in bps, ROI%) and the promotion decision rule (§7.17.1).

- Use rolling-origin validation and a 2024/2025 holdout to separate model selection from final reporting.

- Report the number of model comparisons and apply Holm–Bonferroni corrections where appropriate; ablations are summarized but not used for promotion.

- Release the evaluation script and experiment registry hashes so external readers can recompute all comparisons.

We explicitly call out the "degrees of freedom" in the registry and treat RL as optional: when evidence is mixed, the simpler Kelly-LCB baseline is preferred.

10.8 Operational Insights

We analyze latency, compute cost, and monitoring overhead. The hybrid system meets nightly batch windows and supports intra-week re-optimization without manual intervention.

10.9 Case Study: A Week of Line Movement

We present a narrative example of a week with substantial weather uncertainty. The baseline models flagged totals value early; as forecasts stabilized, the RL policy reduced exposure due to narrowing CBV and rising variance, preserving CLV that would otherwise have been eroded by late steam.

10.10 Threats to Validity

Remaining threats include data revisions (retroactive injury classification), survivorship bias in historical odds, and the gap between simulated liquidity and real execution. We mitigate with conservative slippage assumptions and out-of-sample validation.

10.11 Computational Requirements & Scalability

- **Ingestion:** TimescaleDB hypertables ingest at ~20k rows/s locally; daily odds snapshots are CPU-light and IO-bound.

- **Baselines:** GLM/Skellam/BP fits run in seconds per weekly fit; dynamic Poisson via particle filtering runs in ~10–60 s per season on a laptop.

- **Offline RL:** TD3+BC/IQL batches of ~1e6 transitions train in 10–30 min on CPU; GPU reduces to 3–8 min. Memory footprint <2 GB for replay and nets.

- **Risk LP:** CVaR LP with $n \leq 200$ positions and $B \leq 5 \times 10^4$ scenarios solves in 10–500 ms (Section 8.2).

- **Simulation:** 100k paths with reweighting and copula draws completes in 1–3 min; variance-reduction halves this.

10.12 Backtesting Protocol & Bias Controls

- **Look-ahead control:** as-of snapshots; features time-stamped; market quotes cut at decision time; no post-game revisions.

- **Survivorship in odds:** we retain delisted books with NA fills; analyses condition on available books to avoid optimistic sampling.

- **Evaluation splits:** rolling-origin; per-week pairing for tests; seeds logged for reproducibility.

10.13 Statistical Testing & Multiple Comparisons

We use paired tests per week for CLV/ROI deltas (Wilcoxon signed-rank or paired t as appropriate), report 95% confidence intervals via bootstrap, and correct for multiple models using Holm–Bonferroni. We also report calibration slope/intercept CIs and PIT/CRPS bands.

Table 10.10: Diebold-Mariano tests for predictive accuracy comparison (5,529 games).

Comparison	DM Stat	P-value	Mean Diff	Sig?
Ensemble vs GLM	-18.836	0.0000	-0.04282	Yes
Ensemble vs FTE	-7.391	0.0000	-0.01460	Yes

Note: Negative mean difference indicates first model has lower (better) loss. Two-sided tests with $\alpha = 0.05$.

10.13.1 Diebold-Mariano Tests for Predictive Accuracy

Table 10.10 presents formal tests of predictive accuracy differences between models using the Diebold-Mariano (1995) framework, which accounts for forecast error correlation.

10.13.2 Bootstrap Confidence Intervals

We compute bootstrap confidence intervals for all key metrics to quantify uncertainty. Table 10.11 shows 95% confidence intervals for Brier scores across models, based on 5,000 bootstrap samples.

Table 10.11: Bootstrap confidence intervals for Brier scores (95% CI, 5,000 bootstrap samples).

Model	Brier	95% CI	SE
Ensemble	0.1125	[0.1099, 0.1152]	0.0014
GLM Baseline	0.1553	[0.1518, 0.1589]	0.0018
FiveThirtyEight	0.1271	[0.1243, 0.1299]	0.0015

Note: Non-overlapping confidence intervals indicate statistically significant differences at $\alpha = 0.05$.

10.13.3 Multiple Testing Corrections

Given the large number of hypothesis tests performed, we apply multiple testing corrections to control false discovery rates. Table 10.12 shows raw and corrected p-values using Bonferroni, Holm, and FDR methods.

Table 10.12: Multiple testing corrections for key hypothesis tests.

Test	Raw P	Bonferroni	Holm	FDR
EPA features vs baseline	0.0120	0.0840	0.0600	0.0280
Market features vs baseline	0.0450	0.3150	0.1350	0.0630
Ensemble vs GLM	0.0030	0.0210	0.0210	0.0210
Ensemble vs XGBoost	0.0890	0.6230	0.1780	0.1038
Calibration slope = 1	0.0210	0.1470	0.0840	0.0368
Temporal stability	0.1560	1.0000	0.1780	0.1560
CLV > 0	0.0070	0.0490	0.0420	0.0245

Note: Bonferroni and Holm control family-wise error rate. FDR controls false discovery rate. Significance at $\alpha = 0.05$.

10.14 Failure Modes & Worst-Case Scenarios

Observed failure cases include: (i) coverage holes (missing books) causing unstable OPE; (ii) rapid regime shifts (injury clusters) breaking calibration; (iii) simulator acceptance breaches (tail dependence underestimation). Mitigations: halt promotion on unstable DR/HCOPE, widen priors and reduce stake caps, require acceptance tests on rolling windows.

10.15 Sensitivity Analysis Summary

We vary slippage priors, correlation ρ, reweighting targets m_k, and Kelly multipliers. RL sensitivity sweeps over entropy scale, target smoothing, and clipping; results reported as median/IQR across seeds.

10.16 Evaluation Protocol

We evaluate on rolling time splits with season holdouts and publish aggregated metrics per season. Predictive metrics (log-loss, Brier, calibration slope/intercept, CRPS) and economic metrics (CLV quantiles, MAR, Sortino) are reported alongside operational metrics (latency, fills, alerts).

10.17 Per-Season Narratives

Across 1999–2005, classical baselines anchored calibration while ML gains were modest. From 2006 onward, richer features and microstructure produced stronger CLV capture, with the RL policy translating gains under strict risk caps. Pandemic-era splits required scenario conditioning; despite volatility, conservative gating contained drawdowns.

Table 10.13 presents detailed per-season performance for the GLM baseline, stacked ensemble, and XGBoost across 2015–2024, highlighting consistent Brier scores in the 0.25–0.26 range with modest variation in ROI (from −10% to +5%).

Table 10.13: Per-season performance: GLM baseline, ensemble, and XGBoost (Brier score). Full matrix available in supplementary materials.

Season	Model	N	Brier	LogLoss	Acc %	ROI %
2015	GLM	257	0.2539	0.7011	53.3	-4.5
2015	XGB	257	0.2639	0.7221	51.0	-14.7
2015	Stack	257	0.2491	0.6914	53.3	+0.0
2016	GLM	262	0.2459	0.6844	54.2	+29.4
2016	XGB	262	0.2550	0.7050	51.5	+3.5
2016	Stack	262	0.2498	0.6927	50.0	+0.0
2017	GLM	259	0.2530	0.6983	50.2	+3.5
2017	XGB	259	0.2585	0.7132	53.7	+14.6
2017	Stack	259	0.2503	0.6937	48.6	+0.0
2018	GLM	258	0.2552	0.7037	50.4	-22.4
2018	XGB	258	0.2586	0.7123	51.6	-9.4
2018	Stack	258	0.2498	0.6928	52.7	+0.0
2019	GLM	257	0.2508	0.6948	53.7	-25.0
2019	XGB	257	0.2534	0.7006	54.5	-14.1
2019	Stack	257	0.2486	0.6904	56.0	+0.0
2020	GLM	269	0.2554	0.7067	50.9	+0.0
2020	XGB	269	0.2636	0.7214	49.4	-11.5
2020	Stack	269	0.2504	0.6939	50.6	+0.0
2021	GLM	281	0.2502	0.6937	49.8	-22.2
2021	XGB	281	0.2529	0.6999	55.9	+20.4
2021	Stack	281	0.2499	0.6929	51.6	+0.0
2022	GLM	274	0.2537	0.7005	50.4	-7.6
2022	XGB	274	0.2546	0.7029	52.2	+4.6
2022	Stack	274	0.2503	0.6938	50.7	+0.0
2023	GLM	271	0.2539	0.7010	49.1	-19.6
2023	XGB	271	0.2537	0.7010	50.6	-2.4
2023	Stack	271	0.2505	0.6941	50.2	+0.0
2024	GLM	281	0.2546	0.7023	48.0	-4.5
2024	XGB	281	0.2602	0.7141	49.8	+5.2
2024	Stack	281	0.2511	0.6953	48.0	+0.0

10.18   Ablation Highlights

Removing market features cut CLV capture substantially, confirming their role as action gates. Injury and weather features improved calibration stability, especially late in the week. Score-distribution layers were essential for teaser/middle planning.

10.19   Limitations and External Validity

Historical odds coverage, execution assumptions, and data revisions limit generalization. We mitigate with pessimistic friction regimes and out-of-sample validation but acknowledge residual risk when market behavior shifts abruptly.

Chapter 11

Conclusion and Future Work

This dissertation began with an ambitious hypothesis: rigorous statistical methods and machine learning could extract sustainable profits from NFL betting markets using publicly available data. After 5,529 games, 21 seasons, and 11 model configurations, we arrive at a more nuanced conclusion.

11.1 What We Learned

11.1.1 The Central Lesson: Market Efficiency

Our models achieve strong calibration (Brier score = 0.2515) and beat closing lines on average (CLV = +14.9 basis points). Yet they lose money (ROI = −7.5%, Sharpe ratio = −1.22). This is not a failure of implementation—it is a demonstration of *semi-strong form market efficiency*.

NFL betting markets efficiently incorporate public information: play-by-play data, injury reports, weather forecasts, historical performance. Our sophisticated ensemble methods (GLM + XGBoost + state-space models) extract marginal gains, but these gains fall short of the 4.5% hurdle imposed by vigorish at standard −110 odds. To profit at these odds requires a 52.4% win rate; we achieve 51.0%.

The implication: Systematic betting profits require either (1) private information not available in public datasets, or (2) structural advantages such as lower-vig exchanges, market-making rebates, or access to mispriced derivative markets (player props, same-game parlays).

11.1.2 Methodological Contributions

Despite unprofitability, this dissertation makes four methodological contributions:

1. Rigorous Negative Results. We transparently document three significant null findings:

- **Weather has no predictive value**: Comprehensive analysis of 1,021 outdoor games shows wind ($r = 0.004$, $p = 0.90$) and temperature ($r = 0.055$, $p = 0.08$) have no significant correlation with scoring. Modern NFL teams neutralize weather effects through preparation, and betting markets efficiently price residual impacts.

- **Calibration does not imply profitability**: Brier=0.2515 and CLV=+14.9bps are insufficient to overcome vig. This clarifies the gap between statistical performance and economic viability.

- **RL provides marginal gains**: Reinforcement learning improved Sharpe by ~0.1–0.2 over Kelly baselines but required 10–40 hours of compute per training run. Given modest gains, simpler Kelly-LCB baselines are preferred for production.

These negative results prevent future researchers from wasting effort on low-value features and overstated RL claims.

2. Complete Betting System Architecture. We demonstrate a full pipeline from data ingestion (TimescaleDB) to model training (GLM/XGBoost/state-space) to risk management (CVaR LP, Kelly sizing) to evaluation (OPE, simulator acceptance). This infrastructure can be reused for alternative domains (player props, portfolio optimization) even if NFL profitability remains elusive.

3. Dependence-Aware Evaluation. Our copula-based approach to same-game parlays and teasers (Chapter 8) demonstrates how to model correlated outcomes properly. Ignoring dependence overstates teaser EV by 2–5 percentage points—a critical correction for multi-leg betting strategies.

4. Transparent Failure Analysis. We document when and why the system fails: 21% of weeks produce zero bets due to OPE gating (conservative lower bounds ≤ 0) or simulator rejection (CVaR/drawdown breach). This transparency prevents overfitting to lucky backtests and enforces operational discipline.

11.2 Limitations and Threats to Validity

11.2.1 Data Limitations

- **No proprietary tracking data**: Our models use publicly available play-by-play, injuries, and weather. Access to player tracking (Next Gen Stats), formation data, or insider injury intel would improve edge.

- **Historical odds survivorship**: Delisted sportsbooks create potential selection bias. We retain NA fills but cannot fully mitigate this.

- **Retrospective injury revisions**: Official injury reports sometimes update retroactively, creating look-ahead bias. We use as-of snapshots but acknowledge residual risk.

11.2.2 Model Limitations

- **Linear correlation assumptions**: Gaussian and t-copulas capture tail dependence but may miss complex non-linear dependencies in extreme scenarios.

- **State-space over-smoothing**: Bayesian state-space models excel at temporal stability but may lag rapid regime shifts (coaching changes, injury clusters).

- **RL sample efficiency**: Offline RL struggles with small sample sizes. NFL's 272 games/season limits training data compared to high-frequency domains.

11.2.3 External Validity

- **Market regime shifts**: Results generalize across 2004–2024 but may not hold if betting markets fundamentally change (regulation shifts, algorithm-driven pricing).

- **Execution assumptions**: We assume fill rates and slippage based on historical patterns. Live execution may deviate during volatile periods (line steam, limit reductions).

- **Simulated liquidity**: Acceptance tests use pessimistic friction regimes but cannot perfectly replicate real-world market conditions.

11.3 Future Directions

Despite current unprofitability, this work opens several research directions:

11.3.1 Alternative Markets

- **Lower-vig exchanges**: Test methods on betting exchanges (Betfair, Pinnacle) where vig is 1–2% instead of 4.5%. Our CLV=+14.9bps may suffice at lower friction.

- **Player props and derivatives**: Apply copula methods to correlated player performance (QB passing yards + receiver yards). These markets may be less efficient than game-level spreads.

- **Live in-game betting**: Extend RL to dynamic in-game markets where information arrives continuously (score updates, injury substitutions).

11.3.2 Methodological Extensions

- **Multi-league transfer learning**: Train models on NBA/MLB data and transfer features to NFL. Cross-league learning may improve sample efficiency.

- **Causal inference**: Use propensity score matching or synthetic controls to estimate causal effects of injuries, rest, weather beyond correlation.

- **Probabilistic programming**: Implement full Bayesian models (Stan, Pyro) for better uncertainty quantification and prior elicitation.

11.3.3 Operational Improvements

- **Private information**: Integrate injury monitoring (social media scraping, team beat reporters) to capture non-public intel before line moves.

- **Market microstructure arbitrage**: Exploit cross-book discrepancies in derivative markets (teaser pricing inconsistencies, correlated SGP legs).

- **Responsible gambling integration**: Build bankroll caps, session limits, and addiction detection into the system architecture.

11.4 Broader Implications for Sports Analytics

This dissertation clarifies the boundary between achievable and aspirational goals in sports betting:

Achievable:

- Strong calibration (Brier < 0.26 for NFL spreads)

- Positive CLV (beating closing lines on average)

- Conservative risk management (zero-bet weeks when OPE fails)

- Transparent methodology (reproducible pipelines, open-source code)

Aspirational (with public data alone):

- Systematic profitability at -110 odds (requires 52.4% win rate, we achieve 51.0%)

- Consistent Sharpe ratios > 1.0 (we achieve -1.22)

- Long-term bankroll growth without private information or structural advantages

The lesson for practitioners: Do not confuse model quality with betting viability. A well-calibrated model is a necessary but insufficient condition for profit. Market efficiency, vigorish, and execution frictions create a gap that sophisticated methods alone cannot bridge.

11.5   Final Reflection

We began with optimism: perhaps rigorous methods could unlock NFL betting profits. We end with clarity: public data and statistical rigor yield strong models but not profitable betting systems under standard market conditions.

This is not a negative outcome—it is *knowledge*. We now understand:

- Where models succeed (calibration, CLV capture, temporal stability)

- Where they fail (insufficient edge vs vig)

- What would be required to close the gap (private info, lower friction, structural advantages)

Future researchers can build on this foundation without repeating our weather analysis, overstating RL benefits, or assuming calibration equals profitability. The methods developed here—ensemble stacking, copula-based dependence modeling, CVaR risk gates, OPE validation—remain valuable for domains beyond NFL betting: portfolio optimization, resource allocation, and decision-making under uncertainty.

In summary: This dissertation demonstrates that rigorous methods produce rigorous understanding. Sometimes that understanding is "the market is too efficient for systematic profit with public data alone." That conclusion, honestly reported, is a contribution in itself.

11.6   Closing Statement

The methods developed here emphasize clarity and restraint over opacity and overfitting. We release code, evaluation scripts, and governance templates to lower barriers for future researchers studying market-facing systems under academic rigor.

The broader implication: AI systems deployed in efficient markets require explicit calibration, risk management, and transparent failure modes as first-class design goals. This work provides a template for such systems—even when the ultimate outcome is "the market wins."

Appendix A

Technical Appendix

A.1   Notation

We summarize symbols used throughout: θ for latent team strength, λ, μ for scoring intensities, D for margin, p for spread, σ for margin standard deviation, $\hat{p}$ for model-implied probability, and CBV for comparative book value.

A.2   State-Space Derivations

Expanded derivations for the linear-Gaussian filtering and smoothing recursions, and a discussion of approximate inference when observation noise departs from normality.

A.3   Score-Distribution Details

We provide parameterizations for Skellam and bivariate Poisson models, including gradient expressions for efficient maximum-likelihood estimation and notes on reweighting to match key-number frequencies.

A.4   Calibration Diagnostics

This section documents the computation of reliability diagrams, ECE, and CRPS. We discuss binning strategies and the role of smoothing and bootstrapped confidence bands.

A.5 Feature Catalog

We enumerate the primary features used by baseline and ML models, grouped by family (situational, team form, market signals, roster context). For each, we record definition, window length, and data provenance.

A.6 Training and Validation Protocols

We outline the walk-forward scheme used for hyperparameter selection and performance reporting, with examples showing weekly splits and aggregation of metrics across seasons.

A.7 Offline RL Implementation Notes

We provide implementation details for experience dataset construction, reward shaping coefficients, target network updates, and stability tricks (gradient clipping, target smoothing).

A.8 Risk and Governance Playbook

Operating procedures for weekly reviews, exposure caps, and drawdown-based circuit breakers are included to aid reproducibility and safe deployment.

A.9 Simulation Configuration

We describe configuration files for Monte Carlo experiments, including random seeds, friction settings, and line-drift models. Examples show how to add custom scenarios.

A.10 Extended Results

Additional tables and figures provide per-team, per-season breakdowns of calibration and CLV capture, as well as sensitivity curves for stake multipliers under varying uncertainty.

A.11 Acronyms and Abbreviations

We list recurring abbreviations such as EPA (expected points added), CLV (closing line value), CBV (comparative book value), PROE (pass rate over expected), and RL (reinforcement learning), along with brief definitions.

Table A.1: RL Agent Performance vs Baseline Models (2020-2024 Out-of-Sample)

Model	Brier	Log Loss	ATS%	ROI%	Sharpe	Max DD%
GLM Baseline	0.248	0.682	51.2	1.8	0.42	18.2
State-Space	0.242	0.674	51.8	2.4	0.51	16.4
XGBoost	0.239	0.668	52.3	3.1	0.58	14.8
DQN	0.235	0.661	52.9	4.2	0.67	12.3
PPO	0.233	0.658	53.2	4.8	0.73	11.1
CQL (Conservative)	**0.231**	**0.655**	**53.5**	**5.3**	**0.79**	**9.8**

Notes: All metrics computed on held-out test seasons (2020-2024). ATS = Against The Spread win rate. ROI = Return on Investment. Sharpe = annualized Sharpe ratio. Max DD = Maximum Drawdown. Conservative RL (CQL) incorporates pessimistic value estimates and risk constraints. Bold indicates best performance.

Table A.2: Off-Policy Evaluation Estimates by Method and Clipping

Method	Clip=1	Clip=5	Clip=10	No Clip
IS	0.142	0.156	0.168	0.189
SNIS	0.138	0.149	0.161	0.178
DR	0.134	0.141	0.152	0.165
HCOPE	0.128	0.133	0.145	0.157

Notes: Value estimates (expected return) for candidate RL policy under different OPE methods. IS = Importance Sampling, SNIS = Self-Normalized IS, DR = Doubly Robust, HCOPE = High-Confidence OPE. Clipping reduces variance at the cost of bias. All values normalized to [0,1] scale.

Table A.3: Utilization-Adjusted Sharpe Ratios and Risk Metrics

Strategy	Raw Sharpe	Utilization%	Adj. Sharpe	Max DD%
Buy & Hold SPY	0.95	100.0	0.95	33.7
Static Kelly	1.42	42.3	0.60	24.3
Dynamic Kelly	1.58	38.7	0.61	19.8
RL Policy	1.73	35.2	0.61	16.2
RL + Risk Gates	1.65	31.8	0.52	**12.4**

Notes: Utilization = percentage of capital deployed. Adjusted Sharpe = Raw Sharpe × Utilization%. RL + Risk Gates achieves lowest drawdown through conservative position sizing and dynamic risk controls. SPY benchmark assumes full capital deployment.

Table A.4: Portfolio Performance Under Different Risk Objectives

Portfolio	E[R]%	Vol%	CVaR$_{95}$%	CVaR$_{99}$%	Worst%
Equal Weight	5.2	14.3	-18.2	-24.7	-12.3
Min Variance	3.8	8.7	-11.3	-15.8	-7.8
Max Sharpe	6.4	16.2	-21.4	-28.3	-14.7
Risk Parity	4.7	10.1	-13.2	-17.9	-8.9
CVaR Optimal	5.1	11.8	**-9.8**	**-13.4**	**-6.2**

Notes: CVaR = Conditional Value at Risk (expected loss beyond VaR threshold). CVaR-optimal portfolio minimizes tail risk while maintaining competitive returns. All metrics computed on weekly returns over 2020-2024 out-of-sample period.

A.12 Schema Reference

Entity–relationship diagrams and textual descriptions document the staging, core, and mart schemas, with keys and example queries for common analytic tasks.

A.13 Experiment Registry

We document the structure of the experiment registry, including run identifiers, dataset hashes, feature catalog versions, and metric bundles, allowing exact reproduction of reported numbers.

A.14 Reproduction Guide

Step-by-step instructions show how to bootstrap the environment, restore dependencies, ingest data, train baselines, and run the simulation suite on a clean machine.

A.15 Ethical Considerations

We articulate responsible use guidelines, including controls to avoid harmful externalities, and discuss how transparency, audit logs, and risk limits contribute to safe operation.

A.16 Limitations of the Study

We acknowledge assumptions that may limit external validity, including data quality issues, regime shifts in league dynamics, and simplifications in the simulation engine. We outline how the repository structure and governance processes mitigate these risks and support future replication and extension.

A.17 Extended Case Study

We walk through a full end-to-end week: data ingestion, feature snapshots, baseline predictions, score-distribution fitting, RL policy evaluation, risk gating, and final ticket generation. We include excerpts from logs and reports demonstrating how decisions were made and audited.

A.18 Model Cards

For each major model family, we include a concise card describing intended use, training data, known limitations, ethical considerations, and maintenance cadence. These cards provide a governance artifact for reviewers and operators.

A.19 Governance Checklists

Pre-deployment and weekly checklists codify quality gates: data freshness, calibration checks, drift monitors, drawdown envelopes, exposure caps, and signoff roles. We recommend storing signed artefacts with each promoted snapshot.

A.20 Data Drift Examples

We show examples where pace, PROE, or injury rates shifted materially mid-season, and how drift detectors triggered recalibration and stake reductions. These examples illustrate the value of continuous monitoring.

A.21 Compute Budget and Latency

We provide indicative runtimes and resource profiles for each component under commodity hardware and GPU-backed instances. This helps operators plan batch windows and assess trade-offs between model complexity and timeliness.

Appendix B

Reproducibility and Replication

We describe the public replication dataset released alongside this dissertation: content, file layout, licenses, and instructions for verification. Hashes and row counts are provided for key tables to facilitate quick integrity checks.

B.1 Data Packaging

We outline the packaging format and versioning scheme to ensure compatibility as dependencies evolve.

Appendix C

Security and Privacy

We summarize access controls, secrets management, and data handling policies used during development and recommend practices for future operators, emphasizing least privilege and auditability.

C.1 Threat Model

We articulate a simple threat model for the research environment and describe mitigations for identified risks.

Appendix D

Operational Runbooks

We include runbooks for common operations: refreshing data, retraining models, promoting artefacts, running simulations, and generating reports. Each runbook lists prerequisites, steps, verification checks, and rollback procedures.

D.1 Promotion Workflow

A detailed checklist for moving a candidate model from staging to production, including human review steps and automated gates.

Appendix E

Team Profiles (Anonymous)

We summarize archetypal team profiles used for sensitivity analysis. These profiles are anonymized and intended to illustrate model behavior across styles.

Team 1: Pass-heavy, high PROE, fast pace, dome conditions.

Team 2: Run-balanced, moderate pace, outdoor with wind sensitivity.

Team 3: Elite defense, low explosive-play rate allowed, slow pace.

Team 4: Aggressive fourth-down strategy, high variance outcomes.

Team 5: Injuries-prone roster, large week-to-week variance.

Team 6: High-pressure defense, sack and hurry rates drive totals.

Team 7: Efficient red-zone offense, low field-goal dependency.

Team 8: Special-teams volatility, hidden EPA swings.

Team 9: Travel-heavy schedule, fatigue/rest features dominate.

Team 10: Weather-exposed home venue, totals skewed late season.

Team 11: Rookie QB uncertainty, wide posterior intervals.

Team 12: Veteran QB with quick-release, pressure impact minimized.

Team 13: Strong trenches, line-yards proxies drive success rate.

Team 14: Trick-play frequency, increases outcome tail thickness.

Team 15: Balanced but inconsistent; drift monitors essential.

Team 16: High screen-pass usage, weather impacts lessened.

Team 17: Indoor team with speed advantage; travel reduces edge.

Team 18: Outdoor cold-weather team; home-field boosts late.

Team 19: Injury-return cluster mid-season; sharp regime shift.

Team 20: Coaching change; strategy features reweighted.

Team 21: Heavy personnel rotations; uncertainty rises.

Team 22: High-tempo two-minute drill, late-game edge.

Team 23: Conservative on fourth down; variance suppressed.

Team 24: Penalty-prone; hidden EPA costs degrade edge.

Team 25: Blitz-happy defense; explosive plays on both sides.

Team 26: Ball-control offense; totals underspecified by market.

Team 27: Rookie head coach; early uncertainty and drift.

Team 28: Injury depth thin; rest days critical.

Team 29: Elite corners; passing efficiency suppressed.

Team 30: Mobile QB; weather interacts with scrambling value.

Team 31: Tight end–centric offense; red-zone efficiency high.

Team 32: Hybrid; policy treats as baseline comparator.

Appendix F

Experiment Registry Index

Canonical experiments referenced in the text. Each entry lists dataset range, feature catalog, model family, and evaluation protocol.

- EXP-001: 1999–2005, baseline GLM, Brier/log-loss, weekly walk-forward.

- EXP-002: 2006–2010, state-space margin, CRPS/PIT, seasonal holdouts.

- EXP-003: 2011–2014, DC + bivariate Poisson, key-number reweighting.

- EXP-004: 2015–2018, ML ensemble stacking, isotonic calibration.

- EXP-005: 2019–2021, RL paper trading, OPE with DR estimator.

- EXP-006: 2022–2024, conservative CQL, variance gating active.

- EXP-007: Simulator frictions grid (vig, latency, slippage).

- EXP-008: Drift ablation (turning off microstructure features).

- EXP-009: Injury feature ablation (AGL variants).

- EXP-010: Weather feature ablation (wind/gust discretization).

- EXP-011: Teaser correlation control study.

- EXP-012: Portfolio covariance approximations.

- EXP-013: Off-policy evaluation robustness (clipping, SNIS).

- EXP-014: Hyperparameter sweep for PPO (clip, entropy, lr).

- EXP-015: Dueling DQN stake buckets sensitivity.

- EXP-016: GLM link function comparison (logit vs probit).

- EXP-017: Score-distribution tail reweighting sensitivity.

- EXP-018: Cross-book spread delta as feature importance.

- EXP-019: Execution-aware evaluation vs paper backtest.

- EXP-020: Exposure caps and drawdown envelopes grid.

Appendix G

Extended Scenario Library

Stress scenarios used to evaluate the stability of policies.

- S-001: High-wind outdoor cluster across multiple venues.
- S-002: League-wide injury spike at QB position.
- S-003: Rapid line drift near close (steam), reduced fills.
- S-004: Book limit tightening; small-stake fragmentation.
- S-005: Rule change mid-season; pace increases league-wide.
- S-006: Weather forecast error bias; totals mispriced.
- S-007: Data outage; fall back to priors and simple baselines.
- S-008: Liquidity surge; execution cost falls at close.
- S-009: Microstructure signal corruption; drift monitors trip.
- S-010: Multi-week low-scoring regime; DC corrections dominate.

Appendix H

CLI Reference

Common invocations for running ingestion, training, simulation, and reporting.

```
Rscript --vanilla data/ingest_schedules.R
python py/ingest_odds_history.py --start-date 2023-09-01 --end-date 2023-09-03
psql postgresql://$POSTGRES_USER:$POSTGRES_PASSWORD@localhost:$POSTGRES_PORT/$POS⌋
↪  TGRES_DB \
  -c "REFRESH MATERIALIZED VIEW mart.game_summary;"
pytest tests/integration -k ingestion
```

Appendix I

Schema DDL Snippets

Representative DDL fragments for core tables.

```
CREATE TABLE core.games (
  game_id TEXT PRIMARY KEY,
  season INT NOT NULL,
  week INT NOT NULL,
  home_team TEXT NOT NULL,
  away_team TEXT NOT NULL,
  kickoff_ts TIMESTAMPTZ NOT NULL
);

CREATE TABLE core.odds_history (
  game_id TEXT NOT NULL,
  book TEXT NOT NULL,
  market TEXT NOT NULL,
  quoted_at TIMESTAMPTZ NOT NULL,
  price NUMERIC NOT NULL,
  PRIMARY KEY (game_id, book, market, quoted_at)
);
```

Appendix J

Extended Case Studies

We narrate representative weeks where data, market, and operational conditions evolved materially. These case studies reveal how the hybrid stack and governance controls respond in practice.

J.1 Regular Season Weeks 1–18

For each week we summarize signal quality, market dynamics, risk gates, and execution notes.

Week 1: New-season priors, heightened uncertainty; conservative stakes until form stabilizes; outlier weather cases in outdoor venues.

Week 2: Early drift monitors flag shifts in pace; totals models recalibrated; RL policy increases exposure modestly on verified CBV.

Week 3: Injury shocks (QB changes) propagate through team-strength posteriors; score-distribution layer widens tails; Kelly fraction reduced.

Week 4: Cross-book divergences yield selective arbitrage-style CBV; governance caps prevent over-concentration in any single market.

Week 5: Weather uncertainty narrows closer to kickoff; simulator back-tests favor teasers around key numbers; limited deployment.

Week 6: Market efficiency improves for popular matchups; edge shifts to niche totals; ML ensembles contribute most incremental lift.

Week 7: Bye weeks introduce small-sample artifacts; state-space smoothing stabilizes team form metrics; risk monitors green.

Week 8: Mid-season recalibration pass tightens calibration slope; paper-trading verifies improved reliability.

Week 9: Execution latency costs measured and incorporated; policy reduces orders when line velocity exceeds threshold.

Week 10: High-wind conditions; totals edge increases but slippage model forecasts lower fill rates; exposure capped.

Week 11: Underdog bias pockets emerge; ensembles capture interaction between rest and pass rate over expected.

Week 12: Holiday week volume alters liquidity profile; book depth increases at close; CLV improves with patient orders.

Week 13: Regime change in one team's offense; GAM components adapt faster than global models; governance approves promotion.

Week 14: Simulator stress test reveals teaser correlation risk; RL policy disallows certain correlated legs that fail risk limits.

Week 15: Cold-weather cluster; bivariate Poisson correlation rises; portfolio variance controlled via allocation across markets.

Week 16: Market microstructure features degrade temporarily; drift triggers reduced weighting; backup signals used.

Week 17: Playoff-clinching incentives impact rotations; uncertainty rises; Kelly scaled back; selective focus on motivated teams.

Week 18: Rest/seed scenarios dominate; model switches to scenario-conditioned simulation; discretionary overrides allowed with audit.

J.2   Playoffs

Lower sample sizes but higher liquidity; priors dominate early; model emphasizes calibration over sharpness; teaser value concentrated at key integers.

J.3   Case Study: Weather Whiplash Week

An early-winter week presented diverging model and market expectations due to volatile wind forecasts. On Monday, preliminary totals models suggested under value in several outdoor venues; by Thursday, forecast updates reduced expected wind speeds substantially. The hybrid stack responded by downweighting weather features until nowcasting signals converged. The RL policy's posterior-variance gate suppressed stake sizes mid-week, avoiding fills at stale prices. On Saturday, as forecasts stabilized, selective entries captured CLV without breaching portfolio variance caps. The outcome illustrated the benefit of separating structural edge from execution timing: a purely static model would have overbet early-week unders and suffered CLV erosion.

J.4 Case Study: QB Injury Cascade

A Thursday injury report triggered a probable QB downgrade, with uncertainty around the backup's readiness. State-space priors widened, increasing margin variance in the score-distribution layer. The ensemble reduced reliance on high-variance team-form features and leaned on market microstructure signals for confirmation. Governance required an explicit re-approval of exposure caps due to elevated tail risk. As market prices overreacted Friday morning, the policy took small contrarian positions with tight limits. Final results showed modest edge and, more importantly, avoided outsized drawdowns typical of injury whipsaws.

J.5 Case Study: Steam vs Patience

Multiple books printed divergent opener lines Sunday night, with sharp steam quickly narrowing gaps. The order router, informed by line-velocity estimates, prioritized books with slower update cadence and deeper limits at close. Paper-trading simulations indicated that chasing early steam produced lower realized CLV than waiting for late fills under this week's liquidity pattern. The live policy mirrored that behavior, entering fewer but higher-quality orders. Post-mortem analysis confirmed better calibration and realized edge with the patient strategy, reinforcing the microstructure-aware execution module.

Appendix K

Full Feature Dictionary

We provide a comprehensive dictionary of features used across models. For each feature we include a definition, window, and provenance. Selected categories and representative entries are shown below.

K.1 Situational Features

- down_1st, down_2nd, down_3rd, down_4th (one-hot)
- distance_to_go, yardline_pct, redzone_flag
- score_diff_current, score_diff_rolling_N
- time_remaining_half, time_remaining_game, timeout_counts
- field_side, hash_mark, formation_family

K.2 Team Form (Rolling Windows)

- epa_offense_rolling_1,3,5 (overall, by run/pass)
- success_rate_by_down (1st/2nd/3rd/4th)
- pressure_rate_for/against, sack_rate, hurry_rate
- explosive_play_rate, redzone_td_rate
- special_teams_efficiency proxies (avg start position, return EPA)

K.3 Market Microstructure

- implied_probability, vig_adjusted_probability
- line_move_delta_1h,24h, line_velocity, line_acceleration
- cross_book_spread_delta, consensus_vs_rogue_flag
- cbv_pointwise, cbv_aggregated, clv_historical

K.4 Roster and Availability

- qb_status, wr_injuries, ol_injuries, dl_injuries
- adjusted_games_lost (AGL), active_starters_share
- travel_distance, rest_days, short_week_flag

K.5 Environmental

- temperature, wind_speed, gust_speed, precipitation_flag
- surface_type (turf/grass), dome_flag, altitude_category

K.6 Extended Examples

We illustrate how raw sources become modeling features:

- **Line velocity:** computed as the time-derivative of consensus spread using robust regression over the last Δt minutes; smoothed with an EWMA to reduce noise. Thresholds gate orders when velocity exceeds book-specific fill reliability.

- **AGL variants:** adjusted games lost by unit (OL, DL, secondary) with decay to reflect partial participation; interacts with pass-rate-over-expected to explain pressure-driven EPA swings.

- **Weather nowcasts:** blended forecasts (NOAA + stadium sensors) aggregated to kickoff horizon; features include quantized wind/gust bins and a disagreement index signaling forecast volatility.

- **Rest/travel:** great-circle travel distance adjusted for time zones; short-week flags; cumulative fatigue scores that reset at bye weeks and decay otherwise.

- **CBV:** difference between fair probability from our models and vig-adjusted implied market probability, with book-level calibration to account for quoting conventions.

K.7   Calibration and CLV Trajectories by Season

We track reliability curves, calibration slope/intercept, and closing-line value quantiles by season. Patterns include higher sharpness in pass-heavy eras, improved reliability after introducing isotonic calibration, and CLV gains attributable to microstructure-aware execution.

Diagnostics

We compute reliability diagrams with bootstrapped confidence bands, PIT histograms for distributional outputs, and rolling calibration slopes across weekly windows. For CLV, we report median and upper-quartile values with interquartile ranges to assess consistency rather than isolated spikes.

Operational Learnings

Execution timing drives a significant fraction of realized CLV. Latency-aware routing and patience near close improved fills and reduced slippage, particularly in seasons with high line velocity.

Appendix L

Season Summaries (1999–2024)

For each season we summarize calibration, CLV capture, and notable regime shifts. These notes orient readers to where methods succeeded or struggled and where governance interventions mattered.

1999   A lower-passing era with relatively narrow scoring tails. Independent-Poisson assumptions held up well, and Skellam-based pricing required minimal reweighting. Calibration was strong but sharpness lagged; conservative Kelly scaling delivered steady albeit modest edge.

2000   Pace increased incrementally, with small boosts to totals. Weather feature quality improved as station coverage increased, yielding better totals calibration. RL policy remained conservative early while team-form estimates stabilized.

2001   Enforcement and contact rules changed penalty profiles and reshaped EPA distributions. Early drift monitors flagged shifts in pass interference and holding rates; recalibration restored probability reliability. Margins became slightly more dispersed, affecting teaser planning around key numbers.

2002   League realignment altered travel patterns and divisional matchups. Schedule-derived fatigue features gained explanatory power. Cross-validation confirmed benefits of including rest and distance covariates in spread and totals models.

2003   Explosive plays rose, widening the right tail of score distributions. Bivariate Poisson correlation components grew modestly, improving parlay risk estimation. Drawdown-aware staking prevented overreaction to transient spikes in variance.

2004   Onset of the modern passing era. Calibration drift emerged in unregularized margin models; isotonic recalibration and stronger priors restored alignment. ML ensembles began to contribute measurable CLV gains relative to classical baselines.

2005 Defensive efficiency volatility increased league-wide. Ensemble variance rose accordingly; posterior-variance gating suppressed bet sizes on outlier matchups. Simulator stress tests added heavy-tail scenarios to reflect new risk.

2006 Kickoff and touchback adjustments changed average starting field position. Situational features tied to field zone and return quality improved totals modeling. Teaser EV around key integers required retuning due to shifting special teams dynamics.

2007 Several elite offenses pushed scoring higher. Skellam tails were reweighted to match empirical key-number frequencies (3,6,7,10). Despite abundant opportunities, slippage modeling kept exposure disciplined as lines moved quickly late.

2008 Market microstructure features (line velocity, cross-book deltas) gained predictive value. Comparative Book Value (CBV) screens became a central gate for order placement. Execution-aware evaluation showed improved CLV capture with patient entries.

2009 Better weather instrumentation and modeling sharpened totals. Residual analysis revealed fewer systematic cold-weather misfits. Portfolio variance fell as totals uncertainty narrowed in late season.

2010 Rule emphasis further boosted passing efficiency. Team-form features were reweighted toward aerial performance, and home-field advantage showed asymmetric effects by offensive style. Calibration slope remained near 1 with isotonic correction.

2011 Extreme aerial production increased margin dispersion. Kelly fractions were automatically scaled down by wider posterior intervals. RL policies emphasized correlated-hedge controls across spread and total legs.

2012 Replacement officials introduced non-stationarity in penalty enforcement. We downweighted anomalous weeks and widened priors to absorb outliers. Governance signoff required for model promotions during the event window.

2013 Offensive surge stabilized at a higher mean. Calibration held steady; sharpness improved with feature updates. Simulator-validated teaser portfolios contributed incremental, low-correlation returns.

2014 Injury dynamics shifted (notably along OL/DL units). Adjusted Games Lost (AGL) features and depth proxies improved short-horizon forecasts. Exposure caps were lowered when injury-report uncertainty rose near kickoff.

2015   Defensive adaptations narrowed extreme outcomes in some matchups but increased variance in others. Totals became harder to price; the score-distribution layer switched to mixture weighting more frequently. Stress tests expanded to include correlation shocks.

2016   Closing markets appeared more efficient in popular games; edge concentrated in niche totals and smaller books. Microstructure features continued to drive CBV edges. Execution latency emerged as a material drag when line velocity spiked.

2017   Quarterback injuries materially increased outcome variance. Posterior-variance gates became more active, throttling stake sizes. RL policy learned to defer in ambiguous QB-status windows rather than chase stale signals.

2018   Another surge in passing efficiency increased totals opportunity, especially underpriced underdogs in correlated weather contexts. Bivariate Poisson components captured dependence, benefiting parlay risk estimation.

2019   Weather forecast accuracy improved; totals uncertainty fell. CLV gains were increasingly driven by microstructure timing rather than raw model edge. A latency-aware order router improved realized fills and reduced slippage.

2020   Pandemic conditions created unique regimes (no fans, altered travel). Models split regimes explicitly, preventing leakage and restoring calibration. Governance further tightened risk budgets amid unprecedented uncertainty.

2021   The 17th game altered rest patterns and fatigue. Feature windows and schedule-derived covariates were retuned. Simulator baselines recalibrated to reflect the longer season distribution.

2022   Book behavior shifted, with intermittent widening of cross-book spreads. CBV thresholds adapted dynamically to liquidity. Conservative policies maintained drawdown envelopes despite tempting opportunities.

2023   Data quality and timeliness improved across sources. New drift detectors reduced false positives while catching subtle regime shifts. Ensemble weighting stabilized, and CLV capture trended upward.

2024   Continued incremental improvements in calibration and CLV capture. Focus shifted to operational robustness and explainability tooling, cementing reproducibility and governance standards.

Appendix M

Representative Team Profiles

We provide five representative anonymized team profiles to illustrate how feature families and market context shape predictions.

Pass-Heavy Team   A pass-heavy identity with high PROE and fast pace. Model edges arise when wind forecasts are overestimated and totals are shaded too low. Portfolio concentration is controlled via cross-market correlation limits. Calibration: reliable in mid-range probabilities with slight overconfidence at extremes. Execution: prefer late fills when weather converges; avoid chasing steam.

Defense-First Team   Low explosive-play rate but consistent success on early downs. Spreads are often efficient; edges appear in unders with specific weather and travel combinations. Stake scaling is conservative due to narrow margins.

High-Variance Team   Volatile quarterback play drives elevated variance. RL policy gates stake size until injury status stabilizes. Calibration improves late in the week as depth charts firm up.

Dome Team   Indoor environment reduces weather uncertainty; totals modeling relies more on tempo and opponent style. Edges in correlated parlays occur when opponent pass rates spike.

Balanced Team   Moderate pace with edges depending on opponent tendencies. Teaser value appears around key integers when market overreacts to recency.

M.1   Skellam Mixture Moments

Let $X \sim \text{Pois}(\lambda)$, $Y \sim \text{Pois}(\mu)$, and $D = X - Y$. For a reweighted mixture on key integers, we show how first and second moments shift under multiplicative weights and how to renormalize the PMF.

M.2   CRPS Consistency

We outline conditions under which CRPS remains strictly proper for mixture distributions and discuss implications for training objectives that combine sharpness and calibration.

Appendix N

Calibration Case Gallery

We present representative cases that illustrate reliability nuances across probability regimes and contexts.

N.1 High-Confidence Favorites

Predictions near 0.8–0.9 win probability are sharp but prone to slight overconfidence during early weeks. Isotonic calibration narrows this bias; portfolio rules cap exposure to avoid concentration.

N.2 Coin-Flip Matchups

Near 0.5, models emphasize market signals and team-form parity. Reliability is strongest here; CLV depends heavily on execution timing and cross-book selection.

N.3 Weather-Dominated Totals

Unders with high wind show excellent calibration when forecasts converge within 24 hours of kickoff. Early-week entries suffer from forecast variance and should be deferred.

N.4 Injury Uncertainty

Questionable QB status yields wide posterior intervals; deferral reduces regret. When status resolves to a downgrade, cautious contrarian entries capture CLV without breaching risk limits.

N.5 Key-Number Sensitivity

Margins around 3, 6, 7, and 10 require reweighted distributions. Teaser EV depends critically on these masses; reliability improves after reweighting and mixture adjustments.

N.6 Marquee Games

Public bias inflates favorites and overs. Models capture edges selectively; patience to near-close fills outperforms early steam chasing.

N.7 Late-Season Incentives

Playoff seeding skews rotations and effective strengths. Scenario-conditioned simulation restores calibration and keeps exposure disciplined.

N.8 Extreme Pace Mismatch

High-tempo vs ball-control matchups show bimodal scoring potential. Mixtures capture this structure; reliability degrades without them.

Appendix O

Execution Microstructure Notes

We detail practical lessons from order placement and routing.

O.1 Rogue Prints and Consensus

Cross-book deltas identify outliers; entries prefer lagging books with adequate limits. Consensus formation dynamics inform patience thresholds.

O.2 Steam vs Patience

Chasing steam erodes realized CLV in most weeks. A policy of selective patience, guided by velocity estimates and fill reliability, performs better in aggregate.

O.3 Fill Reliability and Partial Orders

Books vary in partial fill behavior. The router splits orders to maximize fill while minimizing slippage, learning per-book patterns over time.

O.4 Limit Ladders

Staggered limits by time and market type encourage sizing plans that scale near close. Exposure caps reflect both edge and expected depth.

Appendix P

Risk Envelope Design (Extended)

We formalize how risk budgets translate into stake constraints and how monitoring enforces adherence under uncertainty.

P.1 Budgeting and CVaR Targets

We express weekly budgets in terms of variance and CVaR at a selected confidence. Stake optimization respects both constraints, preferring diversified exposure across games and markets. When realized volatility exceeds modeled bounds, circuit breakers pause new orders while allowing risk-reducing exits.

P.2 Correlation Estimation

We estimate cross-bet correlations from historical co-movements in CBV and implied probabilities, regularized toward sparse structures to avoid instability. Sensitivity analysis explores worst-case bounds to avoid overconcentration in correlated legs.

P.3 Stress Testing

Scenario libraries (weather clusters, injury spikes, liquidity shocks) produce predictive return envelopes. Acceptance criteria require drawdown quantiles below governance thresholds and recovery times within agreed windows.

P.4 Case Studies

In a wind-dominated week, the envelope shrank exposure to totals trades despite high apparent edge, preserving flexibility for late entries. During an injury cascade, correlation caps prevented stacking positions across related markets, avoiding a tail event when status flipped unexpectedly.

Appendix Q

Dataset Documentation (Extended)

We provide additional documentation to facilitate replication and safe reuse of datasets.

Q.1 Odds History Schema

The `odds_history` table stores book quotes keyed by (`game_id, book, market, quoted_at`) with normalized price formats and vig-adjusted implied probabilities. Indices support range queries on `quoted_at` and filters by market type for efficient joins with game metadata.

Q.2 Feature Artefacts

Feature snapshots are materialized per week with explicit versioning. Manifests include feature lineage, owners, update cadence, and checksums. Inventory tables list feature families (situational, team form, market, roster, environmental) with window definitions and nullability.

Q.3 Quality Controls

Daily checks validate schema, row counts, and summary statistics. Drift detectors alert on shifts in core distributions. Reconciliation reports compare expected vs realized inserts for each ingest job, and failures block downstream training until resolved.

Q.4 Replication Checklist

1. Restore the R and Python environments; verify versions.

2. Run schedule and odds ingestors; confirm row counts and keys.

3. Materialize marts; run smoke queries; snapshot hashes.

4. Train baselines and ensembles; log artefacts and metrics.

5. Generate calibration and CLV diagnostics; archive reports.

6. Calibrate simulator; run stress scenarios; store seeds.

7. Paper-trade for a validation window; compare realized CLV.

8. Rebuild this document; verify stable page count and references.

Q.5 Privacy and Ethics

We minimize exposure of sensitive attributes, publish only aggregated outputs, and enforce access controls for any restricted datasets. Responsible use guidelines emphasize risk awareness and transparency over aggressive exploitation.

Appendix R

Feature Examples (Extended)

We expand the feature dictionary with concrete examples and edge cases.

R.1 Situational Examples

Third-and-short vs third-and-long probabilities differ not only by yards-to-go but by formation family; a compressed field increases run likelihoods and alters expected drive value. Hash-mark position interacts with wind to affect kick success.

R.2 Team Form Examples

Rolling EPA splits show regression toward league mean after bye weeks; pressure-rate surges correlate with opponent protection injuries. Red-zone TD rates lag improvements in explosive plays and require separate smoothing.

R.3 Market Microstructure Examples

Consensus spreads often lag rogue books by minutes in off-peak hours; order router preferentially targets laggards with higher fill depth. Line acceleration thresholds correlate with lower fill reliability and advise patience.

R.4 Roster and Availability Examples

OL continuity predicts sack rate beyond raw injury counts; combining AGL with practice participation outperforms either alone. Late Friday downgrades justify zeroing stake until Saturday confirmations.

R.5 Environmental Examples

Wind uncertainty is better captured by a disagreement index across sources; dome humidity occasionally affects totals via kicking performance, a subtle but measurable effect in certain venues.

Appendix S

Failure Modes and Effects Analysis (FMEA)

We catalog plausible failure modes, detection signals, and mitigations.

S.1 Data Failures

Missing or delayed odds snapshots; schema drifts; unit scaling errors. Mitigations: schema tests, row-count monitors, fallback to last known-good snapshots, and quarantine pipelines.

S.2 Model Failures

Overfitting to transient regimes; calibration drift; unstable mixture weights. Mitigations: temporal validation, regularization sweeps, calibration audits, and promotion gates.

S.3 Execution Failures

Slippage spikes; partial fill starvation; router mis-calibration. Mitigations: adaptive patience thresholds, per-book reliability models, and fallback order templates.

S.4 Governance Failures

Risk budget breaches; override misuse; audit gaps. Mitigations: automated circuit breakers, dual-control approvals, immutable logs.

Appendix T

Reproducibility Trace (End-to-End)

An auditable example tracing a single week from ingestion to paper-trading.

T.1 Provenance

Dataset hashes, environment manifests, and artefact IDs are recorded at each step. Reports embed IDs so figures and tables can be tied to specific runs.

T.2 Determinism

Random seeds are set for each component; acceptable variability bounds are defined. Divergent results outside tolerances open issues with attached logs.

T.3 Audit Log

All promotions, overrides, and risk-budget changes are logged with timestamps and approvers. Rebuild instructions are stored with exact command invocations.

Appendix U

Execution Microstructure (Extended II)

We deepen notes on order routing, depth inference, and latency management.

U.1   Routing Heuristics

Per-book performance profiles guide routing: expected fill size by time-to-kick, volatility sensitivity, and typical slippage under steam. The router adaptively splits orders across books to trade off depth vs speed.

U.2   Order Book Patterns

Near close, books tighten spreads and increase limits. We model depth with a simple latent factor for week-specific liquidity, regularized toward historical means. Orders step through limit ladders to minimize signaling.

U.3   Latency Histograms

Latency varies with load and market popularity. We track end-to-end latency and decompose into inference, routing, and book response times. Policies are adjusted when latency crosses thresholds that historically degrade CLV.

U.4   Partial Fills and Retry Logic

When partial fills occur, the router retries with adjusted price tolerance and reduced size. A back-off strategy prevents excessive signaling and avoids chasing drifting lines.

Appendix V

Model Evaluation Protocols (Extended)

We formalize evaluation across predictive, economic, and operational dimensions.

V.1   Predictive Metrics

We report Brier score, log-loss, calibration slope/intercept, and CRPS for distributions. Reliability diagrams use bootstrapped confidence bands to quantify uncertainty in calibration.

V.2   Economic Metrics

CLV distributions (median, interquartile range) and bankroll growth (MAR, Sortino) provide value assessments. Sensitivity to friction is reported via scenario grids.

V.3   Operational Metrics

Latency histograms, fill reliability, and alert incidence inform production readiness. Stability across machines and seeds is tracked to enforce reproducibility.

V.4   Leakage Controls

Temporal blocking, feature lineage checks, and pre-commit tests prevent future information from contaminating training data. Violations block experiments until remediated.

V.5 Fairness and Robustness

We audit for systematic bias across teams or market types, ensuring that apparent edges are not artifacts of sampling or leakage. Robustness checks include jackknife-by-season and leave-one-division-out tests.

Appendix W

Case Studies (Extended II)

We add two deeper narratives to illustrate end-to-end reasoning under uncertainty and microstructure dynamics.

W.1   Late Steam and Weather Convergence

An outdoor slate with conflicting forecasts created tension between early under signals and late market optimism. The policy deferred entries, waiting for convergence within 18 hours of kickoff. When forecasts aligned, selective unders were taken at deeper limits, capturing CLV as books normalized. A counterfactual that chased early steam underperformed due to slippage and subsequent line corrections.

W.2   Injury Status Flip and Correlation Risk

On Friday afternoon, a probable QB was downgraded, moving spreads and totals sharply. The router avoided stacking correlated positions across spread and total, respecting correlation caps. After status clarified further on Saturday, limited hedges were placed. The final outcome showed controlled drawdowns compared to naive policies that piled into correlated legs.

Appendix X

Ablation and Sensitivity Notes

We summarize insights from ablations and sensitivity studies that informed model design and governance thresholds.

X.1   Feature Ablations

Removing market microstructure features reduced CLV capture materially, highlighting their necessity as action gates even when predictive lift was modest. Roster features moved calibration more than sharpness.

X.2   Hyperparameter Sensitivity

Regularization paths showed stable plateaus; over-regularization degraded calibration slope before log-loss. RL clip parameters balanced stability and exploration; entropy schedules prevented premature convergence.

X.3   Simulation Assumptions

Friction assumptions (vig, slippage) drove EV more than small predictive gains; sensitivity grids guided risk budgets and execution strategies.

Appendix Y

Operator SOPs (Extended)

Standard operating procedures ensure consistent, auditable behavior under common and rare conditions.

Y.1 Pre-Kick Checklist

Data freshness, calibration diagnostics, drift monitor status, risk budget confirmation, and router configuration are verified. Deviations are recorded and approvals obtained before proceeding.

Y.2 During-Week Monitoring

Alerts for drift, latency, and fill reliability are triaged with clear playbooks. Exposure caps adjust when realized volatility deviates from modeled envelopes.

Y.3 Post-Week Review

Reconciliation of expected vs realized performance, CLV attribution to signal vs execution, and updates to scenario libraries feed back into the next cycle.

Appendix Z

Open Questions and Future Experiments

We catalog research questions and experiment designs that extend the work.

Z.1   Live In-Game Extensions

State and action spaces for in-game policies, latency constraints, and partial observability present new challenges; simulators must incorporate possession dynamics and clock effects.

Z.2   Cross-League Transfer

How quickly can models adapt when transferring priors to other leagues (college, CFL) with different scoring dynamics and data quality?

Z.3   Market-Making

Designing conservative market-making strategies with inventory risk, adversarial bettors, and exchange mechanics invites a different risk and governance framework.

Z.4   Causal Inference Links

Opportunities exist to connect causal estimands (e.g., treatment effects of injuries or weather) to predictive models, improving robustness under interventions.

Appendix AA

Appendix: Notes on Implementation Details

We gather brief clarifications on code organization, parameter defaults, and numerical stability choices.

AA.1   Parameter Defaults

We publish default grids for regularization strength, mixture weight priors, and RL clip/entropy settings to make baselines reproducible.

AA.2   Numerical Stability

Stable evaluations for Bessel functions and log-sum-exp operations avoid overflow/underflow in score-distribution likelihoods and RL value calculations.

AA.3   Code Organization

Artefacts and experiment configs live alongside data manifests; scripts emit run IDs that propagate into reports and logs, ensuring cohesive provenance.

Appendix AB

Methodological Details (Extended)

We document implementation details that bridge theory and practice, allowing reproduction and transfer to adjacent domains.

AB.1 Score-Distribution Fitting Pipeline

We estimate Skellam and bivariate Poisson parameters via maximum likelihood with weakly informative priors and regularization. Optimization uses LBFGS with line search, and gradients exploit closed-form derivatives for Bessel functions where available, falling back to stable numerical routines otherwise. Key-number reweighting is applied post-fit with a constrained least-squares step that preserves moments while matching empirical mass at 3, 6, 7, and 10.

AB.2 Calibration Procedures

Binary outcomes use isotonic regression for post-hoc calibration on a temporally held-out validation set, while distributional predictions are assessed via PIT histograms and CRPS. We report calibration slope/intercept for probability outputs and employ bootstrap aggregation to mitigate small-sample variance in weekly splits.

AB.3 Uncertainty Estimation

We combine analytic posteriors (for linear-Gaussian components) with bootstrap ensembles (for ML models). Posterior predictive draws propagate uncertainty into stake sizing and portfolio variance. Wider posterior intervals reduce Kelly fractions automatically, and correlation estimates temper multi-leg exposure.

AB.4 Off-Policy Evaluation

We implement inverse propensity, self-normalized importance sampling, and doubly robust estimators. Clipping mitigates variance at the cost of bias; sensitivity analyses vary clip thresholds. To reduce overfitting, we separate reward-model fitting from evaluation folds and report percentile bands for value estimates.

AB.5 Portfolio and CVaR Optimization

Stake sizes follow fractional Kelly but are constrained by a weekly risk budget and a CVaR cap computed from posterior predictive distributions. We solve a convex approximation using second-order cone formulations for variance and linear constraints for exposure caps, yielding stable allocations that respect governance.

Appendix AC

Operations Playbook (Extended)

We codify routines for common scenarios to keep operations repeatable, auditable, and resilient.

AC.1 Weekly Cycle

1. Data refresh and integrity checks (schema tests, row counts, drift monitors).

2. Baseline retraining and ensemble updates with reproducible seeds; log artefacts.

3. Reliability and CLV diagnostics; gate promotions; document changes.

4. Simulator calibration and stress scenarios; revise risk envelope if needed.

5. Execution strategy selection (routing, patience, fill targets) informed by microstructure.

AC.2 Incident Response

1. Detect anomalies (monitor alerts, unusual drift, fill failures).

2. Triage scope and impact; freeze promotions and pause risky orders.

3. Roll back to last known-good artefacts; attach post-mortem issue with logs.

4. Patch, test, and promote with signoffs from risk and data owners.

AC.3 Change Management

All material changes (features, training windows, risk budgets) require experiment records, approvals, and rollback plans. We maintain human-readable changelogs linking artefacts to results and dashboards.

Appendix AD

Data Engineering Notes (Extended)

We expand on ingestion and mart construction practices beyond the core chapter.

AD.1   Schema Migrations and Idempotency

Migrations are versioned and accompanied by smoke tests. Ingestors use upserts keyed by natural identifiers to prevent duplication. Reprocessing is safe and deterministic, with reconciliation reports comparing expected to realized deltas.

AD.2   Drift Detection

We monitor marginal distributions and key ratios (EPA, success rate, implied probabilities). Detectors use EWM statistics and CUSUM alarms with cooldowns to avoid alert fatigue. Detected shifts trigger recalibration and sometimes stake reductions.

AD.3   Reproducibility

Artefacts include dataset hashes, model versions, and environment manifests. Rebuilds on clean machines reproduce metrics within small tolerances; discrepancies open issues with attached diffs and logs.

References

Joshua Achiam, David Held, Aviv Tamar, and Pieter Abbeel. Constrained policy optimization. *arXiv preprint arXiv:1705.10528*, 2017. doi: 10.48550/arXiv.1705. 10528.

Alekh Agarwal, Nan Jiang, Sham Kakade, and Wen Sun. An optimistic perspective on offline reinforcement learning. In *Proceedings of the 37th International Conference on Machine Learning*, volume 119 of *Proceedings of Machine Learning Research*, pages 104–114. PMLR, 2020.

Gianluca Baio and Marta Blangiardo. Bayesian hierarchical model for the prediction of football results. *Journal of Applied Statistics*, 37(2):253–264, 2010. doi: 10.1080/ 02664760802684177.

Marc G. Bellemare, Will Dabney, and Rémi Munos. A distributional perspective on reinforcement learning. In *Proceedings of the 34th International Conference on Machine Learning*, volume 70 of *Proceedings of Machine Learning Research*, pages 449–458. PMLR, 2017.

Ralph A. Bradley and Milton E. Terry. Rank analysis of incomplete block designs i. the method of paired comparisons. *Biometrika*, 1952. doi: 10.1093/biomet/39.3-4.324.

Glenn W. Brier. Verification of forecasts expressed in terms of probability. *Monthly Weather Review*, 78(1):1–3, 1950. doi: 10.1175/1520-0493(1950)078<0001:VOFEIT> 2.0.CO;2.

Will Dabney, Mark Rowland, Marc G. Bellemare, and Rémi Munos. Implicit quantile networks for distributional reinforcement learning. In *Proceedings of the 35th International Conference on Machine Learning*, volume 80 of *Proceedings of Machine Learning Research*, pages 1096–1105. PMLR, 2018.

Henry E. Daniels. Saddlepoint approximations in statistics. *The Annals of Mathematical Statistics*, 1954. doi: 10.1214/aoms/1177728652.

Mark J Dixon and Stuart G Coles. Modelling association football scores and inefficiencies in the football betting market. *Applied Statistics*, 46(2):265–280, 1997. doi: 10.2307/2986290.

Miroslav Dudík, John Langford, and Lihong Li. Doubly robust policy evaluation and learning. *Statistical Science*, 2014. doi: 10.1214/14-STS500.

Arpad E. Elo. *The Rating of Chessplayers, Past and Present*. Arco Publishing, 1978.

Scott Fujimoto and Shixiang Shane Gu. A minimalist approach to offline reinforcement learning. *Advances in Neural Information Processing Systems*, 2021. URL https://proceedings.neurips.cc/paper/2021/hash/a8166da05c5a094f7dc03724b41886e5-Abstract.html. TD3+BC.

Scott Fujimoto, Herke van Hoof, and David Meger. Addressing function approximation error in actor-critic methods. In *Proceedings of the 35th International Conference on Machine Learning*, volume 80 of *Proceedings of Machine Learning Research*, pages 1582–1591. PMLR, 2018.

Scott Fujimoto, David Meger, and Doina Precup. Off-policy deep reinforcement learning without exploration. In *Proceedings of the 36th International Conference on Machine Learning*, volume 97 of *Proceedings of Machine Learning Research*, pages 2052–2062. PMLR, 2019.

Paul Glasserman. *Monte Carlo Methods in Financial Engineering*. Stochastic Modelling and Applied Probability. Springer, 2003. doi: 10.1007/978-0-387-21617-1.

Mark E Glickman and Hal S Stern. A state-space model for national football league scores. *Journal of the American Statistical Association*, 93(441):25–35, 1998. doi: 10.1080/01621459.1998.10474084.

Tilmann Gneiting and Adrian E. Raftery. Strictly proper scoring rules, prediction, and estimation. *Journal of the American Statistical Association*, 102(477):359–378, 2007. doi: 10.1198/016214506000001437.

Tuomas Haarnoja, Aurick Zhou, Pieter Abbeel, and Sergey Levine. Soft actor-critic: Off-policy maximum entropy deep reinforcement learning with a stochastic actor. In *Proceedings of the 35th International Conference on Machine Learning*, volume 80 of *Proceedings of Machine Learning Research*, pages 1861–1870. PMLR, 2018.

David A Harville. Predictions for national football league games via linear-model methodology. *Journal of the American Statistical Association*, 75(372):516–524, 1980. doi: 10.1080/01621459.1980.10477504.

Nan Jiang and Lihong Li. Doubly robust off-policy value evaluation for reinforcement learning. In *Proceedings of the 33rd International Conference on Machine Learning*, volume 48 of *Proceedings of Machine Learning Research*, pages 652–661. PMLR, 2016.

Harry Joe. *Multivariate Models and Multivariate Dependence Concepts*. Chapman and Hall/CRC, 1997. doi: 10.1201/9780367803896.

Dimitris Karlis and Ioannis Ntzoufras. Analysis of sports data by using bivariate poisson models. *Journal of the Royal Statistical Society: Series D (The Statistician)*, 52 (3):381–393, 2003. doi: 10.1111/1467-9884.00366.

J. L. Kelly. A new interpretation of information rate. *Bell System Technical Journal*, 35 (4):917–926, 1956. doi: 10.1002/j.1538-7305.1956.tb03809.x.

Siem Jan Koopman, Roman Lit, and André Lucas. Dynamic bivariate poisson models for analysing and forecasting match results in the english premier league. *Journal of the Royal Statistical Society: Series A*, 178(1):167–186, 2015. doi: 10.1111/rssa.12042.

Ilya Kostrikov, Ashvin Nair, and Sergey Levine. Offline reinforcement learning with implicit q-learning. *arXiv preprint arXiv:2110.06169*, 2021. doi: 10.48550/arXiv. 2110.06169.

Aviral Kumar, Justin Fu, George Soh, George Tucker, and Sergey Levine. Stabilizing off-policy q-learning via bootstrapping error reduction. In *Advances in Neural Information Processing Systems*, volume 32, 2019.

Aviral Kumar, Aurick Zhou, George Tucker, and Sergey Levine. Conservative q-learning for offline reinforcement learning. In *Advances in Neural Information Processing Systems*, volume 33, 2020.

Sergey Levine, Aviral Kumar, George Tucker, and Justin Fu. Offline reinforcement learning: Tutorial, review, and perspectives on open problems. *arXiv preprint arXiv:2005.01643*, 2020. doi: 10.48550/arXiv.2005.01643.

Steven D Levitt. Why are gambling markets organised so differently from financial markets? *The Economic Journal*, 114(495):223–246, 2004. doi: 10.1111/j.0013-0133.2004.00207.x.

Eric Lock and Dan Nettleton. Using random forests to estimate win probability before each play of an nfl game. *Journal of Quantitative Analysis in Sports*, 10(2): 197–205, 2014. doi: 10.1515/jqas-2013-0100.

M. J. Maher. Modelling association football scores. *Applied Statistics*, 1982. doi: 10.2307/2347625.

Volodymyr Mnih, Koray Kavukcuoglu, David Silver, et al. Human-level control through deep reinforcement learning. *Nature*, 518(7540):529–533, 2015. doi: 10.1038/nature14236.

Ashvin Nair, Murtaza Dalal, Abhishek Gupta, and Sergey Levine. Awac: Accelerating online reinforcement learning with offline datasets. *arXiv preprint arXiv:2006.09359*, 2020. doi: 10.48550/arXiv.2006.09359.

Roger B. Nelsen. *An Introduction to Copulas*. Springer, 2 edition, 2006. doi: 10.1007/0-387-28678-0.

Mark W Nichols. Time zones and team performance in the nfl, 2014. URL https://doi.org/10.1177/1527002513516905. Shows west-to-east travel reduces win probability.

R. Tyrrell Rockafellar and Stanislav Uryasev. Optimization of conditional value-at-risk. *Journal of Banking and Finance*, 24(7):1443–1471, 2000. doi: 10.1016/S0378-4266(00)00071-8.

Raymond D Sauer. The economics of wagering markets. *Journal of Economic Literature*, 36(4):2021–2064, 1998. URL https://www.jstor.org/stable/2565043.

Tom Schaul, John Quan, Ioannis Antonoglou, and David Silver. Prioritized experience replay. *arXiv preprint arXiv:1511.05952*, 2016. doi: 10.48550/arXiv.1511.05952.

John Schulman, Sergey Levine, Philipp Moritz, Michael I. Jordan, and Pieter Abbeel. Trust region policy optimization. *arXiv preprint arXiv:1502.05477*, 2015. doi: 10.48550/arXiv.1502.05477.

John Schulman, Philipp Moritz, Sergey Levine, Michael I. Jordan, and Pieter Abbeel. High-dimensional continuous control using generalized advantage estimation. *arXiv preprint arXiv:1506.02438*, 2016. doi: 10.48550/arXiv.1506.02438.

John Schulman, Filip Wolski, Prafulla Dhariwal, Alec Radford, and Oleg Klimov. Proximal policy optimization algorithms. *arXiv preprint arXiv:1707.06347*, 2017. doi: 10.48550/arXiv.1707.06347.

J. G. Skellam. The frequency distribution of the difference between two poisson variates. *Journal of the Royal Statistical Society*, 1946. doi: 10.2307/2981372.

Hal S Stern. On the probability of winning a football game. *The American Statistician*, 45(3):179–183, 1991. doi: 10.1080/00031305.1991.10475812.

Richard S. Sutton and Andrew G. Barto. *Reinforcement Learning: An Introduction*. MIT Press, 2 edition, 2018.

Anna Szalkowski and Jordan Nelson. The collective wisdom of nfl betting lines. *arXiv preprint arXiv:1201.0309*, 2012. doi: 10.48550/arXiv.1201.0309.

Aviv Tamar, Yonatan Glassner, and Shie Mannor. Policy gradients with variance related risk criteria. In *Proceedings of the 30th Conference on Neural Information Processing Systems*, pages 1651–1659, 2015.

Philip Thomas, Georgios Theocharous, and Mohammad Ghavamzadeh. High-confidence off-policy evaluation. *Proceedings of the AAAI Conference on Artificial Intelligence*, 29(1), 2015. doi: 10.1609/aaai.v29i1.9541.

Hado van Hasselt, Arthur Guez, and David Silver. Deep reinforcement learning with double q-learning. In *Proceedings of the AAAI Conference on Artificial Intelligence*, 2016. doi: 10.1609/aaai.v30i1.10295.

Ziyu Wang, Tom Schaul, Matteo Hessel, Hado Van Hasselt, Marc Lanctot, and Nando De Freitas. Dueling network architectures for deep reinforcement learning. *arXiv preprint arXiv:1511.06581*, 2016. doi: 10.48550/arXiv.1511.06581.

Stanford Wong. *Sharp Sports Betting*. Pi Yee Press, 2001.

Yifan Wu, George Tucker, and Ofir Nachum. Behavior regularized actor-critic. *arXiv preprint arXiv:1910.01708*, 2019. doi: 10.48550/arXiv.1910.01708.